ESTIMATING SYSTEM AND TRAVELER COSTS DUE TO LANE CLOSURES DURING CONSTRUCTION AND MAINTENANCE OPERATIONS

Ernest Tufuor, Ph.D.
Postdoc Research Associate
Nebraska Transportation Center
University of Nebraska-Lincoln

Li Zhao, Ph.D.
Postdoc Research Associate
Nebraska Transportation Center
University of Nebraska-Lincoln

Mm Haque, Ph.D.
Graduate Research Assistant
Nebraska Transportation Center
University of Nebraska-Lincoln

Laurence R. Rilett, Ph.D., P.E., F. ASCE.
Director, Auburn University Transportation Research Institute
Ginn Distinguished Professor
1220 Shelby Center
Auburn University

John E. Anderson
Executive Director, Central Plains Research Data Center (CPRDC)
Department of Economics
525N College of Business
University of Nebraska-Lincoln

Eric C. Thompson
Director/Chair, Bureau of Business Research
Department of Economics
523A College of Business
University of Nebraska-Lincoln

A Report on Research Sponsored By

Nebraska Department of Transportation and U.S. Department of Transportation Federal Highway Administration

May 2022

TECHNICAL REPORT DOCUMENTATION PAGE

1. Report No. FY21-008	**2. Government Accession No.**	**3. Recipient's Catalog No.**
4. Title and Subtitle Estimating System and Traveler Costs Due to Lane Closures During Construction and Maintenance Operations		**5. Report Date** May 2022 **6. Performing Organization Code**
7. Authors Ernest O.A. Tufuor, Li Zhao, Mm Haque, Laurence R. Rilett, John E. Anderson, Eric C. Thompson		**8. Performing Organization Report No.** **26-1121-0036-001**
9. Performing Organization Name and Address Nebraska Transportation Center 2200 Vine Street P. O. Box 830851 Lincoln, NE 68583-0851		**10. Work Unit No.** **11. Contract** SPR-FY21(008)
12. Sponsoring Agency Name and Address Nebraska Department of Transportation Research Section 1400 Hwy 2 Lincoln, NE 68502		**13. Type of Report and Period Covered** July 2020 – May 2022. **14. Sponsoring Agency Code**
15. Supplementary Notes .		

16. Abstract

Lane closures are used to facilitate activities related to road construction and maintenance or operations. However, there are economic costs associated with lane closures and these may accrue to both the traveling public as well as to traffic agencies. The Nebraska Governor's office has identified maximizing the effectiveness of lane closures as a priority for the Nebraska Department of Transportation (NDOT). The goal of this project is to assist NDOT in effectively managing the operations of work zones to maximize the effectiveness of lane closures under Nebraska conditions. This report summarizes the findings of the current state of the practice in work zone traffic control techniques, work zone traffic operation models and tools, and the value of travel time economic analysis. It was found that the latest and 6th edition of the Highway Capacity Manual (HCM6) has developed a traffic microsimulation methodology for modeling work zones on multilane highways and two-lane highways. It was, therefore, important to calibrate the model under Nebraska conditions. The report presents a calibration methodology for both multilane highways and two-lane highway lane closure cases. The calibration model was tested to determine the sensitivity of the increase in traffic volume, percent of heavy vehicles, work zone lengths, and posted speeds for over 1460 different scenarios. In addition, a state-of-the-science emission modeling software, recommended by the US EPA, was used to model the sensitivity of the vehicle emission performance using the outcome of the calibrated work zone models as a key input. The outcome of the sensitivity analysis is used to develop a lane closure cost simulation model that examines the cost of changes in road user time, emissions, and fuel cost under all of the lane closure scenarios. The economic analysis develops estimates of time, emissions and fuel use costs to simulate the increase in hourly road user costs associated with a lane closure. A working spreadsheet has been developed to assist NDOT engineers to estimate the cost of lane closures for hundreds of closure scenarios.

17. Key Words Traveler Costs, Lane Closure, Construction, Maintenance	**18. Distribution Statement**		
19. Security Classification (of this report) Unclassified	**20. Security Classification (of this page)** Unclassified	**21. No. of Pages** 171	**22. Price**

Form DOT F 1700.7 (8-72) Reproduction of completed page authorized

DISCLAIMER

The contents of this report reflect the views of the authors, who are responsible for the facts and the accuracy of the information presented herein. The contents do not necessarily reflect the official views or policies neither of the Nebraska Department of Transportations nor the University of Nebraska-Lincoln. This report does not constitute a standard, specification, or regulation. Trade or manufacturers' names, which may appear in this report, are cited only because they are considered essential to the objectives of the report.

The United States (U.S.) government and the State of Nebraska do not endorse products or manufacturers. This material is based upon work supported by the Federal Highway Administration under SPR-FY21(008). Any opinions, findings and conclusions or recommendations expressed in this publication are those of the author(s) and do not necessarily reflect the views of the Federal Highway Administration."

ACKNOWLEDGMENTS

The authors would like to thank the research sponsor, the Nebraska Department of Transportation, for their support. Special thanks go to the TAC members chaired by Matt Neemann for their insightful contributions to achieve project goals. We also acknowledge the contributions of NDOT District Engineers in Merrick, York, and Saunders Counties who helped in coordinating a safe and efficient work zone data collection system.

Table of Contents

ABSTRACT 11
1 INTRODUCTION 13
2 LITERATURE REVIEW OF THE CURRENT STATE OF PRACTICE 16
2.1 Work Zone Traffic Control Techniques 16
2.1.1 Work Zone on Multilane Highways 16
2.1.2 Work Zone on Two-Lane Highways 20
2.2 Work Zone Traffic Operation Models and Tools 29
2.2.1 HCM6 Freeway/Multilane Highway Work Zone Model 30
2.2.2 HCM6 Two-Lane Highway Work Zone Model 31
2.2.3 Work Zone Simulation Models 35
2.2.4 Work Zone Model Optimization 37
2.2.5 Work Zone Traffic Analysis Tools 38
2.3 The Value of Travel Time 41
2.3.1 The Size and Sign of the Value of Travel Time 44
2.3.2 Gap between WTP and WTA Measures of Value of Travel Time 46
2.3.3 The Value of Travel Time Savings 47
2.3.4 Meta-analysis in Value of Travel Time 47
3 WORK ZONE SIMULATION MODEL DEVELOPMENT FOR NEBRASKA 49
3.1 Calibration & Validation Method for Simulation Models of Intelligent Work Zones 50
3.1.1 Multilane Work Zone AQD Traffic Simulation Model Development 52
3.1.2 Simulation of the AQD System Using VAP 53
3.1.3 AQD Work Zone Model Calibration 57
3.1.4 Multilane Case Study 63

3.1.5 Multilane Simulation Model Input 66
3.1.6 Multilane Calibration Parameters 70
3.1.7 Multilane Calibration Results 72
3.1.8 Multilane Model Validation 72
3.1.9 Multilane Model Development Concluding Remarks 75
3.2 Calibration & Validation of a Microsimulation Model of Lane Closures on Two-Lane Highway Work Zone 76
3.2.1 Two-lane Highway Test Site and Data Collection System 81
3.2.2 Two-lane Highway Data Processing for Calibration 84
3.2.3 Two-lane Highway Work Zone Proposed Calibration Methodology 87
3.2.4 Two-lane Highway Case Study 92
3.2.5 Two-lane Highway Calibration Results 95
3.2.6 Two-lane Highway Model Validation and Transferability 101
3.2.7 Two-lane Highway Model Development Concluding Remarks 105
4 SENSITIVITY ANALYSIS OF WORK ZONE CALIBRATED MICROSIMULATION MODEL FOR NEBRASKA 107
4.1 Sensitivity Analysis of the Four-lane Work Zone Case 108
4.1.1 Four-lane Work Zone Model Capacity Estimates 110
4.1.2 Four-lane Work Zone Model Performance Estimates 112
4.2 Sensitivity Analysis of the Six-lane Work Zone Case 114
4.2.1 Six-lane Work Zone Model Capacity Estimates 115
4.2.2 Six-lane Work Zone Model Performance Estimates 117
4.3 Sensitivity Analysis of the Two-lane Work Zone Case 122
4.3.1 Two-lane Work Zone Model Capacity Estimates 123
4.3.2 Two-lane Work Zone Model Queue Length Estimates 124
4.3.3 Two-lane Work Zone Model Delay Estimates 125

4.4 Sensitivity Analysis of Vehicle Emission Performance 126

4.4.1 MOVES Work Zone Model & Results – Nebraska Conditions 127

5 THE COSTS OF LANE CLOSURE MODEL 132

5.1 Introduction 132

5.2 Travel Time Costs 134

5.3 Emissions Costs 139

5.4 Fuel Costs 142

5.5 Lane Closure Costs 144

6 CONCLUDING REMARKS 146

REFERENCES 151

APPENDICES 169

LIST OF FIGURES

Figure 2. 1 The layout of the Nebraska AQD system (not to scale) 18

Figure 2. 2 The HCM6 framework for 1L2W work zone lane closure model 33

Figure 3. 1 AQD system realization in simulation 53

Figure 3. 2 Flowchart of the AQD system algorithm. 54

Figure 3. 3 The layout of the AQD System and Data Collection at the Waco IWZ Test Site 65

Figure 3. 4 The Empirical Distribution of CC1 69

Figure 3. 5 Segment Travel Time Calibration Results. 71

Figure 3. 6 Speed and PDMS Display According to the AQD Logic. 73

Figure 3. 7 Validation of Traffic Counts for PCs and HVs at PDMS1 and PDMS2. 74

Figure 3. 8 Test sites and data collection system 83

Figure 3. 9 Empirical data from Highway 30 work zone test site used in microsimulation model calibration for Northbound (NB) and Southbound (SB) 86

Figure 3. 10 Proposed model of two-lane work zone microsimulation calibration 88

Figure 3. 11 Comparison of empirical, uncalibrated, and best calibrated output distributions 97

Figure 3. 12 Validation and transferability of calibrated model parameters 103

Figure 4. 11 Sensitivity analysis for active work zone duration of 1 hour 124

Figure 4. 12 Delay varies over truck percentage, demand, and work zone length (1 hour) 125

Figure 4. 15 Running exhaust algorithm flow chart 127

Figure 4. 14 Output of a sample emissions scenario analysis 129

Figure 4. 15 The impact of traffic volume changes on vehicle emissions 130

Figure 4. 16 The impact of work zone length on vehicle emissions 131

Figure 4. 17 The impact of posted speed on vehicle emissions 131

LIST OF TABLES

Table 2. 1 Intelligent Work Zone Application Evaluation Results 20

Table 2. 2 Potential Advantages and Disadvantages of Traffic Control Techniques 23

Table 2. 3 The 1L2W Traffic Control Practices Among State DOTs 26

Table 2. 4 Example of Maximum Lane Closure Length for 1L2W Traffic Controls 28

Table 2. 5 Capacity of Long-Term Construction Zone on Freeways and Multilane Highways (Source: Exhibit 10-14, HCM6) 31

Table 2. 6 The Main Measurement of the Value of Travel Time 44

Table 3. 1 Desired Speed Distribution 67

Table 3. 2 Parameter Calibration Results 72

Table 3. 3 Comparative Model Outcomes of Mean and Distribution Approach for Saturation Headway. 99

Table 3. 4 Comparative Model Outcomes of Mean and Distribution Approach for Work Zone Travel Time. 100

Table 4. 1 The Total Number of Scenarios 108

Table 4. 2 Estimated Work Zone Capacity as a Function of Truck Percentage 111

Table 4. 3 Other State DOT Operational Work Zone Capacities 111

Table 4. 4 HCM6 Predicted Work Zone Capacities 115

Table 4. 5 Sample Scenario Emission Results 129

Table 4. 6 National Emission Estimates Vs Simulation Estimations 130

Table 5. 1 Method for Calculating the Time Cost of an Hour of Vehicle Travel using U.S. Income and Wages 136

Table 5. 2 Aggregate Value for an Hour of Automobile Travel using U.S. Income and Wages. 138

Table 5. 3 Hourly Value of Increased Travel Time for an Example Lane Closure Project 139

Table 5. 4 Method for Estimate the Cost Per Gram of Greenhouse Gas Emissions..... 140

Table 5. 5 Hourly Value of Increased Emissions for an Example Lane Closure Project..... 142

Table 5. 6 Method for Estimate the Cost Per Joule of Fuel Use..... 143

Table 5. 7 Hourly Value of Increased Fuel Costs for an Example Lane Closure Project..... 144

ABSTRACT

Lane closures are used to facilitate activities related to road construction and maintenance or operations. However, there are economic costs associated with lane closures that may accrue to both the traveling public and traffic agencies. The Nebraska Governor's office has identified maximizing the effectiveness of lane closures as a priority for the Nebraska Department of Transportation (NDOT). The goal of this project is to assist NDOT in effectively managing the operations of work zones to maximize the effectiveness of lane closures under Nebraska conditions.

This report summarizes the findings while evaluating the current state of the practice in work zone traffic control techniques, work zone traffic operation models and tools, and the value of travel time economic analysis. The latest and 6th edition of the Highway Capacity Manual (HCM6) has developed a traffic microsimulation methodology for modeling work zones on multilane highways and two-lane highways. However, this model was not calibrated under Nebraska conditions.

The report presents a calibration methodology for both multilane highways and two-lane highway lane closure cases. Empirical travel data was collected on three active work zones. Two were located on Interstate 80 and one was on State Highway 30 in Nebraska. A traffic simulation model, VISSIM, was used to model these test sites and calibrated to represent local conditions. The calibration model was used to estimate work zones performance measures such as average queue, delays, travel time, and capacity. The model was tested to determine the sensitivity of increase in traffic volume, percent of heavy vehicles, work zone lengths, and posted speeds for over 1460 different scenarios. In addition, a state-of-the-science emission modeling software, recommended by the US EPA, MOtor Vehicle Emission Simulator (MOVES) was used to model

the sensitivity of the vehicle's emission performance using the outcome of the calibrated work zone models as a key input.

The outcome of the sensitivity analysis was used to develop a lane closure cost simulation model that examines the cost of changes in road user time, emissions, and fuel cost under all of the lane closure scenarios. The model utilized changes in travel time, emissions of various greenhouse gases (i.e., CO2, CO, NOx, VOC), and fuel use (gasoline, diesel, CNG, E-85 Ethanol) under lane closure scenarios. The economic analysis developed estimates of time, emissions, and fuel used costs to simulate the increase in hourly road user costs associated with a lane closure. A working spreadsheet has been developed to assist NDOT engineers to estimate the cost of lane closures for hundreds of closure scenarios.

1 INTRODUCTION

Lane closures are used to facilitate activities related to construction and maintenance/operations. However, there are economic costs associated with lane closures and these may accrue to both the traveling public and traffic agencies. While it is sometimes necessary to prohibit lane closures during the day to alleviate traffic congestion, there are consequences of this decision related to project delivery timelines, construction costs, and safety within the work zone. The Nebraska Governor's office has identified maximizing the effectiveness of lane closures as a priority for the Nebraska Department of Transportation (NDOT). The goal of this project is to assist NDOT in effectively managing the operations of work zones to maximize the effectiveness of lane closures under Nebraska conditions.

Lane closure performances can be impacted by traffic control techniques, lane closure characteristics (e.g., length of lane closure, speed limit, etc.), and traffic characteristics (e.g., volume, heavy vehicle). Therefore, accurate evaluation of critical performance measures (e.g., delay, capacity, costs) is key to efficient work zone management and road users' satisfaction. The latest and 6th edition of the Highway Capacity Manual (HCM6) provides methodologies to estimate lane closure capacity reductions and delays related to various work zone conditions. The HCM6 methodology is based on a microsimulation model. It is critical to calibrate this model to represent Nebraska conditions.

The specific objectives of this research project identified by NDOT are four-fold:

1. Calibrate the 2016 Highway Capacity Manual model to Nebraska conditions.

2. Use the calibrated model to provide estimates of capacity reduction, delay increases, and fuel usage increases related to various work zone/lane closure conditions. Specifically, the following work zone/lane closure cases are examined:
    i. Six-Lane Divided Highway: 3 lanes per direction, 1 lane closed
    ii. Six-Lane Divided Highway: 3 lanes per direction, 2 lanes closed
    iii. Four-Lane Divided Highway: 2 lanes per direction, 1 lane closed
    iv. Two-Lane (Undivided) Highway: 1 lane closed (using flagging or traffic signal operation)
3. Analyze each of the scenarios with respect to different lengths of the work zone, traffic volume, percent of trucks, speed limit, and time the work zone will be active.
4. Conduct a detailed economic analysis of the costs of delay, increased vehicle operating costs, and accident costs for vehicles traveling through lane closures for each of the scenarios.

This report presents the methods, findings, and recommendations for analyzing work zone operations on multilane highways and two-lane highways in Nebraska. The report provides the analysis of 1460 different scenarios of lane closure operations. There were 320 scenarios for the 6-lane cases, 240 scenarios in the 4-lane case, and 900 scenarios in the 2-lane case. These scenarios were made up of the combination of different work zone lengths, traffic volumes at varying truck percentages, and posted speeds. The simulation model was run with a startup time of 15 minutes so the model could reach equilibrium conditions. After the steady-state conditions were reached the key performance metrics for each scenario were assumed. Note that the underlying assumption was the traffic is moving normally with no incidents or severe weather. In other words, the analysis was limited to typical travel conditions within each of the facility types

and scenarios. Note the research was focused on traffic volumes under the work zone capacity. If the demand in a given scenario was such the work zone queues were continuously growing (e.g., oversaturated conditions), then that scenario was discarded and not analyzed further.

The remaining part of the report is organized as follows: Chapter 2 reviews the literature on work zone operations in multilane (e.g., 4-lane and 6-lane) and two-lane highways. The chapter also includes the state of practice of the economic analysis of the value of travel time. Chapter 3 presents a methodology for the work zone simulation model. The methodology is used to develop, calibrate, and validate generic work zone models for multilane and two-lane cases under Nebraska conditions. Then, in Chapter 4, the calibrated models are used to undertake sensitivity analyses of the performance of the work zone under 1460 different scenarios. Also, in this chapter, the operational performance of the calibrated model is used as an input to a national state-of-the-science emission modeling software (MOVES) to estimate vehicle emissions under the given scenarios. Chapter 5 presents the lane closure cost simulation model that examines the cost of changes in road user time, emissions, and fuel cost under different lane closure scenarios. The concluding remarks and recommendations are provided in Chapter 6.

2 LITERATURE REVIEW OF THE CURRENT STATE OF PRACTICE

This section reviews the current state of the practice in work zone traffic control techniques, work zone traffic operation models and tools, and the value of travel time economic analysis. The aim is to ensure that no research relevant to this study is overlooked or duplicated and to bridge some of the gaps in the literature.

2.1 Work Zone Traffic Control Techniques

The traffic control technique deployed at a work zone lane closure setup is one of the key factors that can impact work zone performance (e.g., safety, delay, capacity). The selection of a particular technique is a function of the work zone characteristics, that is, the type of road facility (urban or rural), the road category and the lane configuration (highway or freeway), the traffic volume and composition, the construction activities within the work zone, etc. Consequently, there are completely different techniques used for a two-lane highway compared to a multilane freeway. The following subsections discuss the various traffic operation techniques.

2.1.1 Work Zone on Multilane Highways

Work zones are necessary for maintaining and upgrading road infrastructure. However, work zone lane closures contravene drivers' expectations and therefore pose safety concerns e.g., the potential for rear-end collisions, especially on freeways. According to the US Federal Highway Administration (FHWA n.d.), a total of 842 people were killed at work zones across the US in 2019. This is an increase of 11% over the previous year. It is also important to note that nearly a quarter of these fatalities involved rear-end collisions (FARS 2019 Annual Report). Therefore, for multilane highways or freeways where speeds are relatively high and there are dynamic changes in traffic and work zone areas, it is very important to properly manage the

controls before and within the work zones to balance safety and mobility (Ullman & Schroeder 2014). This objective is often achieved by using intelligent transportation system data collection and analysis for real-time actionable driver information.

A typical ITS setup involves the use of portable speed sensors and cameras integrated with dynamic message signs. On freeways, there is often a dynamic queue detection system as part of the ITS setup to alert approaching drivers of stopped or slow-moving vehicles and avoid rear-end collisions (Paracha and Ostroff 2018). In 2015, the FHWA launched the intelligent work zone initiative to assist state DOTs to better manage work zones to improve safety and mobility. Typically, the intelligent work zone applications serve a combination of the following purposes:

- Advanced queue detection (AQD)
- Speed monitoring
- Travel time display
- Incident detection and surveillance
- Over-height vehicle warning

A typical advanced queue detection system (AQD) designed and deployed by the Nebraska Department of Transportation (NDOT) is shown in Figure 2.1. The system consists of four components:

- Non-intrusive speed detectors placed at or near the taper of the work zone,

- Portable dynamic message signs (PDMS) placed on both sides of the road a few miles upstream of the work zone,

- A computer server with an analysis module for processing pre-defined speed and message algorithms, and

- A wireless communication protocol (e.g., LTE) to transmit data.

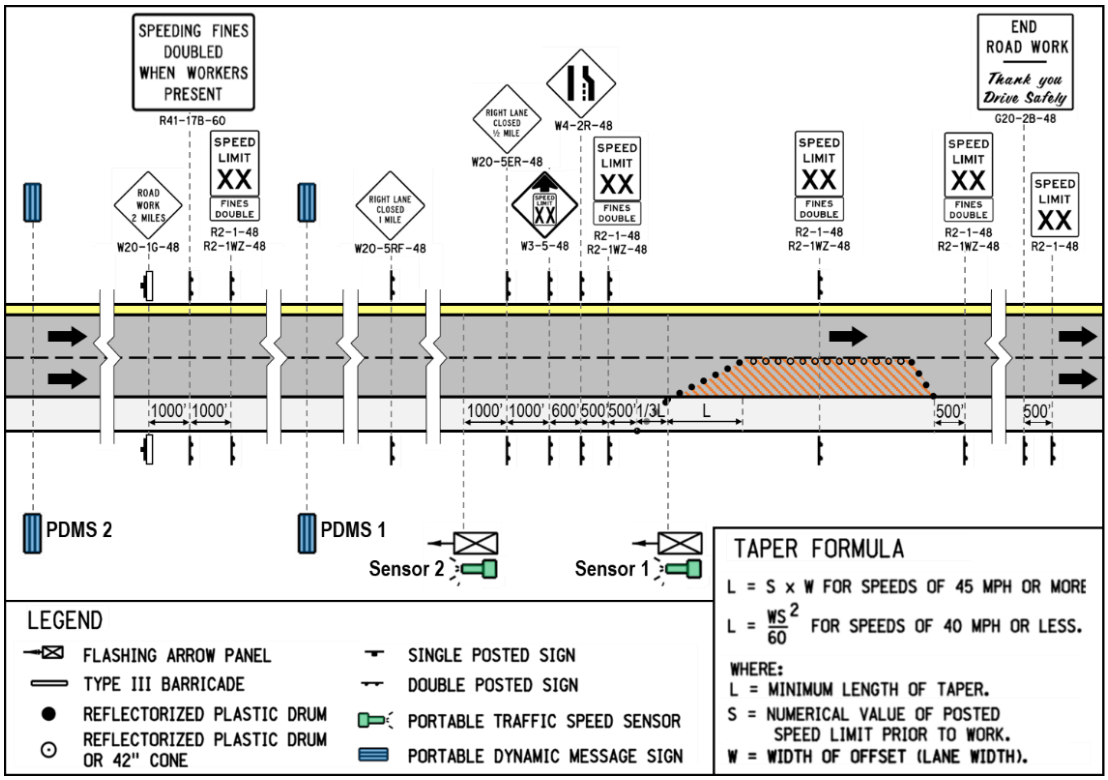

Figure 2. 1 The layout of the Nebraska AQD system (not to scale)

The operation logic of the AQD system is the speed detectors obtain instantaneous vehicle speeds and send them to the analysis module. The analysis module calculates a rolling average speed in a given time window (e.g., 3-min). Based on the speed condition, the system identifies which pre-defined message should be displayed on the PDMS.

In Nebraska, freeway AQD systems are configured so that when the rolling average speed at the work zone is estimated to be i) lower than 25 mph, the upstream PDMS displays a "Stop traffic ahead, prepare to stop" message; ii) between 25 and 45 mph, the upstream PDMS displays a "Slow traffic ahead, slow down" message; and iii) higher than 45 mph, the upstream PDMS displays four asterisks at the corners of the board as default placeholders. It should be noted the messages displayed on the PDMS follow MUTCD standards (FHWA MUTCD 2009). While the approach advocated in this paper is demonstrated using the NDOT AQD systems, other work zone AQD systems could be used without a loss in generality.

It is important to note the ITS work zone setup requires substantial expenditure and significant engineering efforts customized or project-specified to achieve effective and reliable results. For example, it cost Kansas DOT a total of $1.65 million (55% of the total construction works budget) to set up an ITS work zone for the construction of the I-35/Homestead Lane Interchange in Johnson County, Kansas (Bledsoe et al. 2014).

Several state DOTs have deployed and evaluated the effectiveness of the intelligent work zone setup for freeways. It has been found that the ITS work zone system improved safety and mobility. A sample of these evaluation results can be found in Table 2.1.

Table 2. 1 Intelligent Work Zone Application Evaluation Results

State DOT	Source	Project Type	Findings
Arkansas	Li et al. (2016)	I-30 varied locations	Improved worker safety
California	Edara et al. (2013)	I-5 section in Santa Clarita	This resulted in a 78% diversion
Illinois	USDOT & FHWA (2004)	I-55	Decrease in moving violations and crashes
Massachusetts	MassDOT (2014)	Callahan Tunnel Rehabilitation	No gridlock conditions on network
Michigan	USDOT and FHWA (2008)	I-131 section in Kalamazoo	Reduction in forced merges
North Carolina	USDOT and FHWA (2008)	I-40 section between NC801 and SR1101	Inconsistencies in data – issues with system implementation
Ohio	Zwahlen and Russ (2001)	I-17 section near Dayton	Appr. 88% of travel times on message signs were within a 4-min error margin
Texas	TTI (2018)	I-35 expansion	Managed mobility and improved safety

2.1.2 Work Zone on Two-Lane Highways

Two-lane highways facilitate mobility for people and goods through rural and sub-urban locations, carrying bi-directional traffic movements with the availability of one lane for each direction. When one lane is closed for construction, the traffic from both directions alternatively shares the common open lane, which causes significant capacity reduction and increases travel delays.

2.1.2.1 Traffic Operation Techniques

The traffic movement in one open lane on two-lane highways, often regarded as a one-lane two-way (1L2W) operation, can be controlled using techniques that can be generally grouped into four types, as described below.

- **Human flaggers,** control traffic at each end of the one-lane section using flags generally showing stop or slow signs. Human flagger is the most frequently used method for 1L2W operations (Farid et al. 2018). If the one-lane section is short and the flagger can see both ends of the direction, one flagger can be used. Otherwise, two flaggers are needed at both ends of the work zone and should communicate with each other (FHWA 2009). For example, using the flag transfer method, the last vehicle approaching the one-lane section is asked to carry the flag to the flagger on the other end (Ohio MUTCD 2012; Ohio TEM 2014). Important factors to consider when choosing the human flagger technique are topography, length of lane closure, alignment, time of work (e.g., nighttime, or daytime), and work duration (short term or long term). For example, the human flagger method is more likely to be applied for short-duration operations (e.g., several hours) in the daytime (Finley et al. 2014).

- **Automated flagger assistance devices** (AFAD), are designed to perform similar tasks as flaggers without needing them to stay near the traffic lanes. The AFAD system typically includes a gate arm that descends to the down position across the approaching traffic lane when traffic is stopped. It ascends to an upright position when the traffic is allowed to proceed (FHWA MUTCD 2009). To improve the conspicuity of the arm, a flag should also be added to the end of the gate arm.

AFADs can be either STOP/SLOW paddles or RED/YELLOW lenses. AFADs are commonly used for the site for short-term use with sufficient sight distance and a relatively short length of the closure. The most common factors considered when choosing AFADs include topography, length of the closure, sight distance, and duration of work.

- **Pilot cars** are used in the work zone to guide the queued vehicles in the right direction through a 1L2W work zone. This technique is typically used for long and/or complex one-lane section work zones to eliminate driver confusion about the complex situation and maintain the travel speed of vehicles within the work zone. Note while the pilot cars are in operation, flaggers are needed to stay on both ends of the work zone to monitor the arriving traffic to the one-lane section. The most common factors when considering the pilot car method are sight distance and length of the closure.

- **Portable traffic signal** (PTS) regulates traffic similar to the conventional signalized intersection but with only two phases. The PTS system consists of traditional traffic signal phases, i.e., red, yellow, and green, which can be programmed to work as a pre-timed or actuated signal control system. The only difference of the PTS is the duration of red clearance time will be longer as the traffic from the opposite direction needs to be cleared before traffic can proceed through the one-lane section. The important factors considered for the selection of PTS technique adoption are the length of the closure, sight distance, topography, and duration of work.

Whereas the human flaggers, AFADs, pilot cars, and PTSs are mostly used for 1L2W work zone traffic operational control, a combination of these techniques or other assistive techniques may be applied depending on the work zone conditions and the preference of the concerned local agencies. For example, AFADs can be used in addition to the human flaggers if 1) vehicle queues extend beyond the advance warning sign or 2) the sight distance from the back of the queue and the approaching vehicle is not sufficient.

In summary, the advantages and disadvantages of the application of the four techniques (Farid et al. 2018; Finley et al. 2014), as can be found in **Error! Reference source not found.**.

Table 2. 2 Potential Advantages and Disadvantages of Traffic Control Techniques

Techniques	Advantages	Disadvantages
Human flagger	• Least expensive • Quick set-up and removal time. • Handle irregular, emergency, or unprecedented situations	• Safety concern for flaggers. • Flagger fatigues and stress. • Personnel management can be problematic
AFAD	• Better driver response • Quick set-up and removal • Flaggers do not expose to traffic • One can operate multiple devices	• Potential for device malfunction and need for maintenance • Training and expertise required • More expensive
pilot car	• Clear travel direction guidance • multiple access points • Safer for construction workers	• Incur additional waiting time • May result in work zone intrusion • Require additional personnel
PTS	• Better driver response • Suitable for long-term operation • No vehicle-flagger conflict. • Save human effort	• Expensive • Potential for device malfunction • Long set-up and removal time • Coordinate with roadside signals

The four traffic operation techniques are generally modeled using either flagger control or signal control, which is described below.

1. Flagger control model

The flagger-related control techniques (e.g., human flagger, AFAD, pilot car) can dynamically change the right of way with real traffic flow conditions. Therefore, the flagging control is similar to a vehicular actuated signal control in operation. In the flagger control operation, the right of way can be provided using three methods: 1) distance gap out(Washburn et al. 2008), which alters the right of way with a specific gap distance of approaching vehicles; 2) prespecified queue length (Al-Kaisy and Kerestes 2006), which alters the right of way after a prespecified queue length is formed behind the stop-bar; and 3) fixed green time (Zhu 2015), which alters the right of way after a pre-specified time. In practice, a combination of these methods may be used in determining the right of way under flagger control operation.

2. Signal control model

A 1L2W work zone under PTS control is similar to a two-phase signalized intersection in operation. Therefore, the signal control plan needs to determine the optimal green time and the cycle length. HCM6 provides an equation for calculating the optimal green time at the 1L2W work zone (Schoen et al. 2015; Zhu 2015). As can be seen in Equation 2.1, the optimal green time is a function of the work zone length.

$$g_{opt} = \begin{cases} 20 & 0.0375l < 20 \\ 0.0375l & 20 \le 0.0375l \le 60 \\ 60 & 0.0375l > 60 \end{cases} \qquad \text{Eq. 2.1}$$

where g_{opt} = optimal effective green time for one direction (s)

l = work zone length (ft)

It should be noted there are a couple of drawbacks associated with the HCM6 optimal green time model. First, the equation does not consider the effect of traffic demand. Second, the optimal green time is derived from a field study with a work zone length of 800 feet. Therefore, the use of the same signal timing for various ranges of traffic demand and work zone length may not necessarily maximize the operational efficiency (e.g., reduce delay and/or increase capacity).

The classic pre-timed signal control models that can be adopted in determining the 1L2W work zone signal control plan (i.e., cycle length, green time) are 1) Webster model, which adjusts the lost time due to the work zone clearance time (Webster 1958); and 2) Schonfeld model, which is originally a queuing theory-based model (Schonfeld 1999) and can be used for a work zone signal timing plan.

These three traffic control models may be adopted in different traffic volume scenarios (Hua et al. 2019). For a low or moderate volume, the flagger model and actuated signal control model perform better than the pre-timed signal control models. The flagger control model with optimized gap-out distance performs better in minimizing stop delay and queue length under low volume (less than 200 pcu/h/direction) or high volume (420 ~ 580 pcu/h/direction). The actuated signal control model performs better in minimizing queue length under moderate volume (220 ~ 400 pcu/h/direction). For a high-volume scenario where pre-timed signal control may be appropriate, the Webster model outperforms the Schonfeld model for vehicle throughput.

2.1.2.2 Traffic Control Practices

In a survey of the 1L2W operation techniques on a rural highway conducted by Farid et al. (2018), it was found that thirty-seven state DOTs use the human flagger control frequently or exclusively, making it the most used traffic control technique. Comparatively, the PTS and the pilot car are less used, and the AFAD is the least used method among the four operation

techniques mentioned before. **Error! Reference source not found.**.3 summarized the traffic control practices when adopting different techniques among State DOTs.

Table 2. 3 The 1L2W Traffic Control Practices Among State DOTs

Reference	Human flagger	AFAD	PTS	Pilot car
Nebraska DOT (2017)				should make a round trip within 15 minutes
Florida DOT (2017)		the distance between two AFADs to be less than 800 ft	only used when the flagger can control for signal malfunction	use along with PTSs when work zone distance is greater than 0.5 mi
Iowa DOT (2015)	use single flagger in adequate sight distance when volumes < 2000 vpd, closure length < 100 ft		use "green revert" and "rest in absence of actuation" functionalities for actuated PTS	
Kansas DOT (2015)			allows PTS left unattended or one flagger operation if both ends are visible to each other	max speed should be 40 mph and reduced to 20 mph near the activity area with the workers present.
Michigan DOT (2010)	use single flagger if work zone is short and visible from both ends, volumes < 400 vpd and speed < 45 mph			
Minnesota DOT (2014)	use single flagger when there is adequate visibility and ADT < 1500 vph			the last vehicle from a platoon greater than 300 ft should not enter the work zone
Missouri DOT (2017)		not allow for long-term stationary operation; need to place a protective vehicle at 150 ft from the activity area.		

Montana DOT (2014)	not approve one flagger operation if more than 10 vehicles stop at flag station 50% of the time		
Nevada DOT (2017)			the last vehicle from a platoon greater than 300 ft should not enter the work zone
Oregon DOT (2016)	not allow one flagger in nighttime operation, closure length > 200 ft, sight dist. < 750 ft, ADT > 400 vpd		for nighttime operations or the approaching vehicles cannot see one flagger station to another
Pennsylvania DOT (2014)		the min all-red clearance ranges from 12 to 45 seconds	
Virginia DOT (2015)	allow single flagger in adequate sight distance and traffic volumes < 500 vph	allow AFADs with ADT < 12,000 vpd	

In addition, Minnesota, Florida, Virginia, and Kansas allow the use of a single flagger for two AFADs under many conditions such as unobstructed view of the AFADs, unobstructed view of approaching traffic from both directions, and the flagger's ability to accurately read the AFADs' indicators.

State DOTs may have their own criteria to select traffic control methods, which may include the maximum length of the closure, maximum vehicle delay, traffic volume, and speed (Farid et al. 2018). In general, the human flagger is used in short lane closures, while the pilot car is used in longer lane closure cases. Table 2.4 lists examples of State DOTs allowing the

maximum length of the lane closure when applying the appropriate traffic operation control techniques in the 1L2W work zone.

Table 2. 4 Example of Maximum Lane Closure Length for 1L2W Traffic Controls

Traffic Control Technique	Maximum lane closure length (additional conditions in parentheses)	Example DOTs
Human flagger	2000 feet, 100 feet (single flagger)	Iowa
	500 feet (single flagger)	Minnesota
	3 miles (along with PTSs)	Missouri
	2000 feet	Ohio
	1 mile	Oregon
	2 miles, 200 feet (single flagger)	South Carolina
	1 mile (flag transfer)	Virginia
AFADs	800 feet	Florida
	0.5 miles	Missouri
	2 miles	South Carolina
	800 feet	Virginia
	800 feet	Washington
PTSs	960 feet, 1340 feet (< 3 days)	Iowa
	1000 feet	Oregon
	1500 feet	Washington
Pilot car	2.5 miles (ADT < 2500) 2 miles (ADT: 2500-5000) 1.5 miles (ADT > 5000)	Iowa
	3 to 5 miles	Oregon
	4 miles	Pennsylvania

Maximum vehicle delays may vary from 5 to 30 minutes based on traffic control techniques and the preference of different DOTs. For example, for the pilot car control technique, Iowa and Nevada DOTs allow a maximum vehicle delay of 15 and 30 minutes, respectively. Under the human flagger technique, South Carolina DOT allows a maximum delay of 5 minutes when work zone length is less than 1-mile, 7.5 minutes for work zone length from 1 to 2 miles, and 20 minutes in case side roads are present within the work zone.

Even though human flaggers are required to wear high-visibility safety apparel and are expected to position themselves with utmost safety and precaution, crashes involving human flaggers still occur which can result in serious injury (Finley et al. 2015). Flaggers' fatigue and stress are common issues, which are generally addressed by rotating flagger personnel throughout the duration of work activities. To provide safety to human flaggers in the work zone, various devices such as portable rumble strips, and portable changeable message signs have been used (Farid et al. 2018). These devices intend to warn drivers of the work zone ahead and prepare them for a possible stop. AFADs can also improve the human flaggers' safety by allowing them to stay far from traffic exposures. In addition, flaggers' safety can be improved by replacing flaggers with a PTS system. The PTSs have several advantages such as the safety of the human flagger, increased workforce productivity, better communication with motorists, and long-term nighttime projects (Carlson et al. 2015; Daniels et al. 2000; MUTCD 2009).

2.2 Work Zone Traffic Operation Models and Tools

Safety, delay, and capacity are the most important traffic performance measures in a work zone lane closure case. Lane closures contravene drivers' expectations and therefore pose safety concerns e.g., the potential for rear-end collisions, especially on freeways. If closures are not properly managed, they may drastically reduce roadway capacity and increase vehicle delays. In the case of the two-lane work zone, these performance measures become more critical as both directions of traffic use a single lane in turns. Consequently, effective traffic control techniques at two-lane work zones are crucial to reduce excessive delays and improve safety and capacity.

Work zone traffic control strategies can be modeled using a deterministic approach (e.g., applying equations and a spreadsheet) or a stochastic approach (e.g., using a traffic microsimulation model). Variables that may impact the performance of the traffic control

techniques include work-zone length, the speed at the work zone, traffic volumes, etc. One of the goals of this research is to model and study the impact of these variables on work zone performance under Nebraska conditions.

2.2.1 HCM6 Freeway/Multilane Highway Work Zone Model

The latest and 6th edition of the Highway Capacity Manual (HCM6) listed five factors that influence the work zone capacity of a freeway/multilane highway. These factors include the lane configuration (e.g., a reduction from 2 lanes to 1 lane or 3 lanes to 2 lanes), hard or soft barrier type (e.g., concrete or cone), area type (e.g., urban or rural), lighting conditions (day or night), and lateral distance (0-12 ft). Based on these variables, the HCM6 estimates the work zone capacity (C) by adjusting the average queue discharge flow rate (QDR) using Equations 2.2 and 2.3 formulated in the NCHRP Report 03-107.

$$QDR = 2093 - 179f_{AT} + 9f_{LD} - 154\, f_{LCSI} - 194f_{BT} - 59f_{D} \quad \text{Eq. 2.2}$$

$$C = \frac{100QDR}{(100 - \alpha)} \quad \text{Eq. 2.3}$$

Where,

f_{AT} = area type; urban = 0, rural=1

f_{LD} = lateral distance from the nearest open lane to the work zone

f_{LCSI}= lane closure severity index; $\frac{1}{(Open\ ratio\ x\ number\ of\ open\ lane(s))}$

f_{BT} = barrier type; concrete = 0, cone, barricade = 1, and

f_{D} = day or night; day = 0, night = 1

$\alpha = 7\%\ (HCM2016)$

The HCM6 methodology includes both short-term and long-term capacity estimation methods. The difference between short and long-term work zones comes from the duration and

barrier separation type. The capacities of long-term work zones are often higher than short-term work zones as the portable concrete barriers provide better separation than plastic barriers and regular drivers become familiar with long-term work zones. The short-term method suggests a base capacity of 1,600 pc/h/ln. The long-term method varies from state to state as well as the configuration (number of lanes open normally to number of lanes open at work zone). The long-term work zone capacity values provided by HCM6 can be found in Table 2.5. More detailed information can be found in the NCHRP Report 03-107 and the HCM6.

Table 2. 5 Capacity of Long-Term Construction Zone on Freeways and Multilane Highways (Source: Exhibit 10-14, HCM6)

State	Capacity by Lane Closure Configuration (normal – reduced), pc/h/ln					
	2–1	3–2	3–1	4–3	4–2	4–1
TX	1,340		1,170			
NC	1,690		1,640			
CT	1,500-1,800		1,500-1,800			
MO	1,240	1,430	960	1,480	1,420	
NV	1,375-1,400		1,375-1,400			
OR	1,400-1,600		1,400-1,600			
SC	950		950			
WA	1,350		1,450			
WI	1,560-1,900		1,600-2,000		1,800-2,100	
FL	1,800		1,800			
VA	1,300	1,300	1,300	1,300	1,300	1,300
IA	1,400-1,600	1,400-1,600	1,400-1,600	1,400-1,600	1,400-1,600	1,400-1,600
MA	1,340	1,490	1,170	1,520	1,480	1,170
Default	1,400	1,450	1,450	1,500	1,450	1,350

2.2.2 HCM6 Two-Lane Highway Work Zone Model

The latest and 6th edition of the Highway Capacity Manual (HCM6) has developed a methodology for modeling two-lane work zones. The HCM6 incorporated a two-lane work zone methodology, which is derived from Project NCHRP 03-107 (Schoen et al. 2015). The project included six work zone sites, with work zone lengths ranging from 800 feet to two miles, for the data collection in Washington.

The work zone sites had their traffic controlled by a flagger, PTSs, and a pilot car. The travel speed of vehicles within the work zone was measured to develop the average travel speed (ATS) model. The model required estimation of base free-flow speed (BFFS) which was estimated by regression analysis as a function of the posted non-work zone speed limit. Among the six sites, three sites (length of closure ranging from 800 to 1600 feet) were used to develop the model where flagger and PTS traffic control techniques were used.

A VISSIM simulation model was developed and calibrated using field data from an 800 ft work zone site operated by the flagger control method. A mathematical model was developed based on the calibrated VISSIM model that can calculate the capacity and vehicle delay of two-lane highway work zones under the pre-timed signal control strategy (Zhu 2015). It was found that the mathematical model was able to reproduce delay with mean absolute prediction errors between one to three percent. The flagger control and fixed-time signal control were studied and compared. It was found that at low traffic demand the flagger control method works better. For a work zone site studied in the research, flagger control produced 10 to 20 percent lower vehicle delay.

Figure 2.2 shows the HCM6 analytical method for the two-lane highway work zone model. As seen, the HCM6 procedure for two-lane highways has six key steps. The first step is to obtain traffic information, roadway geometric condition, and work zone data. The next step is to estimate the average travel speed within the work zone. This can be estimated using the non-work zone posted speed limit and considering speed adjustment factors for work zone lane and shoulder width, the number of access points within the work zone, and the percentage of the no-passing zone.

Step 3 is to estimate the saturation flow rate. This model uses 1.89 seconds of saturation headway, which is further adjusted by travel speed (Watson et al. 2015). The adjustment considers no change of base saturation headway if the travel speed is over 45 mph. However, for travel speed under 45 mph, the base saturation headway is adjusted by travel speed.

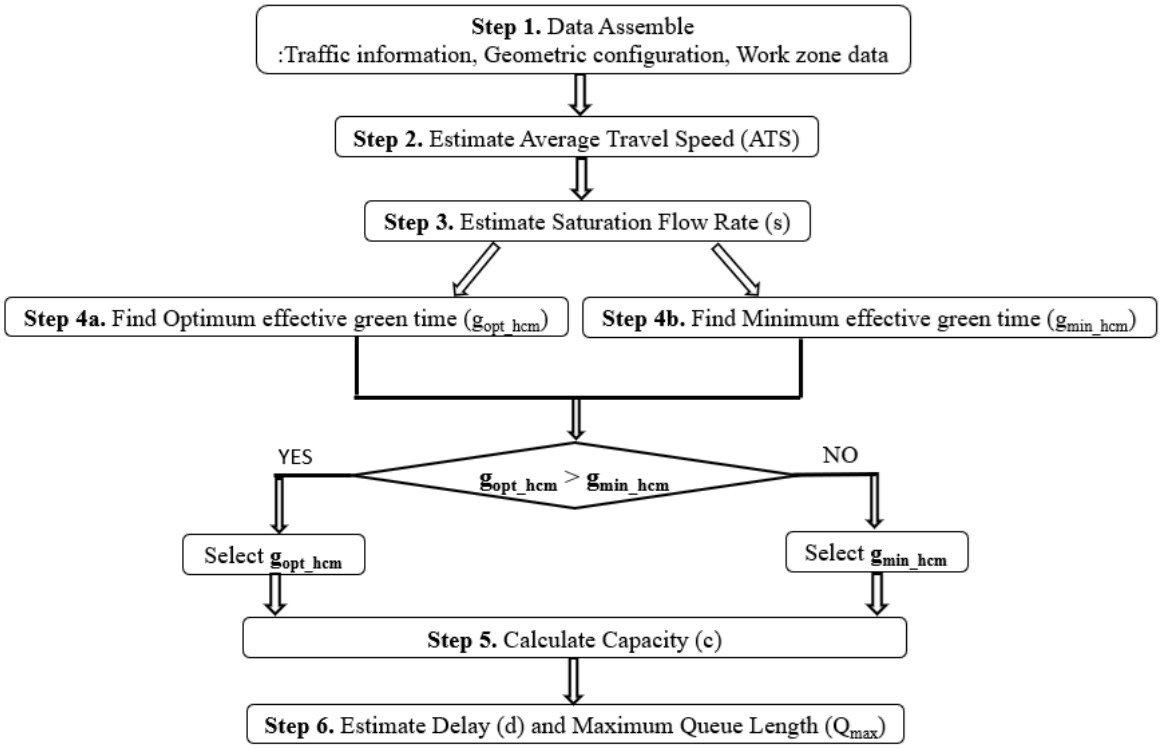

Figure 2. 2 The HCM6 framework for 1L2W work zone lane closure model

Step 4. Estimation of effective green time. This is one of the most important factors of capacity and control delay. For the flagger control method, under balanced directional demand conditions, the HCM6 provides an effective optimal green time equation where the work zone length is the only input. The HCM-6 also has a minimum green time equation in case the optimal green time is shorter than the minimum green time.

Step 5. Capacity estimation for both traffic directions. Capacity is the function of selected effective green time, saturation flow rate, and cycle length. The effective green time is selected from step 4 after the minimum effective green time requirement is fulfilled. The cycle length utilizes the work zone length and ATS information to calculate the clearance time of the work zone for both directions. The saturation flow rate is found in Step 3. This capacity model is analogous to signalized intersection capacity determination techniques.

Step 6. Estimation of control delay and maximum queue length. The directional control delay is the summation of the uniform delay and incremental delay. The maximum queue length is estimated using the traffic demand, clearance time, lost times, and effective green time. HCM6 provides an equation for calculating the optimal green time at 1L2W work zones as discussed in Section 2.1 equation 2.1 (Schoen et al. 2015; Zhu 2015).

When researching the HCM6 methodology on lane closures at work zones, a few drawbacks were found.

1. The HCM simulation model uses a 5% truck percentage. However, the observed percent of heavy vehicles under Nebraska conditions ranged from 25% to 35%.
2. To incorporate the impact of trucks, HCM uses PCE which is based on a two-lane highway, not under work zone conditions.
3. The HCM assumes a saturation headway of 1.89 seconds, whereas the preliminary field observations ranged from 3.5 to 4.5 seconds.
4. The work zone travel speed, on average, was 20% to 30% slower than the HCM prediction.

5. The HCM6 optimal green time model does not consider the effect of traffic demand. The optimal green time is derived from a field study with a work zone length of 800 feet. Therefore, the use of the same signal timing for various ranges of traffic demand and work zone lengths may not necessarily maximize the operational efficiency (e.g., reduce delay and/or increase capacity). The classic pre-timed signal control models that can be adopted in determining the 1L2W work zone signal control plan (i.e., cycle length, green time) include 1) Webster model, which adjusts the lost time due to the work zone clearance time (Webster 1958); and 2) Schonfeld model, which is originally a queuing theory-based model (Schonfeld 1999) and can be used for a work zone signal timing plan. These three traffic control models may be adopted in different traffic volume scenarios (Hua et al. 2019). For a low or moderate volume, the flagger model and actuated signal control model perform better than the pre-timed signal control models. The flagger control model with optimized gap-out distance performs better in minimizing stop delay and queue length under low volume (less than 200 pcu/h/direction) or high volume (420 ~ 580 pcu/h/direction). The actuated signal control model performs better in minimizing queue length under moderate volume (220 ~ 400 pcu/h/direction). For a high-volume scenario where pre-timed signal control may be appropriate, the Webster model outperforms the Schonfeld model for vehicle throughput.

2.2.3 Work Zone Simulation Models

When field measurements of work zone performance measures for various traffic conditions are not feasible, often a simulation model is used to conduct an alternative analysis.

Simulation studies are beneficial to represent the stochastic nature of traffic found in a real-world situation. It is worth noting that, even though microsimulation models have been extensively applied for transportation-related studies, it has not been widely used in the case of two-lane work zone conditions.

With the help of simulation, vehicle delays, queue lengths, and capacity are typically modeled as a measure of the two-lane work zone performance (Cassidy and Han 1993). Using VISSIM, one of the most used microsimulation tools, Zhu modeled a flagger-controlled two-lane work zone (2015). A 300 feet gap-out distance (i.e., 300 feet sensor) was used to imitate the flagger behavior. The findings from the field calibrated VISSIM model aided to develop an analytical work zone model capable of estimating performance measures such as capacity, control delay, and average queue length. Another work conducted by Hua et al. used the VISSIM simulation model to estimate performance measures such as average delay, queue length, and throughput under different signal control techniques (Hua et al. 2019).

The impacts of the work zone on the capacity for a lane closure on a two-lane highway may also be simulated using FlagSim (Washburn et al. 2008). The FlagSim simulation model used a gap-out distance with a maximum green time of 300 seconds to imitate the distance gap method. Three flagging operations can be simulated: distance gap method, maximum queue length method, and fixed-timed method. Field data with a wide range of traffic conditions and impacts of grade are used (Watson et al. 2015) to calibrate the model. The FlagSim generated work zone traffic flow data are used to develop analytical models to calculate work zone travel speed, saturation flow rate, queue delay, and queue length. A common guideline of using microsimulation tools can significantly compensate for the underlying shortcomings.

The guidelines for applying traffic microsimulation modeling software provide approaches for developing and applying the microsimulation model to transportation analysis problems (Wunderlich et al. 2019). The overall goal of this guideline is to encourage comprehensive experimental design based on varying travel conditions, rather than using an "average" day. More emphasis has been put on selecting criteria statistically valid and derived from field observation. This process is considered in the calibration process adopted in this report. Among different criteria of applying different microsimulation software, the calibration can be considered the most crucial task for the analysis being trustworthy and reliable. The two-lane work zone can be modeled as a two-phase signalized intersection in simulation considering two critical aspects, 1) modeling of clearance interval without vehicular conflict, and 2) modeling of the right of way allocation technique similar to field observation. The NCHRP (Project 03-106) report provides a guideline for two-lane work zone calibration using VISSIM (Zhu 2015; Schoen et al. 2015). Calibration data typically involve speed, headway, travel time, average cycle length, and average stop time.

2.2.4 Work Zone Model Optimization

Optimization techniques are applied to work zone models to balance the trade-off between delay and operation costs. Typical optimization techniques may compare the queueing delay model and user/agency cost model to find the optimal strategy. These techniques often require accurate data collection before the model application (Huang and Shi 2008). Variables that can be optimized include:

(1) **work zone length;** a shorter length of work zone decreases the delay while increasing the operational cost. Capacity can be increased with relatively shorter work zone length in the

case of moderate to high traffic demand (Ceder 2000; Schonfeld and Chien 1999; Chen and Schonfeld 2007; Zhu 2015).

(2) **speed;** an increase in travel speed decreases the project cost (Chien et al. 2002). A higher travel speed within the work zone also increases the capacity (Zhu 2015).

(3) **traffic flow/headway;** higher headways cause the traffic flow to exceed work zone capacity (Huang and Shi 2008). Typically, high traffic flow is associated with adversely impacting the work zone performance measures.

(4) **cycle length;** a longer cycle length increases the delay cost while decreasing the operational cost (Schonfeld and Chien 1999). While a longer cycle length may increase delay, a shorter cycle length may cause occasional cycle failure and aggressive driving behavior.

(5) **control type;** to maximize the work zone operation, traffic signal assignment should be based on actual traffic demands (Zhu 2015). The actuated traffic signals maximize the green phases to leverage traffic demand from both directions, which may be an appropriate replacement for the flagger control method (Son 1999; Shibuya et al. 1996).

(6) **work zone duration/start and end time;** the optimal work zone durations and schedules vary dramatically with different input parameters (Chien et al. 2002). Thus, highway agencies need to consider maintenance breaks versus uninterrupted work when scheduling work zone activities and the tradeoff between the agency costs and the user costs.

2.2.5 Work Zone Traffic Analysis Tools

Optimization techniques are applied to work zone models to balance the trade-off between delay and operation costs. Typical optimization techniques may compare the queueing delay model and user/agency costs.

Traffic analysis tools help to strategize prior to starting a work zone and to monitor the work zone performance. The tools help the practitioner to estimate the mobility impacts of the work zone, which are crucial for assessments of factors such as safety, economic, and other work zone-related impacts (Hardy and Wunderlich 2008). Analysis tools associated with mobility impacts and road user costs can use a spreadsheet-based HCM method (FHWA WZ RUC 2011; Ellis et al. 1997).

Most of these spreadsheet-based tools are developed based on HCM methodologies or adapt the partial application of it. These tools mainly use traffic demand data and capacity to estimate the mobility impact, and they are often used for the early stages of a project as the tools often adapt a simplistic approach. Below are some of the most popular tools for analyzing work zone impacts on mobility and user cost.

- ***WorkZoneQ-Pro*** is a work zone software used for performance measures (e.g., capacity, speed, queue length) and user cost for lane closure cases for freeway and two-lane work zones. For two-lane highway lane closure, delay and queue length are computed based on the HCM6 methodology. However, the signal timing is not based on the HCM6 recommendation. Furthermore, travel speed estimations are not based on HCM6, as WorkZoneQ-Pro considers the effects of work intensity and the speed control techniques while estimating the travel speed. Three sources have been reported to form the user cost estimation: 1) FHWA Report on work zone road user costs, 2) American Transportation Research Institute Report, and 3) State DOTs default values.
- ***QUEWZ*** is a work zone road user cost estimation software tool used for freeways and was originally developed for Texas DOT (QUEWZ-98). The QUEWZ estimates costs for three segments of a freeway work zone, 1) the work zone itself (a freeway segment with

reduced capacity due to lane closures), 2) speed-change areas where vehicles decelerate to and accelerate from the work zone, and 3) a queueing area upstream from the work zone, where vehicles queue when incoming traffic demand exceeds the work zone's capacity (Ishimaru and Hallenbeck 2019).

- ***QuickZone*** is a sketch-planning tool developed by FHWA. QuickZone can estimate travel delay time, queuing, and delay costs per vehicle hour for roadway segments under the work zone and for the alternative segment. This tool uses a deterministic delay estimation algorithm to estimate traffic delays and queuing. While the interface is simple and easier to use, it may require more time and effort than similar spreadsheet-based tools (FHWA WZ RUC 2011; Edara 2006).
- ***CA4PRS*** (*Construction Analysis for Pavement Rehabilitation Strategies*), is a decision-support tool for transportation agencies that helps to select effective and economical strategies for highway maintenance and rehabilitation projects (CA4PRS Software FHWA, 2019). The software has three interactive analytical modules: 1) a scheduling module to calculate project duration, 2) a traffic module to quantify the impact (e.g., delay) of work zone lane closures on the traveling public, and 3) a cost module to estimate total project costs.

It has been shown that applying only deterministic approaches, as shown in most of the above-mentioned tools, always results in underestimating work zone delays (Chien et al. 2002). For example, Chitturi and Benekohal (2004) compared the output of QUEWZ and QuickZone with observed data from freeway work zones. The authors reported that when there is queuing QUEWZ overestimated capacity and when there are no queues, capacity is underestimated. QUEWZ also underestimated the observed average queue length and overestimated average

speed. For QuickZone, the authors reported that queue length and total delay were generally underestimated.

There have been several work zone evaluation methodologies proposed in the literature. One such typical example that NDOT usually refers to is the work zone queue length and delay methodology proposed by Chiturri and Benekohal (2010). The authors presented a methodology that can be used to quantify the mobility impact by considering the effects of cars and heavy vehicles' speeds and delays separately. The impact of the vehicle types on speed variation is used to compute the capacity of the work zone at operating speeds from speed-flow curves. Then the work zone queue length and delay (both moving delay and queue delay) are computed from the speed and capacity estimates. It is important to note that a deterministic procedure e.g., an input-output analysis is used to estimate the work zone queue delay, and the moving delay is computed from delay-based passenger car equivalent values for work zones. Also, the methodology might underestimate delays for non-breakdown conditions because the authors assumed that for no flow breakdown conditions vehicles will maintain speed at the upstream of the lane closure zone, which is atypical.

2.3 The Value of Travel Time

The value of travel time (VTT) is one of the most important conceptions in transport economics and its estimation has been the topic of extensive academic and applied work. It is widely used in transport policy analysis, such as high-speed rail construction, congestion costs, quality improvements to local bus service and inter-urban train services, and infrastructure improvements. It is also used in composing a generalized cost for use in forecasting travel demand. There is an agreement that the practice of most governments is to maintain a standard

VTT, which applies to all amounts of time, even if these could clearly be labeled as gains or losses.

The value of travel time for a particular individual may vary significantly based on some characteristics:

- The characteristics of the traveler (e.g., income level).
- The purpose and type of trip (e.g., commuting, personal, recreation, or business-related).
- Travel conditions (e.g., traffic congestion or poor weather).
- The transportation mode (e.g., bus, car, or walk).
- The time of trip (e.g., going home at the end of the day versus going to work in themorning).
- The length of travel (e.g., long or short distance).
- The location (intercity/interstate versus local trips or urban/rural).

The widely used theory of time allocation and how the value of travel time is estimated is often referenced to Becker (1965). In Becker's theory, time could be converted into money by assigning less time to consumption and more time to work, which describes economic decisions under limited time allocation. Therefore, the first concept of the VTT was that consumption has a time cost of not earning money (Jiang 2004). Different researchers employed different approaches for estimating the value of travel time. The first approach involved the development of a regression model to explain variations in the value-of-time estimates across studies as a function of important variables, such as journey purpose, mode used and mode valued, type of data, GDP, and distance. Waters (1995) analyzed an

international comparison of values of time.

However, a problem with this method is that collected variable data cannot possibly cover all sources of variation in the value of time; for example, researchers cannot control different income levels across studies, nor different sample selection strategies in general, and the estimated values of time may be a function of the size or sign of the time variation involved. However, the variables about which researchers have collected information are expected to represent the principal influences on the value of time, and it is assumed that the net effect of unexplained variation in the value of time is randomly distributed across studies and is accounted for by the regression model's error term.

For each value-of-time estimate, corresponding information was collected about the year and quarter of data collection and associated GDP and RPI, sample size, distance and whether the journeys could be classified as urban, suburban, or inter-urban, the type of data used in estimation, journey purpose, the choice context, the mode used and the mode valued, the location, the purpose of the study, and the means of presenting. Researchers conducted the national value of time studies in many countries (UK, Sweden, Finland, France, etc.) considered the experimental data collection methods such as stated preference and results based on conventional revealed preference method. Wardman (1987) conducted an empirical study using stated preference data to determine the distribution of individual values of time. Ahsen et al. (2002), Richardson (2004), Antoniou et al. (2007), Tseng and Verhoef (2008), and Xumei et al. (2011) also employed a stated preference approach for estimating VOT.

There are two other approaches to the valuation of travel time: revealed preference (RP), based on observation of alternative travel choices involving different costs; and stated preference (SP), based on hypothetical choices made by individuals of routes and modes, again

involving different costs, using market research type techniques. Merkert (2017) concludes that there seems to be anagreement in the literature that RP is more appropriate to evaluate willing-to-pay (WTP) for existing links while SP is more useful when evaluating hypothetical choice alternatives (such as the entry of a competitor or new product on certain routes) of existing or new links with significant changes in the levels of service and fares which are not observed in real markets. David Metz (2008) finds the RP valuations to be significantly larger than the SP valuations for both business and non-business trips.

Considering the value of travel time is calculated based on different angles, the summary of the main measurement methods is in Table 2.6.

Table 2. 6 The Main Measurement of the Value of Travel Time

Measurement	Description	Authors
Income	Treat the value of travel time as an increasing function of income levels	Athira et al (2014), Small et al. (1999), Mark Wardman et al. (2016)
GDP	Value of travel time is equal to the ratio of GDP per capita andworking time per capita	Lasmini Ambarwati et al. (2017), Weibin Kou et al. (2017), Mark.W. et al. (2016)
Regression estimation	Revealed preference (RP), basedon observation of alternativetravel choices involving different costs	David Metz(2008), Brownstone and Small (2005), Fezzi (2004)
	Stated preference (SP), based onhypothetical choices made by individuals of routes and modes,again involving different costs	Ahsen et al (2002), Richardson (2004) Antoniou et al (2007), Tseng and Verhoef (2008) and Xumei et al (2011), Algers et al (1998), Kouwenhoven (2018), Calfee (1998)

2.3.1 The Size and Sign of the Value of Travel Time

With regard to theory, the value of time will vary with the size and sign of the time variation if the utility function is non-linear with respect to time. In addition to constraints on

the transferability of time and rescheduling activities, the value of travel time can theoretically be defined as the opportunity cost of travel minus the direct utility from spending time during the trip (Kouwenhoven 2018). In this context, income is important in calculating the monetary value of travel time. The value of travel time is often reported as a percentage of the hourly wage to facilitate comparison across different studies. Johnson (1966) explaines that the reason why the value of non-work time equals the wage rate is the absence of work time in the utility function.

In many papers, the official appraisal practice in many countries increases values of time directly in line with income. Athira et al. (2014) reveal that income and trip length has a substantial influence on the value of travel time. As income increases, VOT also increases. However, Small et al. (1999) and MVA Consultancy et al. (1994) have concluded such reporting does not implicitly assume a relationship between the value of time and income through the surveys they conducted. In addition, Mark Wardman et al. (2016) provide a wealth of cross-sectional evidence indicating the income elasticity is somewhat less than one and there is lack of convincing support for the convention that treats VTT as hourly time. They developed a model to measure VTT via per capita gross domestic product (GDP) based on purchasing power parity (PPP) exchange rates (GDP_PPP). Weibin Kou et al. (2017) think VOT could be calculated by partial of the travel timechange and travel cost change. Lasmini Ambarwati et al. (2017) think the value of travel time is equal to the ratio of GDP per capita to working time per capita. Algers (1998) assumes the cost of travel equals labor income. Shires (2009) estimates an income elasticity of about 0.5 for business travel, 0.7 for commuting, and 0.5 for other passenger transport.

2.3.2 Gap between WTP and WTA Measures of Value of Travel Time

Some scholars analyze the value of travel time from the angle of WTP and WTA. As the normal definition, willingness to pay (WTP) is the maximum amount of money a consumer (a buyer) is willing to sacrifice to purchase a good/service or avoid something undesirable. In contrast, willingness to accept (WTA) is the minimum monetary amount a person is willing to accept to sell a good or service, or to bear a negative externality. In a Hicksian framework equivalent loss is associated with willingness to pay (WTP) and equivalent gain is associated with willingness to accept (WTA). The gap between equivalent loss and equivalent gain is explained by income effect (Willig 1976). When evaluating consumers' choices between different transportation alternatives, the value of time is a fundamental concept. The value of time is calculated as a trade-off ratio of the time coefficient to the cost coefficient. VTT depends on several parameters and varies from country to country, industry to industry, and even from individual to individual. Becker (1965) is probably the first to introduce the allocation of time over various activities in the analysis of consumer behavior, thus offering the micro-economic framework needed to establish the shadow price of time savings.

Some scholars report there are gaps between WTP and WTA in previous studies (Ramjerdiet al. 1997; Algers et al. 1998; Hultkrantz and Mortazavi 2001). However, these studies do not address the nature of these gaps. De Borger and Fosgerau (2006) recently examine the nature of the gaps between WTP and WTA measures of the value of time by using the theory of reference-dependent preferences, which is the first study that addresses the nature of WTP–WTA disparities in the value of time (Farideh Ramjerdi et al. 2007). Hanemann (1991) offers an alternative explanation and suggests the large gap between equivalent loss (EL) and equivalent gain (EG), and hence WTP and WTA, can be explained by income and

substitution effects. Zhao and Kling (1998) look into real options for explaining the gap. They suggest that observed WTA and WTP diverge from equivalent loss and equivalent gain can be explained by commitment costs. Using data collected for the 1994 Swedish Value of Time Study, Farideh Ramjerdi et al. (2007) examine the evidence on the WTP and WTA gap in the Swedish Value of Time and explained WTA estimation is usually bigger than WTP.

2.3.3 The Value of Travel Time Savings

Some researchers estimate VTT via VTTS (value of travel time savings). VTTS can be defined as the willingness to pay for time reallocation between two alternative activities (Huq, 2007). The VTTS is usually derived as the marginal rate of substitution between travel time and cost coefficients, typically as found in discrete-choice models of stated-preference data, revealed-preference data, or a combination of these (e.g., Small et al. 2005). Jiang (2004) interprets the VTTS as consisting of the value of re-assigning time to other activities, as well as the value of the direct change in the utility of travel. Therefore, the VTTS is relevant to the following factors: 1) alternative uses of the saved time to other activities, 2) travel environments, and 3) individual socioeconomic environments. But Andrew Daly (2019) thought VTTS is misleading in estimating VTT since that unlike money, time cannot be stored or borrowed.

2.3.4 Meta-analysis in Value of Travel Time

Many scholars employ meta-analysis in transport research trying to go beyond traditional literature reviews that just list findings of previous papers, especially in recent years. Shires (2009) defines meta-analysis as the statistical analysis of analyses. A number, usually large, of previous research studies is analyzed using statistical methods. Button (1995) uses 29 observations and explained the VTTS from travel purpose, mode, and country group in a linear

regression. None of these variables emerged as statistically significant, which may result from the small sample size. Rietveld (2000) carries out a regression analysis to apply meta-analysis to explain price elasticities of transport demand (various modes). Wardman (2004) performs a regression analysis explaining the natural logarithm of the VTTS, which obtained many significant coefficients (travel purpose, mode, distance class, GDP, stated versus revealed preference). Shires (2009) conducts an international meta-analysis of the value of travel time and finds significant effects for purpose (business, commuting). Comparisons with existing literature suggest that the results derived from the meta-analysis might prove a useful tool for the estimation of the value of travel time where it is not possible to estimate it by direct methods.

3 WORK ZONE SIMULATION MODEL DEVELOPMENT FOR NEBRASKA

The state-of-the-art literature review presented in Chapters 2 and 3 on work zone traffic control techniques and the existing traffic operation analysis models and tools show that:

- The most common practice for a two-lane highway work zone operation control is the human flagger technique, with or without the help of a pilot car. Human flagger operation is mostly based on the concept of the actuated signal control technique and thus can be modeled as a two-phase actuation traffic control using microsimulation.
- Intelligent or smart work zone systems are used to control freeways or multilane highway work zones and to provide real-time actionable information to approaching drivers. The automatic queue detection system is one type of smart work zone setup that has been promoted by the FHWA because it has been shown to successfully reduce the average travel speeds and their variations. Therefore, multilane work zones can be modeled by mimicking vehicle speed reductions using microsimulation
- However, simulation guidelines for work zone model calibration are not adequately addressed. Additionally, the recommendation of many existing models for work zone travel speed and optimized signal timing allocation warrants further validation.

A typical way to model work zone operations, as recommended in the HCM6, is to investigate the impacts of various factors on work zones using a microsimulation platform with the aid of a robust empirical data. Therefore, this chapter explains how a traffic microsimulation model was developed and calibrated under Nebraska conditions for both multilane/freeway work zones and two-lane highway work zones. It should be noted that each section of this chapter

constitutes a technical paper peer-reviewed and presented at the 101st Annual Meeting of the Transportation Research Board.

3.1 Calibration & Validation Method for Simulation Models of Intelligent Work Zones

Work zones have become an essential and integral feature of U.S. highways. A work zone is set up when there is a need for resurfacing, restoration, or rehabilitation on an existing roadway, which usually requires the closure of a traffic lane. The goals of work zone management are to 1) maintain an efficient flow of traffic, and 2) decrease, and hopefully eliminate, the risk of injury and death to construction workers and the traveling public.

Traditionally, the upstream of the work zone is equipped with static message signs that convey advance notifications or visual guidance to drivers. However, static signage cannot provide motorists with real-time information on expected queuing, travel time, delay, or speed at the work zone. This is particularly problematic if the roadway geometry is such that drivers cannot see downstream queues or when the queues extend upstream to locations that drivers may not expect to find them.

To overcome these issues, intelligent work zone (IWZ) systems have been adopted over the last two decades. The basic characteristics of these IWZ systems are that they need to be automated, reliable, and portable. In addition, they should have the ability to obtain and analyze current work zone traffic conditions in real-time and communicate actionable information to motorists.

One IWZ that has been deployed recently is automatic queue detection (AQD) systems. A typical AQD system includes detectors for speed detection near the taper of the work zone and a portable dynamic message sign (PDMS) upstream of the work zone. A computation algorithm

is used for processing speeds to identify certain traffic conditions (e.g., slow-moving or stopped), and to feed the upstream PDMS with predefined warning messages. In this way, motorists will be forewarned when they encounter slower traffic and/or queued vehicles downstream.

Several studies have concluded that AQD systems effectively improve mobility and safety (Hourdos et al. 2017). In addition, many state Departments of Transportation (DOTs) have adopted guidelines for implementing AQD systems at work zones (Hourdos et al. 2017; Roelofs and Brookes 2014; Pesti et al. 2018; Ullman and Schroeder 2014; Hallmark et al. 2020; Domenichini et al. 2017; Bham and Leu 2018). Not surprisingly, the use of AQD systems has become increasingly popular over the past decade. However, some design features including the location of the detectors, the spacing of the dynamic message signs, and the effectiveness of the warning system vary across state DOTs because a consensus on best practices has not yet been achieved by the transportation engineering profession (Huebschman et al. 2003; McCoy and Pesti 2002; Strawderman et al. 2013; Khazraeian et al. 2017).

The application of microsimulation models, for the analysis of complex issues such as the IWZ systems, has become a common practice in transportation engineering because of their convenience and cost-effectiveness (Appiah et al. 2012; Zaidi et al. 2012; Pesti et al. 2013; Appiah et al. 2011). This is particularly true in situations where designed experiments are impossible to conduct because of ethical considerations. As an example, conducting a designed experiment on where to best locate PDMS and what message to display on them would open the DOT to liability issues in the case of a serious car crash that resulted in injury or death. Consequently, almost all field AQD research is based on observational studies.

Interestingly, there has been no study that involves the use of calibrated and validated microsimulation tools to analyze the effectiveness of speed reduction strategies used in the freeway AQD systems. It is hypothesized in this research that a well-calibrated microsimulation model will be useful for studying the traffic impact of AQD systems and, potentially, help identify where the AQD system components should be placed.

The objective of this section is to develop a guideline for calibrating and validating a microsimulation model that can be used to perform replicable, reliable, and detailed analyses of the AQD system at freeway IWZs. Specifically, the section will first introduce the field deployment of AQD systems. Then, a general process of the simulation development and calibration for the AQD system is provided. Next, a test site is selected to demonstrate the calibration process and validation results. Finally, a discussion and recommendations are provided at the end of the section.

3.1.1 Multilane Work Zone AQD Traffic Simulation Model Development

The initial development of the simulation model includes developing a basic model of a generic AQD work zone including lane geometry and configuration, work zone merging locations, initial speed distributions by vehicle type, traffic demand, etc. The second step is to code the AQD system logic within VISSIM using the VisVAP. This is done through a series of surrogate settings. First, a pair of loop detectors are placed in each lane at the beginning of the work zone taper. Then, two desired speed decision points are added upstream of the loop detectors at two locations, as shown in Figure 3.1. The distances of the two locations from the detectors, *d1* and *d2*, correspond to the actual distances of the two PDMS sets to the field detectors, respectively.

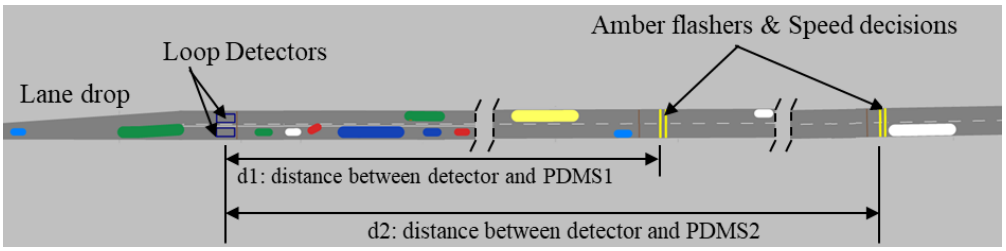

Figure 3. 1 AQD system realization in simulation

In the simulation model, a flashing amber signal is used to assist the analyst in identifying what message would be displayed on the PDMS under the current speed conditions. The flashing amber, whether it is active or not, does not affect the simulated drivers' speeds.

Intuitively, for the simulation model to accurately represent reality, the model has to replicate what drivers do when they encounter a given PDMS message. Essentially, the driving behavior in response to the PDMS warning message is achieved through the use of desired speed distributions input by the users. Note that the desired speed refers to the vehicle's operational speed that is not being impeded by another vehicle. For a given vehicle, the actual operating speed may be influenced by other vehicles in its near vicinity. Therefore, the distribution of the desired speeds at each PDMS location needs to be obtained such that the distribution reflects free-flow traffic at that location. The method for ensuring this will be discussed in detail later in the section.

3.1.2 Simulation of the AQD System Using VAP

In this study, the AQD system logic, as shown in Figure 3.2 (a), is coded using the VisVAP application. VisVAP is a graphical editor that has the ability to retrieve information (e.g., instantaneous vehicular speed) from the virtual loop detectors in the VISSIM model as the simulation model is running. It then uses the information to ascertain current conditions (e.g.,

average traffic speed), which is then used to identify which desired speed distribution the simulated vehicles will follow. There are three critical components to the AQD system logic as seen in Figure 3.2 (b). The three parts are discussed in detail below.

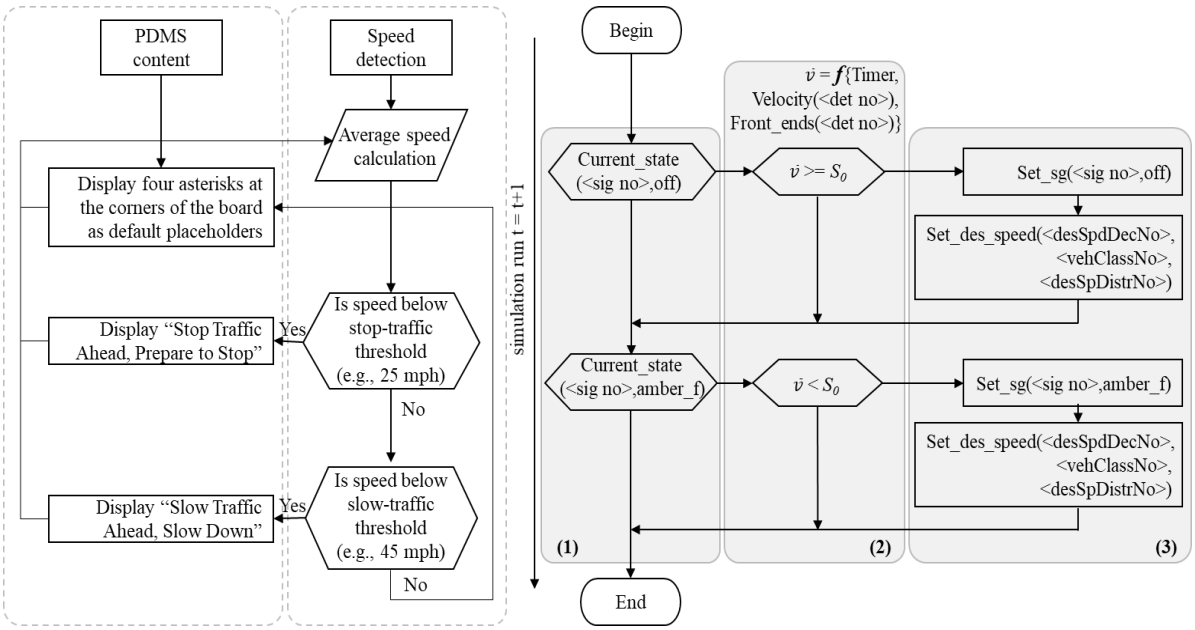

(a) AQD system logic (b) VAP realization codes

Figure 3. 2 Flowchart of the AQD system algorithm.

1. Signal states check

In this section, the flashing amber is used to identify the current signal states (e.g., on/off) in the VAP logic. More importantly, the flashing amber is used as a substitute for the warning message displayed in the simulation. This flashing amber allows a user to monitor whether the warning message is activated or not as the simulation runs.

As illustrated in Figure 3.2, at each step of the simulation run, the flashing amber should always be in one of two states: on and off. Specifically, when the flashing amber is in the "off" state, no warning message is deemed to be posted in the simulation model. However, when the flashing amber is in the "on" state, it visually indicates that one of the two warning messages is activated. The current traffic condition (e.g., speed) is estimated at each time step to determine which desired speed distribution the vehicles should follow and whether the flashing amber should be activated.

2. Travel speed conditions

The loop detectors in VISSIM are able to collect various types of data such as speed, count number, headway, and the presence and occupancy of a vehicle. These data are used within the simulated AQD evaluation system to identify current speed conditions, identify what message to present on the PDMS, and identify desired speed distribution to use at the PDMS locations in simulation. The rolling-average speed, where the average is taken over K minutes, is estimated in VisVAP using Equation 3.1.

$$\bar{v}_t = \frac{\sum_{i=t-K}^{t-1} v_i}{K}, \forall\, t = 1,\ldots, \mathrm{T} \qquad \text{Eq. 3.1}$$

where,

K	Duration of rolling average speed (minutes)
$\bar{v}_t$	K-minute rolling average speed at time period t (mph)
vi	Average speed of vehicles during time period i (mph)
T	Number of time periods

The rolling average speed $\bar{v}_t$ is then compared to a speed threshold S0, which is defined according to the traffic conditions at the work zone (i.e., free-flow, slow-moving, or stopped traffic). Note that currently, the NDOT AQD system assumes the speed threshold (S0) is 45 mi/h. This value can be identified on a site-by-site basis.

As an example, for the NDOT AQD system, the rolling average speed is taken over *K=3* minutes. When the estimated average speed value $\bar{v}_t$ is greater than S0 then it is assumed that there is no congestion and the PDMS does not display a message.

3. Desired speed distribution

In VISSIM, vehicles are assigned speeds at the location where the user indicates the use of a "desired speed decision". The simulated vehicles will follow, if possible, the desired speed distribution defined by the user. The goal is to reflect actual driver behavior when the drivers "see" a given message on the PDMS.

It is important to note that the quality of the desired speed distribution affects the accuracy of the microsimulation results. Therefore, it is critical the desired speed distributions should reflect the actual conditions at the work zone. For example, consider a situation where drivers in the field are observed to slow down an average of 5 mph when seeing a warning message. If drivers in the simulation are modeled as slowing down an average of 10 mph when the message is active, the results show the AQD system operating better than it would in the field.

By definition, the desired speed distributions should be obtained from empirical observations of free-flowing vehicles in the field. This is because VISSIM uses this information

to model what the drivers would do when they are free to choose their speeds in the absence of any other vehicles. Similarly, the modeler should know the desired speed distribution associated with each message that is displayed on the PDMS. This would also be collected from field data under free-flow conditions.

Once these distributions are obtained, each one is input into VISSIM using a cumulative distribution function disaggregated by vehicle type (e.g., passenger cars (PCs) and heavy vehicles (HVs)). In summary, for the Nebraska AQD system, there is a total of six desired speed distributions for an AQD simulation model: two for each PDMS location, two for each message display (e.g., warning or no warning message), and two for each vehicle type. These desired speed distributions are based on empirical measurements at the site.

3.1.3 AQD Work Zone Model Calibration

This study follows a standard microsimulation model calibration protocol (Schoen et al. 2015; Wunderlich et al. 2019). Specifically, a 15-min warm-up time is used, which is about twice the free-flow travel time on the entire road network. This provides enough time for the network to reach steady-state conditions. Five different random seeds are used to replicate the simulation scenarios for each combination of parameters to be calibrated. The average of the five simulation runs is then compared to the field data.

Three sequential steps are used for model calibration, which is, to estimate the desired speed distribution data, modify the car-following headway data, and finally calibrate the HV acceleration/deceleration parameters. These three steps are discussed as follows:

Step 1: Estimate the desired speed distributions. It is assumed drivers respond to the warning display (e.g., begin to slow down) immediately when they pass through the PDMS location. In this study, this means as vehicles pass through the PDMS they are assigned a desired speed that follows a specific desired speed distribution. In this section, it is assumed that the underlying desired speed distribution is normal with a mean of $\hat{\mu}$ and a standard deviation of $\hat{\sigma}$ (i.e., $N(\hat{\mu}, \hat{\sigma})$). The desired speed distributions are obtained from the field data when the traffic is under free-flow conditions. It should be noted the speed distributions are disaggregated by vehicle type (e.g., car and trucks) because it has been shown in the Western U.S. free flow speeds can vary greatly according to vehicle type (Zhou et al. 2019; Hurtado and Rilett 2021). In addition, the desired speed distributions are disaggregated by locations (i.e., PDMS1 vs. PDMS2) and by displayed messages (i.e., SLOW vs. STOP). In summary, the simulation model requires six-speed distributions, and each of these are based on empirical studies conducted on the test bed.

Step 2: Measure empirical car-following headways. Three parameters that directly contribute to the safety distance of car-following are the focus of the calibration step. These aree selected based on the literature review which indicated they have a great impact on the VISSIM driver behavior in work zones (Dong et al. 2015; Jehn and Rod 2019; Yeom et al. 2016). They are: 1) the standstill distance CC0, in feet, which refers to the desired minimum distance between two standing vehicles (i.e., lead and following) when both are stopped; 2) the time headway CC1, in seconds, which refers to the desired time between the lead and following vehicles; and 3) following variation CC2, in feet, which refers to the longitudinal oscillation as a driver moves closer to the lead vehicle. The safety distance is defined in VISSIM as the minimum distance a driver will keep in the car-following status. The minimum safety distance is a function of CC0

and CC1 at a given speed v. The third parameter, CC2, is used to represent a static buffer. The car-following distance *dx_safe* variable is a function of all three parameters as shown in Equation 3.2.

$$dx\_safe = cc0 + 1.47 * v * cc1 + cc2 \quad \text{Eq. 3.2}$$

This study focused on calibrating the desired time headway *CC1* because it has the greatest influence on car-following behavior (Dong et al. 2015). A previous study recommended that using the empirical headway distribution to calibrate the model would be ideal (Jehn and Rod 2019). In other words, the calibration step will attempt to identify parameter values CC0, CC1, and CC2 such that the resulting simulated headways and empirical headways are equivalent.

The empirical headway is defined as the time difference between any two successive vehicles from the same lane when they cross a given reference line, which is calculated using Equation 3.3.

$$h_{ij} = T_{ij} - T_{i(j-1)} \quad \forall j = 1, \ldots, J \quad \text{Eq. 3.3}$$

where,

i = lane number

j = vehicle number, the vehicle j is behind the vehicle (j-1)

h_{ij} = headway of vehicle j in lane i, seconds

T_{ij} = timestamp at the reference line of vehicle j in lane i, seconds

The headway measured in the field cannot be directly applied to the model. This is because, in VISSIM, *CC1* represents the time gap between the first vehicle's rear bumper and the successive second vehicle's front bumper in the same lane. In other words, *CC1* does not include the time for the vehicle to clear the reference line. Thus, the distribution of *CC1* is identified from the empirical headways using Equation 3.4.

$$cc1_{ij} = h_{ij} - \frac{L_{i(j-1)}}{V_{i(j-1)}} \quad \forall j = 1, \ldots, J \qquad \text{Eq. 3.4}$$

where,

$cc1_{ij}$ = *CC1* for vehicle *j* in lane *i*

$L_{i(j-1)}$ = the length of the front vehicle *j-1* in lane *i*

$V_{i(j-1)}$ = the speed of the front vehicle *j-1* in lane *i* at the reference line

Apart from *CC1*, the parameters *CC0* and *CC2* are also closely related to the car-following headway. It is hypothesized that *CC0* and *CC2* will be larger than, or at least equal to, the default values under work zone conditions (Yeom et al. 2016). In this section, the parameters *CC1*, *CC0,* and *CC2* were identified from empirical observations. Note they could also be part of the calibration step.

Step 3: Calibrate HV acceleration parameters. The default acceleration curves for simulating HV movements in VISSIM are based on data from Western European conditions. It is hypothesized this assumption might not be directly applicable to modeling the U.S. HV fleet

(Jehn and Rod 2019). Therefore, it is decided to calibrate the acceleration parameters, including deceleration, to reflect the HV characteristics at the test site.

In VISSIM, the default desired acceleration of HV is modeled as a distribution where the acceleration is a function of HV speed. Equation 3.5 shows the functional form for modeling the relationship between the desired acceleration, $f_a(v)$, and the vehicle speed v (Appiah et al. 2012). Similarly, the desired deceleration, $f_d(v)$, is modeled as a constant function in VISSIM, which can be expressed using Equation 3.6.

$$f_a(v) = \begin{cases} k_1 & 0 \le v < c \\ k_1 e^{-k_2(v-c)} & v \ge c \end{cases} \quad \text{Eq. 3.5}$$

$$f_d(v) = \varphi \quad \text{Eq. 3.6}$$

where,

k_1 = scale parameter, ft/s^2

k_2 = growth rate, h/mi

c = shift parameter, mph

φ = constant value, ft/s^2

In VISSIM, the default values of parameters k_1, k_2, and c for HVs are 2.5 ft/s^2, 0.03 h/mi, and 20 mph, respectively, according to the curve fitting in Equation 3.5. The default value of parameters φ for HVs is -1.25 ft/s^2.

Consequently, this study considers the four parameters related to HV acceleration and deceleration functions (k_1, k_2, c, and φ) as unknowns that need to be calibrated. The objective of the calibration procedure is to minimize dissimilarities between field observed data and simulation output data, which can be expressed using Equation 3.7.

$$min\{f(x)\}, x = (k_1, k_2, c, \varphi) \quad \text{Eq. 3.7}$$

The search for the optimal combination of the parameter vector (k_1, k_2, c, φ) is based on a complete enumeration approach until a minimum value of $f(x)$ is reached. It should be noted that an automatic algorithm may become necessary for parameter optimization when the objective function is complex with more parameters and thus the search space is large.

The above objective function is, by definition, related to a measure of accuracy. In this section, the Root Mean Square Error (RMSE) statistic is used to determine the calibration accuracy. The RMSE statistic calculates the difference between the empirical data and simulated output, given a time interval (e.g., 15 minutes), which is expressed in Equation 3.8.

$$RMSE = \sqrt{\frac{1}{T}\sum_{t=1}^{T}\left(\frac{\frac{1}{N_t}\sum_{n=1}^{N_t}E_{nt} - \frac{1}{N_t'}\sum_{n=1}^{N_t'}S_{nt}}{\frac{1}{N_t}\sum_{n=1}^{N_t}E_{nt}}\right)^2} \quad \text{Eq. 3.8}$$

where

E_{nt} = the empirical measure of n-th vehicle during t-th time interval (s)

S_{nt} = the simulated measure of n-th vehicle during t-th time interval (s)

t = time interval, $t = 1, 2, \ldots, T$

n = vehicle number, $n = 1, 2, \ldots, N_t$

N_t = total number of vehicles in t-th time interval

In this section, the calibration objective is controlled such that an optimal set of values for parameter vector (k_1, k_2, c, φ) will satisfy both min{RMSE(k_1, k_2, c, φ)} and RMSE(k_1, k_2, c, φ) < 20% based on previous best practice as described in the literature (Lu et al. 2014; Kan et al. 2019).

3.1.4 Multilane Case Study

In this section, a field intelligent work zone (IWZ) test site with AQD systems on a freeway is selected to demonstrate the simulation calibration process. The test site, on the westbound I-80 located near Waco, Nebraska, is a four-lane freeway, with one lane closed. The work zone is approximately four miles long, starting at mile-marker 365.4 and ending at mile-marker 361.4, and is active from April through October 2020. The original (e.g., non-work zone) speed limit is 75 mph. A 65-mph speed limit sign is set up at two miles upstream of the work zone and the speed limit is reduced to 55 mph at the taper of the work zone. Once the work zone ended the speed limit returns to 75 mph.

The test site is equipped with a standard NDOT AQD system. A microwave Doppler radar detector is located at the taper of the work zone (detector mile-marker = 365.4). in addition, the first pair of the PDMS1 sets and the second pair of the PDMS2 sets are located 1.2 miles and 3.2 miles, respectively, upstream of the detector on both sides of the road (PDMS1 mile-marker = 366.6 and PDMS2 mile-marker = 368.6).

The AQD systems at the test site provide three types of data. First, the average speed, number of vehicles, and other data (e.g., vehicle class, headway) are obtained by the detector at the work zone taper. Second, the warning message and duration of any changes are obtained by the PDMS sets located upstream of the work zone. Third, surveillance cameras near the work

zone merging area are also available which allows the researchers to visually check the work zone operations.

In addition to data provided by the AQD system, an additional data collection effort is conducted by the research team. The goal is to obtain data including traffic counts, vehicle headways, and travel time at or near the two upstream PDMS sets, respectively. As shown in Figure 3.3, three Miovision Scout kits, each including a camera and a WiFi receiver, are installed 0.5-mile upstream, 0-mile, and 0.5-mile downstream of the PDMS that are marked as locations A, B, and C, respectively. The 0.5-mile spacing is chosen based on past data collection experiences and engineering judgment in that this spacing is long enough to capture the variability in speeds over space.

It should be noted the Miovision Scout kits "ABC" are installed in two phases: phase 1 from September 2 to September 5, 2020, for data collection at the PDMS2, and phase 2 from September 8 to September 11, 2020, for data collection at PDMS1, respectively. In this study, data from PDMS2 on September 3, 2020, and PDMS1 on September 9, 2020, are selected and processed to obtain traffic counts, vehicle headways, and travel time at 15-min time intervals from 8 am to 8 pm.

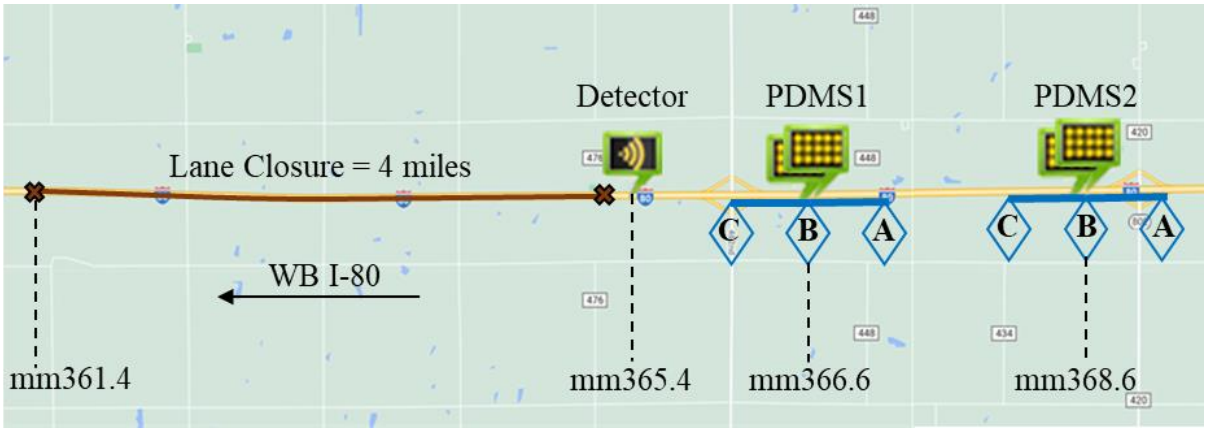

Figure 3. 3 The layout of the AQD System and Data Collection at the Waco IWZ Test Site (mm = mile-marker)

To obtain travel time, all the three Miovision Scout kits at stations A, B, and C are used. Each Miovision Scout kit includes a WiFi receiver to capture MAC addresses from the moving vehicles on the road. The travel times, i.e., time differences, on segment AB and segment BC represent the traffic performance when vehicles traveled before and after the PDMS, respectively. An automatic MAC address matching algorithm is developed to obtain the segment travel time. Meanwhile, the research team also measures the segment travel time using the Miovision Scout cameras at each station.

Specifically, five vehicles are randomly selected at a 15-min interval to manually match the video footage and calculate the travel time, which provides "ground truth" data to verify the large amount of travel time data obtained from the MAC address matching method. The Welch Two Sample t-test rejects the hypothesize that the means of travel time obtained using the two methods are different at the 0.05 significance level at both PDMS1 (on segment AB: t-stat = 0.18, p-value = 0.855; on segment BC: t-stat = 0.19, p-value = 0.856) and PDMS2 (on segment AB: t-stat = 1.39, p-value = 0.164; on segment BC: t-stat = 0.96, p-value = 0.337). This indicates the validity of the large amounts of travel time obtained using the media access control (MAC) matching algorithm.

To obtain vehicle headways, 10 to 15 successive vehicles, in each lane, are measured at station B when their front bumpers pass the same reference line in the video. A maximum headway is defined in order to classify whether a vehicle is in "free flow" condition (e.g., not affected by other vehicles). In other words, the headway data is deemed valid when there is no slow traffic queued up to any of the PDMS and drivers are in a free speed choice when they pass through the PDMS. In this study, traffic conditions at the PDMS location when i) 15-min flow rate less than 1000 passenger car per hour per lane and ii) speed drop less than 25% of the free-flow speed are used to determine the free-flow traffic at PDMS locations (Dong et al. 2015; Transportation Research Board 2010). Finally, the filtering condition resulting in the maximum headway for PCs and HVs are six seconds and eight seconds, respectively.

At this test site, the AQD system is initially designed to convey three types of messages to the public for three traffic conditions, i.e., no warning, slow traffic warning, and stop traffic warning. Unfortunately, the detected speed data is accidentally truncated at 27.5 mph due to the temporary failure of detector firmware during the data collection period. Because of this, there are only two types of message status the PDMS displays, namely 1) the "no warning" status that does not display any warning message, and 2) the "warning" status that only reflects a slow traffic status, regardless of whether a stop traffic warning is required. These two PDMS displays are triggered according to the speed threshold S_0 = 45 mph, as can be seen in Figure 3.3.

3.1.5 Multilane Simulation Model Input

Apart from the basic model input with empirical data from the test site (e.g., traffic volume, HV percentage, etc.), it is argued in this section that information related to the desired

speed distribution and car-following headway are critical input requirements of the simulation model. These two steps are indispensable before conducting the model calibration.

1. Desired speed distributions

The empirical travel speeds on segment AB (before PDMS1 or PDMS2) and segment BC (after PDMS1 or PDMS2) are obtained through the measured length of the road segment dividing the segment travel time, respectively. The mean and standard deviation of travel speed samples are listed in Table 3.1.

Table 3. 1 Desired Speed Distribution

	Mean (mph)		Std. dev. (mph)		Sample size		$N(\hat{\mu}, \hat{\sigma})$
	S_{AB}	S_{BC}	S_{AB}	S_{BC}	S_{AB}	S_{BC}	S_B (mph)
No warning message scenario							
PDMS 1	68.1	64.4	3.6	4.1	1242	1148	(66.3, 3.85)
PDMS 2	71.4	68.2	4.4	4.9	2511	2719	(69.8, 4.65)
Warning message scenario							
PDMS 1	57.6	51.6	4.1	2.8	325	319	(54.6, 3.45)
PDMS 2	70.9	65.7	5.0	5.8	1068	1205	(68.3, 5.40)

It may be seen in Table 3.1 that the average traffic speeds are higher around PDMS2 than around PDMS1 (i.e., 69.8 > 66.3 mph under no warning scenario, and 68.3 > 54.6 mph under warning scenario). It is hypothesized this occurred because the work zone speed regulations are reduced from 75 to 65 mph in the road segment where the PDMS2 is located and reduced from 65 to 55 mph in the road segment where the PDMS1 is located.

More importantly, at both PDMS1 and PDMS2 locations, the average traffic speeds when there is no warning message are higher compared to the average traffic speeds when a warning message is on display (i.e., 66.3 > 54.6 mph at PDMS1, and 69.8 > 68.3 mph at PDMS2). This is

evidence the warning message displayed on the PDMS is functioning as intended: when a warning message is provided, the traffic speed, on average, is reduced.

To incorporate the speed obtained from the segments before and after the PDMS, the average values of the means and standard deviations from segment AB and segment BC are calculated respectively. The results are listed in the last column in Table 3.1. It is hypothesized that the desired speeds (S_B) at PDMS locations are normally distributed, i.e., $S_B \sim N(\hat{\mu}, \hat{\sigma})$. Therefore, four desired speed distributions constructed using S_B data, i.e., warning and no warning scenarios at PDMS1 and PDMS2, respectively, are configured as the input of the simulation model.

2. Car-following headways

According to Equation 3.4, *CC1* is adjusted so that the empirical headway excludes the vehicle's passing time (i.e., vehicle length divided by its speed). In this study, an average vehicle length of 12 ft and an average speed at each of the two PDMS (i.e., S_B) is used to calculate the adjustment. The distributions of the empirical headway used as CC1 for PCs and HVs at PDMS1 and PDMS2 are shown in Figure 3.4.

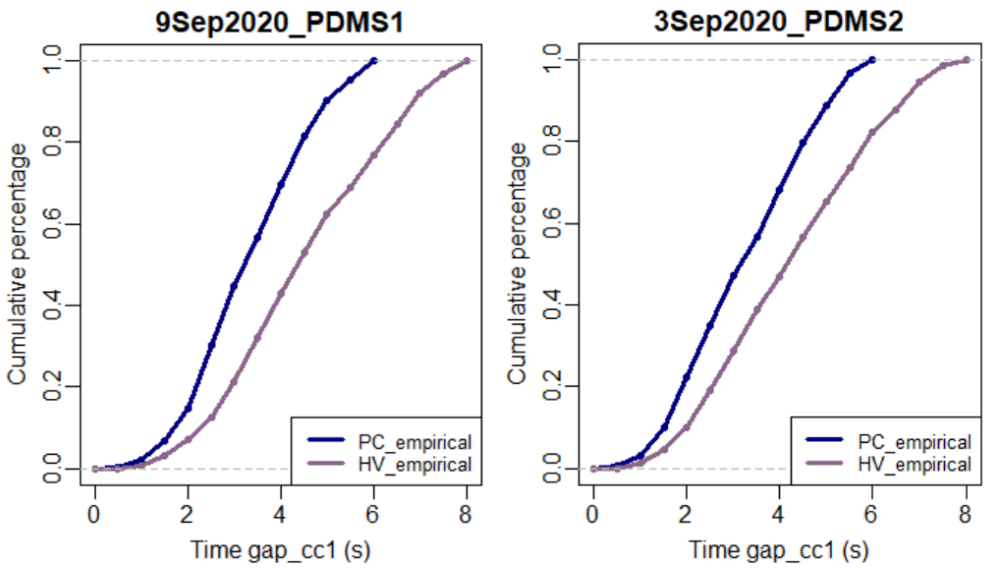

(a) Distribution of CC1 at PDMS1 (b) Distributions of CC1 at PDMS2

Figure 3. 4 The Empirical Distribution of CC1

In addition, *CC0* and *CC2* are obtained according to the literature search. Specifically, CC0 is set as 10 ft based on a project conducted by Dong et al. (2015), who found that CC0 ranges from 8 ft to 12 ft using field data collected on I-80 in Iowa. In addition, CC2 is set as 20.31 ft based on the recommendation of the FHWA Traffic Analysis Toolbox (Wunderlich et al. 2019). To obtain a more accurate calibration model, it is recommended to collect CC0 and CC2 per test site when conditions permit. Alternatively, these parameters may also be part of the calibration process if the user is not comfortable using parameter values obtained elsewhere.

All other VISSIM car-following parameters (i.e., *cc3* - *cc9*) are kept at their default levels (Wunderlich et al 2019). Note the variables chosen are based on past calibration experience and have the largest impact on work zone behavior (Dong et al. 2015; Jehn and Rod 2019; Yeom et al. 2016). It is important to note that the exact car-following parameters are site-specific. A user

may choose to calibrate or modify any of the microsimulation parameters as part of the calibration methodology without a loss in generality.

3.1.6 Multilane Calibration Parameters

In this case, the travel times at Segment AB and Segment BC are used to search the optimal parameter sets (k_1, k_2, c, φ) for the calibration of the HV acceleration characteristics. Figure 3.5 shows the travel time obtained from the automatic MAC address matching method and the video manual matching method in grey dots and blue dots, respectively. Specifically, the travel time collected at PDMS1 under a scenario of the work zone with congested traffic is shown in Figure 3.5 (a), while the travel time collected at PDMS2 under a scenario of the work zone with free-flow traffic is shown in Figure 3.5 (b).

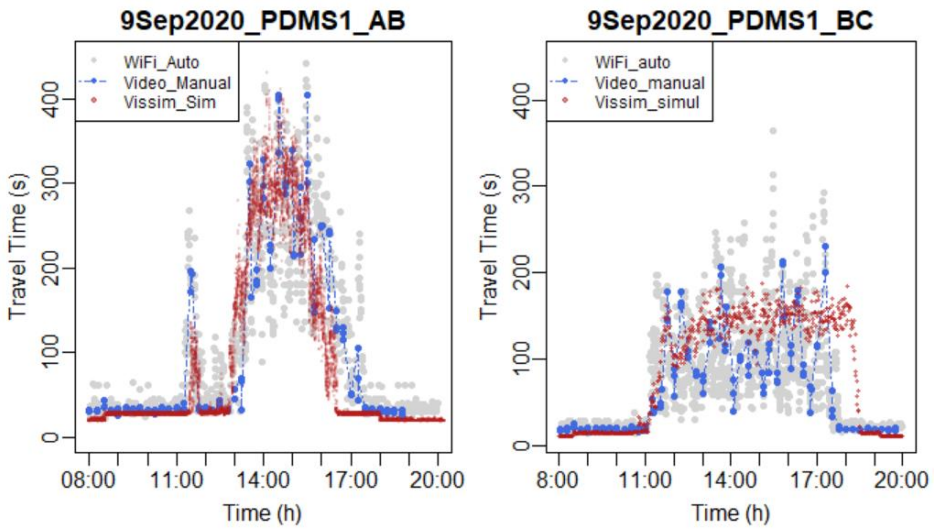

(a) Travel times before PDMS1 (AB) and after PDMS1 (BC) under congested traffic

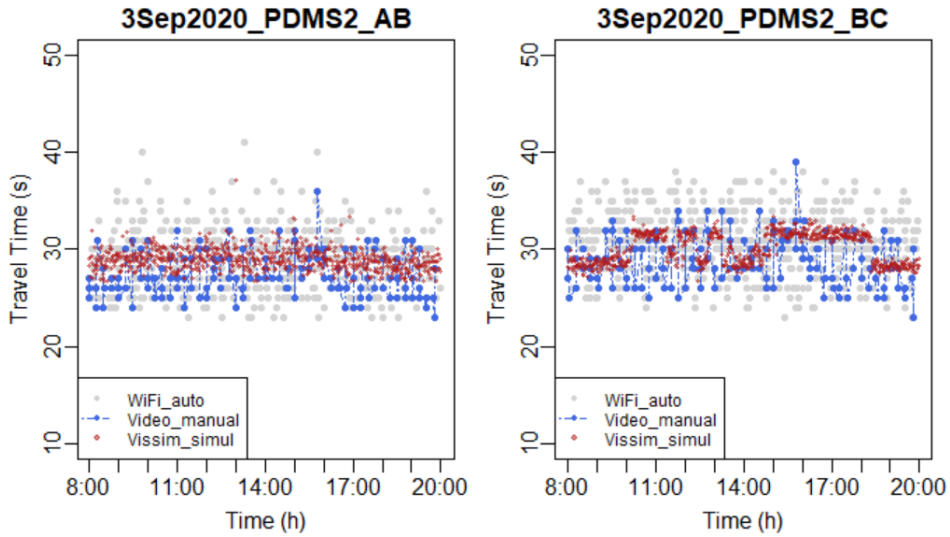

(b) Travel times before PDMS2 (AB) and after PDMS2(BC) under free-flow traffic

Figure 3. 5 Segment Travel Time Calibration Results.

This study considers reasonable search ranges that k_1 is [2, 14] ft/s^2 with an increment of 3 ft/s^2, k_2 is [0.03, 0.07] h/mi with an increment of 0.01 h/mi, c is [0, 20] mph with an increment of 5 mph, and φ is [-8, 0] ft/s^2 with an increment of 4 ft/s^2. The four sensitive parameters and their acceptable ranges construct a combination of 75 scenarios. As five runs for each scenario are performed, it results in a total of 375 simulation runs.

The simulated travel time from a scenario that generated the lowest RMSE is marked as red dots and superimposed on the field data in Figure 3.5. The travel time obtained from the VISSIM simulation output is compared to the travel time obtained using Miovision WiFi automation. The Welch Two Sample t-test rejects the hypothesis that the means of travel time obtained using the two methods are different for both PDMS1 and PDMS2 at the 0.05 significance level. The results indicate the calibration is promising.

3.1.7 Multilane Calibration Results

The scenario that generates the minimum RMSE, representing the least discrepancy between the simulation model and the field observation, is determined through the calibrated parameter values. The results of the calibrated parameters for the HV acceleration characteristics are listed in Table 3.2.

Table 3. 2 Parameter Calibration Results

Parameter	Default Value	Search Range	Search Increment	Calibrated Value
k_1 (ft/s^2)	8.2	[2, 14]	3	11
k_2 (h/mi)	0.048	[0.03, 0.07]	0.01	0.07
c (mph)	12.4	[0, 20]	5	15
φ (ft/s^2)	-4.1	[-8, 0]	4	-4

The calibrated parameters are based on data from the Nebraska test site. However, the calibration methodology is applicable to any location. The key, based on an extensive literature study, is to use as much empirical and local data as possible (Appiah et al 2012).

3.1.8 Multilane Model Validation

The simulation model is validated using two approaches. First, the simulated AQD logic is checked for the reproduction of warning patterns. Second, the traffic volumes at the PDMS1 and PDMS2 are compared using data from a different day at the test site.

Figure 3.6 (a) and Figure 3.6 (b). show the patterns of speed-triggered-warning messages over the data collection periods from field data versus simulation data at PDMS1 and PDMS2, respectively. The PDMS displaying no warning message is color-coded in green while the PDMS displaying a warning message is color-coded in red. The black dots represent the raw

speed data collected by the AQD detector. At the test site, a 3-min rolling average speed is calculated using Equation 3.1 and is drawn with black lines in Figure 3.6.

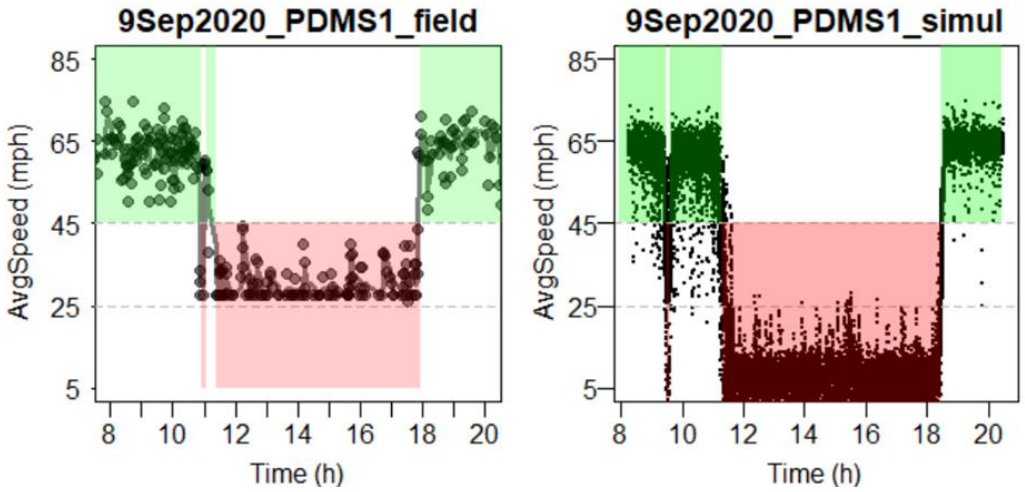

(a) Field observation versus simulation validation for PDMS1

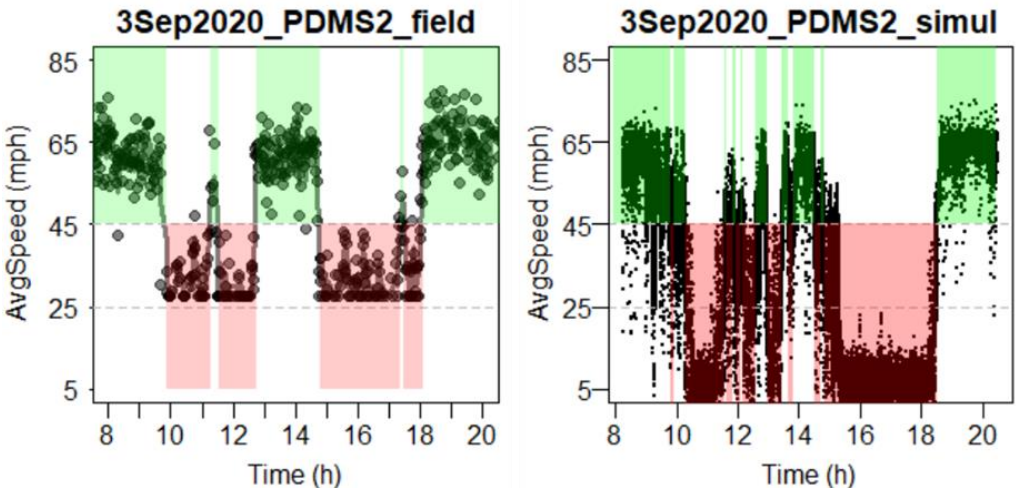

(b) Field observation versus simulation validation for PDMS2

Figure 3. 6 Speed and PDMS Display According to the AQD Logic. (Note that the red area represents warning status while the green area represents no warning status)

As can be seen in Figure 3.6, the field observed patterns at both PDMS1 and PDMS2 locations are essentially replicated by the calibrated simulation model as seen by comparing the

speed profiles with the associated warning message. Specifically, the correct match of the speed-triggered warning time (i.e., time duration indicated by red color) and the no-warning time (i.e., time duration indicated by the green color) is 91.4% at PDMS1 in Figure 3.6 (a) and is 89.8% at PDMS2 in Figure 3.6 (b). The slight shifts and differences between the field measured data and the calibrated output data are acceptable due to the fact that simulation models are incapable of reproducing the complexity and randomness of the real-world traffic conditions (Khazraeian et al 2017).

Furthermore, the calibrated model is also validated using traffic volumes. Specifically, traffic flow data at 15-min intervals at PDMS1 and PDMS2 for both PCs and HVs are used. A comparison of the observed and simulated traffic flow for PCs and HVs is shown in Figure 3.7.

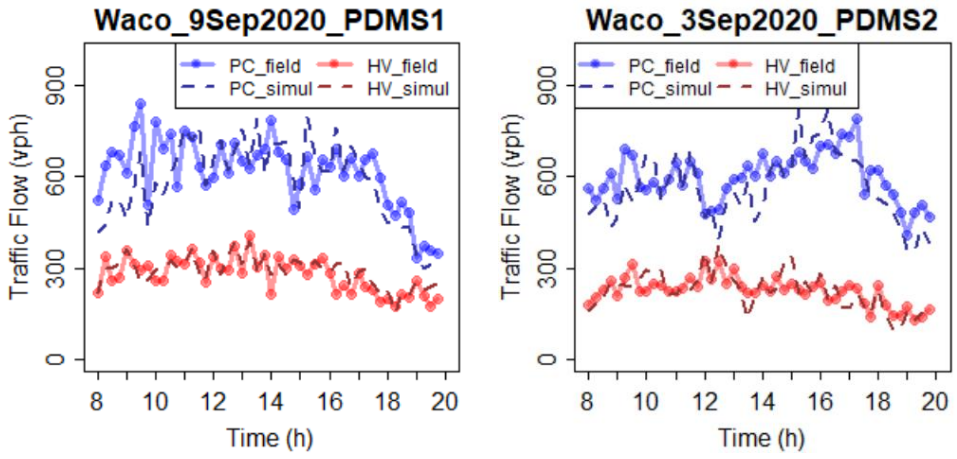

Figure 3. 7 Validation of Traffic Counts for PCs and HVs at PDMS1 and PDMS2.

At the PDMS1 location, the means of traffic flows calculated using field data and the simulated data are 615 and 586 veh/h for PCs and 279 and 288 veh/h for HVs, respectively. Welch Two Sample t-test data indicates there are no significant differences between field

observation and simulated output for PCs (t = 1.19, df = 91.57, p-value = 0.235) and HVs (t = -1.01, df = 91.81, p-value = 0.314).

Similarly, at the PDMS2 location, the means of traffic flows are 597 and 564 veh/h for PCs and 225 and 224 veh/h for HVs, respectively. Welch Two Sample t-test data also indicates no significant differences for PCs (t = 1.67, df = 85.35, p-value = 0.099) and HVs (t = 0.03, df = 86.19, p-value = 0.975). Therefore, the results indicate the simulation model with the calibrated parameters reliably reproduces the traffic conditions at the test site.

3.1.9 Multilane Model Development Concluding Remarks

This study recommends calibrating the freeway IWZ equipped with an AQD system in three steps: 1) configure the desired speed distributions, by scenario, from empirical data; 2) identify the car-following headways from observation and/or from the literature; and 3) calibrate the HV acceleration characteristics. Specifically, ($\hat{\mu}$, $\hat{\sigma}$), (*CC0*, *CC1*, *CC2*), and (k_1, k_2, c, φ) are the three groups of calibrated parameters closely related to driver behavior under the AQD system. Empirical data collected from a test site is used for demonstrating the calibration process in the case study. A user may choose to calibrate the same, more, or fewer parameters than are used in this section. The goal is to demonstrate the methodology and not argue which set of microsimulation models should be observed in the field and which should be calibrated. It should be noted that using simulation will not remove the need for the local DOT to study the safety and efficiency of the work zone implemented.

It is worth mentioning that, due to issues with the AQD system, the case study does not differentiate the warning status of the traffic between slow traffic (i.e., speed between 25 and 45 mph) and stopped traffic (i.e., speed below 25 mph). It is argued that although the detection of

the speed data may affect the understanding of the lower queued speed at the work zone site, it does not necessarily affect the simulation of the AQD system in terms of when to start and end the warning message on PDMS.

Traffic simulation of the IWZ is beneficial in that it provides a cost-efficient method to assess the work zone impact before the system is installed. As a follow-up study, the calibrated simulation model could be used in various studies of the AQD system (Pesti et al. 2013) such as:

- PDMS locations for the optimal distance upstream of the work zone;
- Speed thresholds for different traffic statuses and types of warning messages;
- Rolling interval for averaging vehicle speeds at each detector location;
- Detector spacing between speed detectors deployed upstream of the lane closure; and
- The impact of platooning of connected and automated heavy vehicles on interstate freeway work zone operations.

3.2 Calibration & Validation of a Microsimulation Model of Lane Closures on Two-Lane Highway Work Zone

Two-lane highways are notoriously difficult to model because passing maneuvers take place in the opposing lane of traffic. When work zones are present, the modeling task, in one sense, becomes easier because passing is not allowed. However, in another sense, the modeling task becomes more complicated because of the complex interactions between the driver and the work zone control system.

Work zones along two-lane highways can have three forms: i) shoulder closure, ii) lane shift, and iii) lane closure. The third scenario, lane closure, has the greatest impact on traffic operations (Transportation Research Board 2016). In this scenario, the lane closure forces the traffic traveling in both directions to share a single available lane in an alternating manner. Therefore, lane closure on two-lane highways causes a significant capacity reduction and the simulation model needs to capture this change.

The sixth edition of the Highway Capacity Manual (HCM-6) (Transportation Research Board 2016) characterizes operations on a two-lane work zone lane closure in a similar manner to operations at a two-phase signalized intersection. In other words, it is modeled as an interrupted traffic flow condition. Therefore, similar to the signalized intersections, the capacity of a two-lane work zone is a function of the underlying saturation headways. In contrast to a regular signalized intersection, the lost time for work zones is significantly higher because the clearance time is considerably larger. Note that the clearance time is essentially the work zone travel time. Intuitively, the cycle length and work zone capacity are functions of the work zone travel time. Therefore, saturation headway and work zone travel time are the two key factors that influence the operational performance of a work zone.

Access to the work zone is controlled by three common methods: temporary traffic signal, flagger, and/or a pilot car. The temporary traffic signal control is regulated with a fixed-timing strategy or actuated-timing strategy (Farid et al. 2018; Hua et al. 2019; Washburn et al. 2008). On the other hand, the flagger control technique dynamically changes the right of way in response to real-time traffic flow conditions. Therefore, operationally, the flagging control behaves in the same manner as an actuated signal control technique. A pilot car can be used regardless of which access control approaches (e.g., human flagger or temporary traffic signal

controls) are used. Pilot cars are used for two primary reasons: i) when the work zone length is relatively long, and/or ii) rigorous work activities are being performed within the work zone which may hamper unmonitored traffic moving along the work zone (Farid et al. 2018).

Recently, microsimulation tools have been used to model two-lane work zones. For example, the HCM-6 used the VISSIM microsimulation model to estimate the optimum signal timing strategy for two-lane work zones (Zhu 2015; Schoen et al. 2015). The VISSIM model was calibrated using work zone data from the test site at Preston-Fall City Road SE (near the I-90 corridor) in Washington State. It should be noted this work was based on the average conditions of the work zone. The results from this study were implemented within the HCM-6 (TRB 2016; Schoen et al. 2015). Hua et al. (2019) used the VISSIM simulation model to estimate performance measures including average delay, queue length, and throughput under different signal control techniques. Washburn et al. (2008) developed a microsimulation model, FlagSim, to analyze the impacts of work zones on the capacity for a lane closure on two-lane highways.

While there is a rich literature on calibrating and validating microsimulation models for signalized intersections, studies regarding calibration methods on two-lane work zones are limited (Tawfeek et al. 2018). In fact, the only study to address this issue is NCHRP Report 03-107 (Schoen et al. 2015) which calibrated a two-lane work zone. However, this study used measures of central tendency (e.g., mean values) to calibrate the model.

Because traffic agencies are interested in the range of traffic conditions that will occur on a work zone, and not simply the average conditions, it is critical to use calibrated models that can capture not only average operational conditions but also the expected variability in traffic operations. Previous studies have shown if an analyst needs a distribution of a traffic metric (e.g.,

distribution of queue lengths) rather than a measure of central tendency (e.g., mean queue length) then it is best to calibrate the model using empirical data that captures the distribution of a given parameter. For example, Kim et al. (2005) used a nonparametric statistical technique to calibrate microsimulation models in order to study travel time distributions on bus priority lanes. The authors used different parameters and showed that simple metrics, such as the mean absolute error, led to poor calibration results. When the model was calibrated with a microsimulation model using the distribution of key traffic parameters, the calibration results were significantly improved. Tufuor et al. (2020) calibrated the Highway Capacity Manual (HCM-6) travel time reliability model to capture empirical travel time distribution. Furthermore, Tufuor and Rilett (2021) showed that when the microsimulation model was calibrated using distributions of empirical data, it could replicate empirical travel time distributions at a 5% significance level. Because the distribution of delay, queue length, travel time, etc. is required to analyze how a work zone is operating, it is hypothesized that using the full distribution of empirical data during the calibration step will result in a more useful model. In the case of two-lane work zones where traffic is traveling in both directions, the microsimulation model needs to accurately model the distribution of saturation headways and work zone travel times. This is the primary motivation of this section.

In the simulation model used in the HCM-6, only one parameter (e.g., CC0, standstill distance between two vehicles) was calibrated. In addition, the calibration process itself was manual in nature (Schoen et al. 2015). In this section, it was hypothesized that i) calibrating more parameters, particularly those related to headway and car following, ii) calibrating the model using the distribution of key traffic parameters, and iii) conducting the calibration process

automatically will lead to better and more robust models that can be utilized by traffic agencies in design and operation of work zones.

The major objectives of this section are as follows:

i. Demonstrate that neither an uncalibrated work zone model nor a model calibrated based on the measure of central tendency will provide adequate results when a user requires the model to identify the distribution of key traffic metrics (e.g., work zone travel times, saturation headways, etc.);
ii. Propose a microsimulation calibration methodology for two-lane work zones that uses the distribution of key performance measures as input;
iii. Demonstrate the efficacy of the proposed calibration approach using empirical work zone data for two test sites in Nebraska; and
iv. Validate the calibrated microsimulation model using data not used in the calibration procedure and discuss the spatial transferability of the calibrated model.

The remainder of this section is organized as follows. The next section discusses data collection efforts and empirical data statistics for model development. Then a microsimulation calibration methodology is proposed that is designed for work zones on two-lane highways. Subsequently, a test site in Nebraska is used to demonstrate the proposed automated calibration methodology using empirical data. The calibration results when using i) measures of central tendency and ii) the actual empirical distribution are compared and contrasted using statistical inference techniques. Lastly, the calibrated model is validated using empirical work zone data that is not used in the calibration step and the spatial transferability of the calibrated model is discussed.

3.2.1 Two-lane Highway Test Site and Data Collection System

Two work zone test sites active in the fall of 2020 are selected for this section. The first test site is on U.S. Route 30 southwest of Clarks, Nebraska as shown in Figure 3.8 (a). The non-work zone speed limit is 65 mph, and the annual average daily traffic is 1600 (Nebraska AADT, 2021). The work zone length is 1.1 miles. Access to the work zone is controlled using flaggers and a pilot car.

The second site is located on U.S. Highway 77 south of Winnebago, Nebraska as shown in Figure 3.8 (b). The non-work zone speed limit is 65 mph, and the annual average daily traffic is 3000 (Tufuor and Rilett; 2021). The work zone length is 1.5 miles. Similar to the first site, a flagger and pilot car are used for traffic control in the work zone.

The data collection system includes three components: i) two Miovision Scout detectors, ii) two Wavetronix HD detectors, and iii) a Contour camera. Figure 3.8 (c) shows pictures of these devices in the field. The Miovision and Wavetronix HD detectors are placed in the field while the Contour camera is placed in the pilot car operating in the respective work zone.

The layout of the data collection system is shown in Figure 3.8 (d). It may be seen the Wavetronix HD and Miovision devices are placed inside the work zone and near the flagger position at both ends of the work zone. A contour camera equipped with GPS is installed in the pilot car. Within the work zone, the flagger either shows the “SLOW” sign or the “STOP” sign. The flaggers communicate by short-range radio to ensure the information provided to drivers is consistent.

The contour camera is used to obtain the relative speed and geographical coordinates of the pilot car within the work zone and obtains a video record. The contour camera confirms the work zone is operating under normal conditions and there are no issues (e.g., pilot car stopping to facilitate the movement of construction equipment) that would make any of the collected data invalid.

The Wavetronix HD is used to record length-based vehicle classification, headways, and the instantaneous speed (i.e., spot mean speed) of each vehicle as they enter and exit the work zone. The Miovision device can identify and store MAC address signatures and timestamps from passing vehicles with electronic devices that are WiFi-enabled. This information is later used in the lab to "match" MAC addresses and to estimate the distributions of work zone travel times. Most importantly, the Miovision detectors are also used to record visual activities at the work zone entry and exit points.

(a) Highway 30 test site near Clarks city, Nebraska

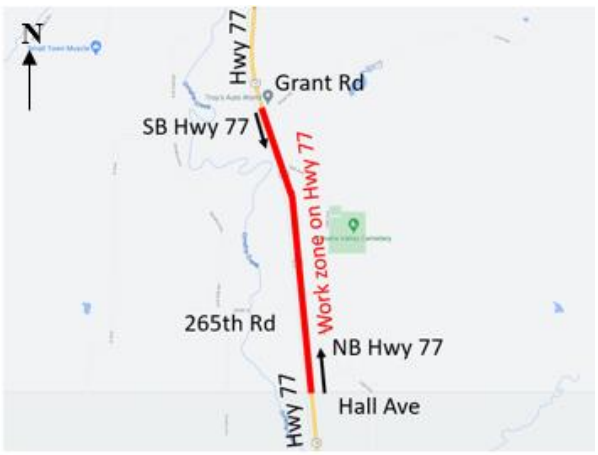

(b) Highway 77 test site near Winnebago, Nebraska

(c) Data collection devices installed at the work zone test sites

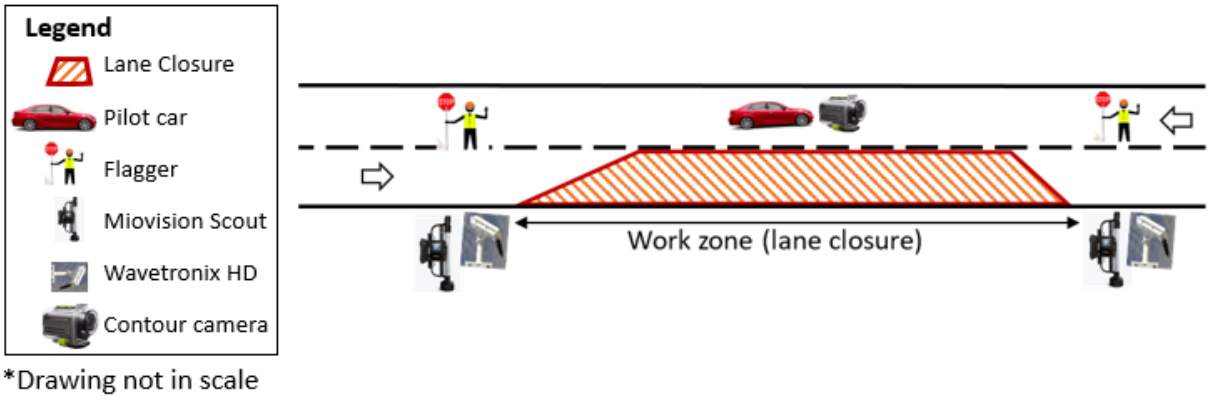

(d) Schematic diagram of a work zone and the layout of the data collection system

Figure 3. 8 Test sites and data collection system

Note that MAC addresses are only collected from WiFi-enabled vehicles. In order to consider all individual vehicles' information for the modeling approach, the research team decides to use the Miovision video data. Approximately twenty hours of active work zone video are collected on October 12, 13, and 14 at the Highway 30 test site, and twelve hours of video are collected on October 30 and 31 at the Highway 77 test site. Traffic volumes, vehicle classification, saturation headways, and work zone travel times are manually observed through video footage.

3.2.2 Two-lane Highway Data Processing for Calibration

Among the twenty hours of active work zone data collected from the Highway 30 test site, six hours of data are used for the model calibration purpose. These six hours represent the most congested times and occur from 4 pm to 6 pm on October 12, 2020, and from 2 pm to 6 pm on October 13, 2020.

The headway is defined and measured using the time between two consecutive vehicles' front axles passing a specific point near the flagger. Following the standard practice defined in the HCM-6, the first three vehicles discharged from the queue are ignored (TRB, 2016). Saturation headway data are estimated from a total of 1145 vehicles from Miovision video record. Figures 3.9 (a & b) show the distribution of saturation headway in the northbound and southbound directions, respectively.

It may be seen in Figure 3.9 (a) that the mean saturation headway for northbound and southbound directions are 4.1 seconds and 4.0 seconds, respectively. These are represented by the dashed blue lines in Figures 3.9 (a) and (b). Note that using Equation 26-B4 of the HCM-6

results in an estimated saturation headway of 2.2 seconds for this test site. This result is shown by the black dashed lines. A Welch two-sample t-test is used to test whether these observed and estimated saturation headways are statistically different. Both tests reject the null hypothesis that HCM-6's prediction and field observation are the same at the 5% significance level for both the northbound (t-stat= 28.6, p-value<0.001) and the southbound (t-stat= 26.7, p-value<0.001) directions.

The work zone travel time is measured as the difference in timestamps between when the vehicle enters the work zone, defined by the fixed location of the upstream flagger, and exited the work zone, defined by the fixed location of the downstream flagger. Travel time data are estimated by manual observation from the Miovision video. Travel times for a total of 1381 vehicles, of which 632 were traveling northbound and 749 were traveling southbound, are obtained using this method.

Figures 3.9(c) and 3.9(d) show the distribution of work zone travel times for the northbound and southbound directions, respectively. As can be seen in these figures, the travel times within the work zone range from 90 to 200 seconds. The mean values are approximately 140 s and 150 s for northbound and southbound directions, respectively. The mean values are marked in dashed blue lines in Figures 3.9(c) and 3.9(d).

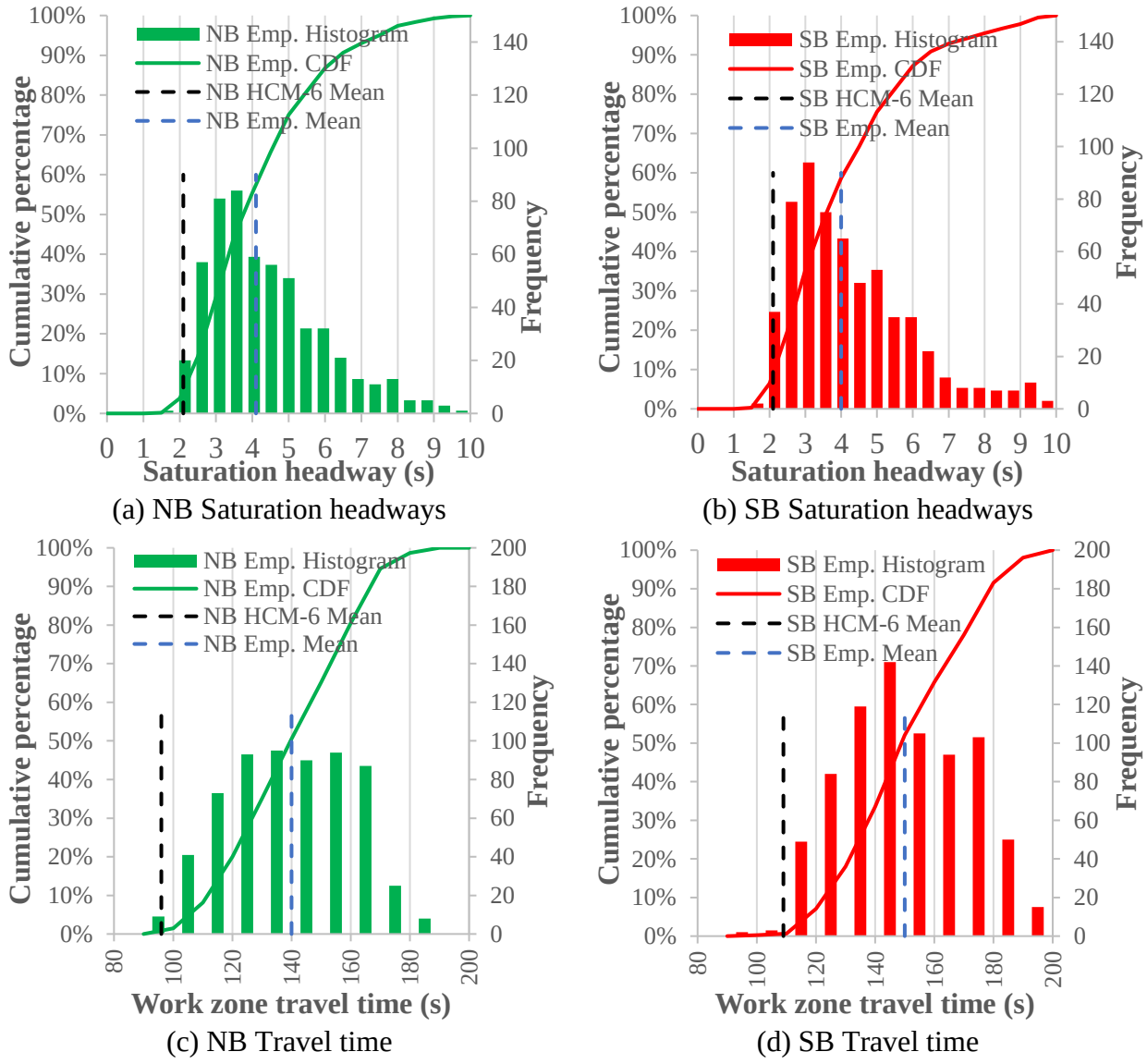

Figure 3. 9 Empirical data from Highway 30 work zone test site used in microsimulation model calibration for Northbound (NB) and Southbound (SB)

The HCM-6 work zone travel time estimation methodology uses factors such as posted speed limit (outside of work zone), lane and shoulder width, and access point density. The exact formulae are labeled Equation 26-B1 and Equation 26-B2 in the HCM-6 (TRB, 2016). Using these equations, the forecast work zone travel times are estimated to be 96 s and 109 s for northbound and southbound directions, respectively. These are shown as the dashed black lines

in Figure 3.9 (c) and Figure 3.9 (d). It may be seen the predicted work zone travel times using the HCM-6 are much lower than the observed travel times. This is confirmed by the Welch two-sample t-test, which rejects the hypothesis that HCM-6's prediction and field observation are the same at the 5% significance level. This was true for both northbound (t-stat= 53.2, p-value<0.001) and southbound (t-stat=-55.2, p-value<0.001) directions.

The results of the statistical tests from both saturation headway and travel time indicate the mean headway and travel time measured from the test site are significantly different than the corresponding headway and travel time means predicted using the appropriate HCM-6 methods. The results indicate the HCM-6 model could not accurately estimate the saturation flow rate and the work zone travel time for the test site. For these reasons it is decided to use a microsimulation model, similar to that used in the original HCM-6 research, to see if it can capture the stochastic features and variable nature of headways and travel times at the test site. Therefore, the first step is to calibrate the microsimulation model to local conditions (FHWA 2016), followed by a validation of the model. Therefore, the next section proposes the calibration method.

3.2.3 Two-lane Highway Work Zone Proposed Calibration Methodology

The general goal of the proposed calibration methodology is to calibrate the microsimulation model so that it can replicate the distribution of the empirical performance measures. This section introduces the proposed methodology and the following section demonstrates the methodology using the Nebraska test site introduced in the previous section. Figure 3.10 shows the flow chart of the proposed calibration model. It may be seen there are three major steps, each described in this section.

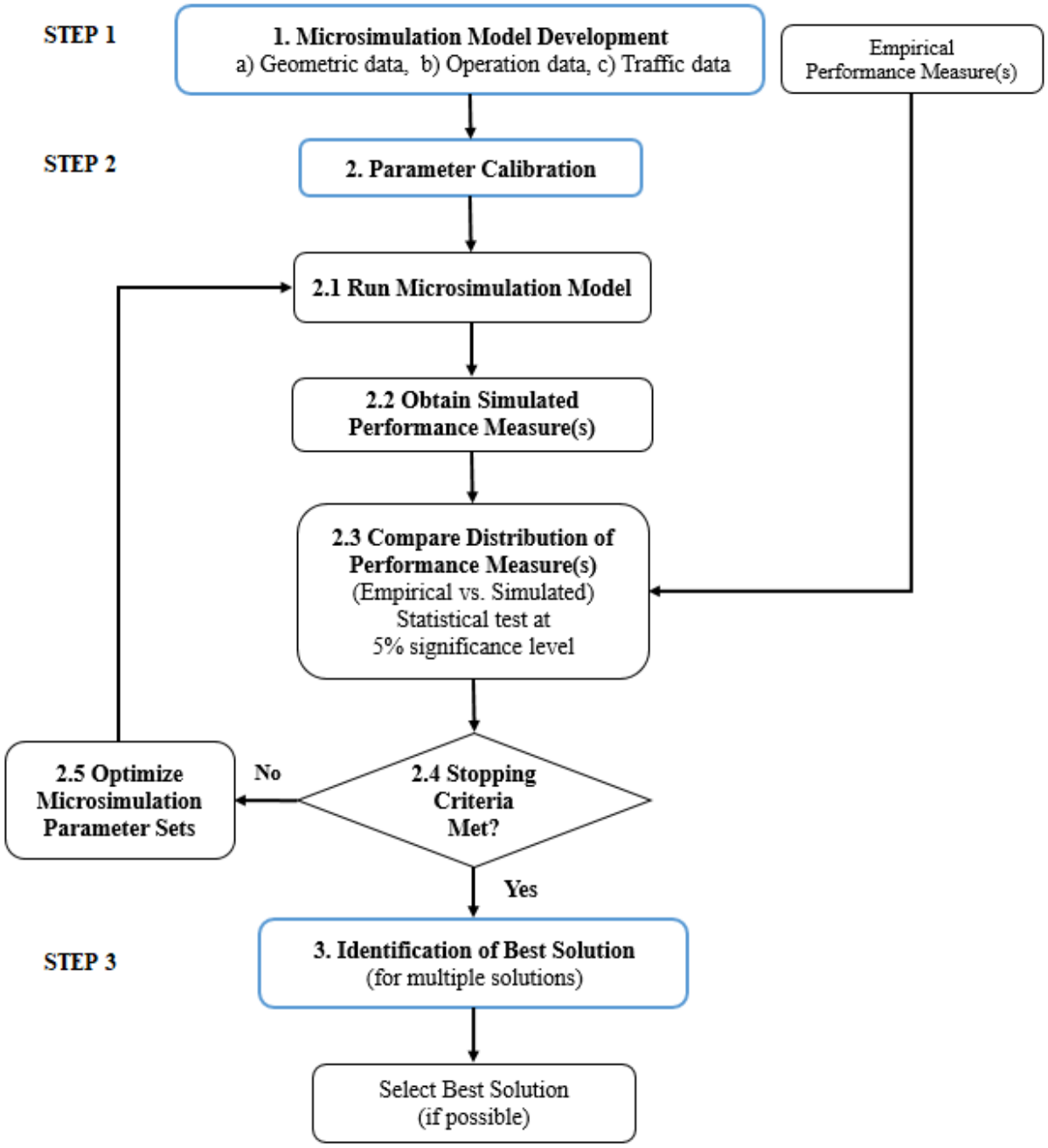

Figure 3. 10 Proposed model of two-lane work zone microsimulation calibration

Step 1. Microsimulation Model Development. There are several available traffic microsimulation tools that can be used for model development including TransModeler™, AIMSUN™, TRANSIMS™, PARAMICS™, CORSIM™, and VISSIM™. A comparison of traffic modeling of these tools is provided elsewhere (Kochenderfer and Wheeler, 2019). A key part of the model development is to obtain local data that represents the work zone under consideration. This includes geometric data (e.g., horizontal curvature, vertical curvature, segment lengths, grades, etc.), operation data (e.g., work zone traffic control, signage, speed limits, etc.), and traffic data (e.g., vehicle volumes, truck percentages, etc.). The data is used to develop the microsimulation model. A key requirement for all simulation models is driver behavior information. All simulation models model driver behavior in different ways using various types of car-following models, lane-change models, gap-acceptance models, etc. The underlying model theory, as well as the associated parameters and their values, need to be understood by the user. Lastly, it is desirable to have empirical data for key performance measures (e.g., queue length distribution, travel time distribution, etc.) so the quality of the model can be ascertained. This information is also used in the calibration step described below.

Step 2. Parameter Calibration. It is important to note that all commercially available microsimulation models have parameters users can adjust to control the internal driver behavior (e.g., car-following, lane changing, etc.) logic to represent local conditions. Each parameter has a default value. While default values may be used, it has been shown the best results are obtained if the parameters are calibrated to local field data (FHWA 2016). The first decision that needs to be made by the analyst is to identify which parameters need to be calibrated. Intuitively, the parameters that directly affect the performance measures of key metrics should be adjusted in the calibration process. The goal is to adjust the microsimulation parameters, within realistic bounds,

such that the simulation model produces performance metrics that match those measured in the field. Note the analyst may use previously calibrated parameter values (e.g., from a previous calibration effort) without a loss of generality. As shown in Figure 3.10, Step 2 is an iterative process consisting of a number of sub-steps as described below:

Step 2.1: In the first iteration, the simulation model is run using the default or previously calibrated parameters. In later iterations, the current parameter set, from Step 2.5, is used. It is common practice to run the simulation model N times and to use the average of the *N* simulation runs.

Step 2.2: The analyst chooses the data used to qualify the operations of the work zone. Typical performance measures are travel time, queue, delay, etc. Preferably this information is in the form of a distribution. In Step 1, empirical performance data is collected. Now, the simulated distribution of each of the selected performance measures is obtained from simulation runs conducted in Step 2.1.

Step 2.3: In this step, the empirical distribution of each performance measure from Step 1, is compared to the corresponding distributions from the simulated data from Step 2.2. There are several techniques that can be used to compare a given distribution. Some authors have used non-statistical tests such as mean absolute error and mean absolute percentage error. These give a measure of how close two distributions are but do not have a statistical basis for making conclusions. It is argued in this section distribution-free statistical tests such as the Kolmogorov-Smirnov (KS) test, Mann-Whitney-Wilcoxon test, etc. should be used (Tufuor et al. 2020; FHWA 2016).

Step 2.4: In this step, a decision is made whether the algorithm should stop or continue to the next iteration. This decision could be based on whether a statistically valid solution has been found. Alternatively, the user can choose to run the algorithm for a set number of iterations. At each iteration, the stopping criteria are checked to determine whether the calibration process should be continued or not.

Step 2.5: Based on the simulation results of the last iteration, the optimization algorithm identifies a new set of parameters that hopefully result in a "better" outcome. Several optimization algorithms could be used for this objective. These include the simplex method, the genetic algorithm, and simulated annealing (FHWA 2016; Spiegelman et al. 2010). Once this parameter set is identified, the logic moves back to Step 2.1 and repeats itself until the stopping criterion is met (checked in Step 2.4). It is important to note there is no guarantee the methodology will find a parameter set that can replicate the empirical distributions of interest. Therefore, it is argued the best approach is to run the methodology until a pre-defined number of iterations are completed (Agdas et al. 2018; Kramer 2017) to avoid creating an endless loop.

Step 3. Identify "Best" solution, if possible. The calibration procedure may identify zero solutions, one solution, or multiple solutions. When the optimization algorithm produces multiple sets of parameters that satisfy the statistical test, further criteria are required to determine the "best" parameter set. The analyst may choose to select the parameter set that results in the least error when the simulation outcome is compared to the observed data, or the parameter set that best represents the local driver behavior.

3.2.4 Two-lane Highway Case Study

As a demonstration of the simulation calibration process, the proposed approach is applied to an existing two-lane one-lane closed work zone on US Highway 30.

Step 1 Microsimulation Model Development. While any simulation model can be used with the proposed methodology in this section as discussed, VISSIM (version 2020) is chosen in this section because i) it has the capability of modeling all operational aspects of work zones, and ii) it was used as an aid in developing the HCM-6 macroscopic work zone equations. The six hours of empirical traffic data from the Highway 30 test site are used in developing the VISSIM simulation model. As previously mentioned in the "Calibration Data Processing" section, traffic demand, flaggers' movement, saturation headway, and travel time data are estimated from Miovision video record. Therefore, data including traffic demand and the proportion of heavy trucks are used as input for the microsimulation model. In addition, work zone information including work zone length, posted work zone speed limit, and work zone traffic control strategies are incorporated into VISSIM. Note that the flaggers' operations are modeled using the VISSIM traffic signal control. Therefore, information related to this logic (e.g., green time allocation, cycle time, etc.) is used. The performance data, such as empirical saturation headway and work zone travel time, are collected and prepared to be used in Step 2.

Step 2 Parameter Calibration. The calibration of the VISSIM work zone simulation model used in the HCM-6 only considered one driver behavior (e.g., standstill distance, CC0). All the other parameters were set to their default values. A preliminary calibration is done by the authors using the same HCM-6 calibration approach. It is found the calibrated model does not match field observations. Consequently, the authors decide to use a more comprehensive

approach. Seven parameters identified in previous research as affecting work zone performance are chosen for calibration (Mathew and Radhakrishnan 2010; Buck et al. 2017; Chitturi 2007; VDOT 2020). These are: CC0 (standstill distance), CC1 (headway time), CC2 (following variation), CC3 (threshold for entering "following" mode), CC4 (negative following threshold), CC5 (positive following threshold), and CC6 (speed dependency of oscillation). A detailed description of these model parameters can be found elsewhere (PTV 2020). It should be noted the lane-changing parameters are set to the default values because lane change behavior is not possible within the two-lane work zone. The details of Step 2 used in this section are described below.

Step 2.1: The VISSIM simulation model is run using the data gathered in Step 1.

Step 2.2: The saturation headway distribution (SHD) and the work zone travel time distribution (WZTTD) are identified as the key performance measures because they directly reflect the quality of operations of two-lane work zones. Therefore, simulated SHD and WZTTD data are collected from VISSIM.

Step 2.3: The simulated and empirical SHD and WZTTD are compared. Specifically, KS tests are used in this section to test the null hypothesis that the simulated SHD (WZTTD) and the empirical SHD (WZTTD) are statistically similar at a 5% significance level (Wackerly et al. 2014). Note that performance measures other than SHD or WZTTD may be used without a loss of generality.

Step 2.4: For this section, 600 iterations are used as the stopping criterion. Note that an analyst can choose less/more without a loss in generality.

Step 2.5: In this step, a genetic algorithm is used to optimize microsimulation parameter sets. It is found the genetic algorithm operators, e.g., the crossover rate and mutation rate, ranged from 50% to 90% and 1.0% to 2.5%, respectively (Tufuor et al. 2020; FHWA 2016). For the Highway 30 test site, the mid-rate of the crossover (e.g., 70 %) and mutation (e.g., 1.75%) rates are used. The generation gap is set to 75% (Appiah et al. 2011; Yao et al. 2012; Angelova and Pencheva 2011). It should be noted the best genetic algorithm parameters to use are a function of the application, which needs to be identified through a combination of prior experimentation and experience. Detailed information regarding genetic algorithms can be found elsewhere (Kramer 2017).

Because *N*, the number of simulation runs in Step 2.1, is set to five and the total number of iterations is set to 600, there are a total of 3000 *(= 600 x 5)* simulation runs conducted during the calibration in an automated process.

Step 3 Selection of "Best" Parameter Set. After the completion of Step 2, six solutions are found that produced simulated results statistically similar to the field-observed SHD and WZTTD for both the northbound and southbound directions of traffic flow. The best parameter set is determined based on the lowest mean absolute error calculated using Equation 3.9. Therefore, the parameter set that provides the lowest MAE is determined as the optimal result of calibrated parameters. Note that in Equation 3.9, the bin is referred to as the interval between selected ranges. For example, for SHD, a bin width of 0.5 seconds is used from 0 to 10 seconds, generating a total number of 19 bins. Note that the selection of bins/bins width may depend on user preferences.

$$\text{MAE} = \frac{\sum_{i=1}^{n} |S_i - E_i|}{n} \qquad \text{Eq. 3.9}$$

Where,

S_i = frequency of bin *i* of the simulated distribution

E_i = frequency of bin *i* of the empirical distribution

n = number of bins.

3.2.5 Two-lane Highway Calibration Results

The proposed calibration model is recommended based on the distribution of the chosen traffic metric(s) as described in the Case Study section. In this case, the goal is to identify traffic simulation parameter values that result in the simulated saturation headway distribution and the simulated travel time distribution being statistically similar to their empirical counterparts. This section refers to this as the Distribution Calibration approach. However, the proposed method in Figure 3.10 can be used to match the mean of the performance measure. In practice, users may base their calibration on matching a measure of central tendency (e.g., mean, median, etc.) of the chosen traffic metrics (FHWA 2021). This section refers to this as the Mean approach when discussing the findings of calibration efforts using both approaches.

Results of the Distribution Approach

Figure 3.11 shows the graphical presentation cumulative distribution function (CDF) graph of the empirical, uncalibrated, and 'best' calibrated solutions for SHD and WZTTD for both directions using the Distribution approach. Figure 3.11 uses dotted and dashed lines to represent the results from northbound and southbound directions, respectively. The dark, red, and green colors show empirical, uncalibrated, and best-calibrated results, respectively.

Figure 3.11(a) shows the shape of CDF for empirical and uncalibrated SHD are visually different (i.e., dark lines vs. red lines). Therefore, not surprisingly, it shows the default parameters from microsimulation model (i.e., uncalibrated) are not able to capture the field

observed condition. After using the proposed calibration method utilizing the Distribution approach, from visual inspection, the shape of calibrated and empirical CDF closely matches (dark lines vs. green lines). Data representing Figure 3.11(a) reveals that for the northbound direction, the calibrated SHD has an interquartile range (IQR) of 2.7-4.8 s, against the empirical SHD's IQR of 2.8-5.0 s. In contrast, the uncalibrated SHD has an IQR of 1.3-2.5 s. On the other hand, for the southbound direction, the IQR of calibrated, empirical, and uncalibrated SHD are 2.7-4.8 s, 2.7-5.0 s, and 1.3-2.4 s, respectively. Most importantly, it is found using the KS test that there is no statistically significant difference between the empirical and calibrated SHD at a 95% confidence level.

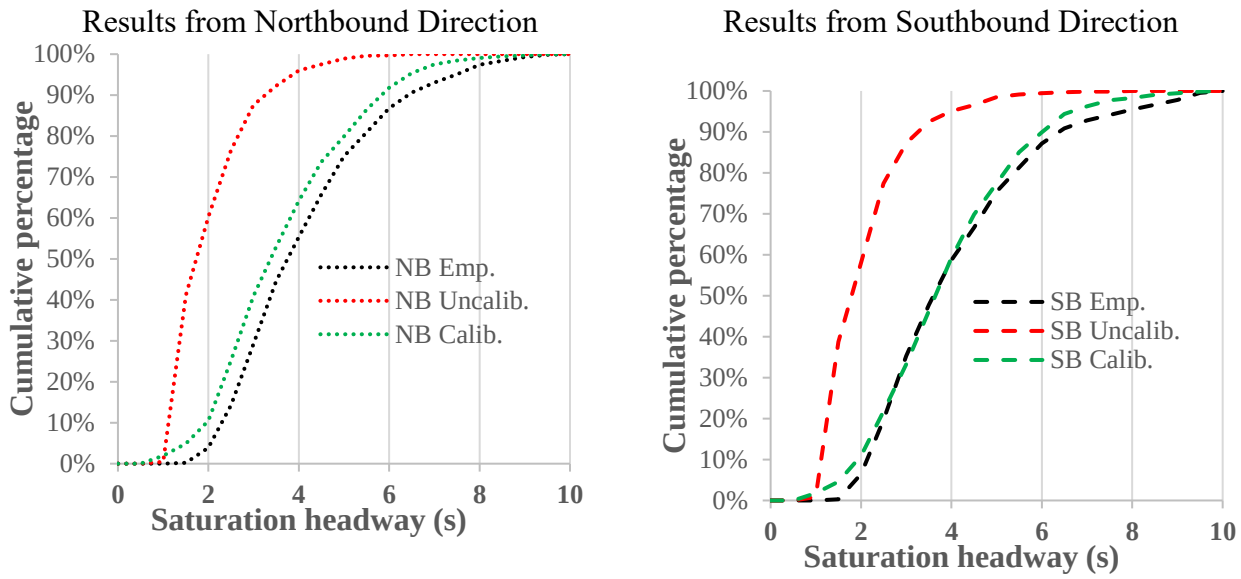

(a) Comparisons of the cumulative distribution of saturation headway

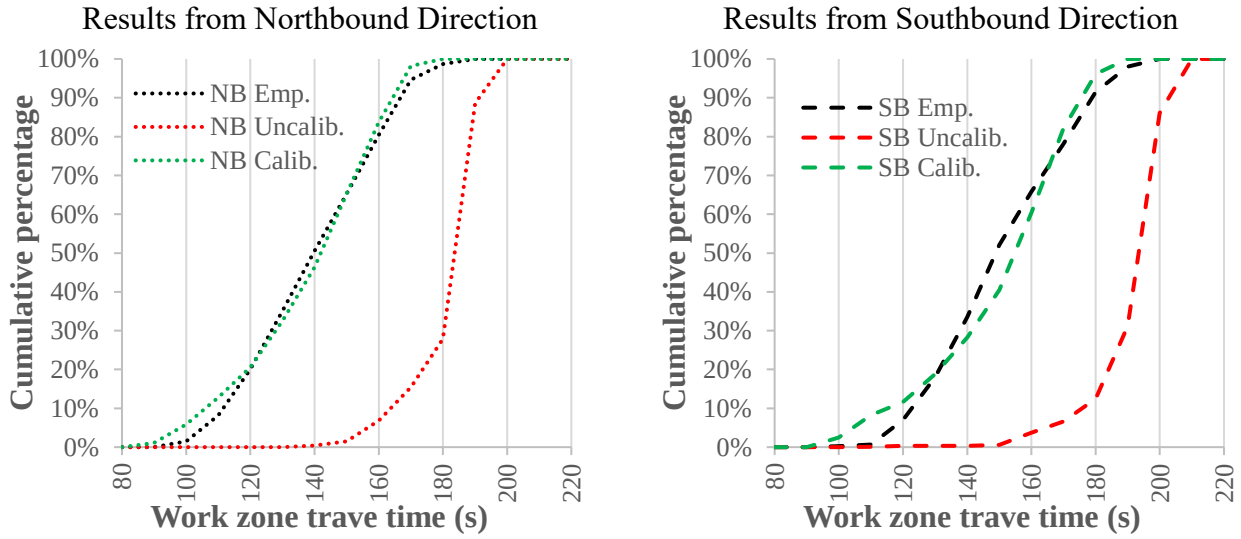

(b) Comparisons of the cumulative distribution of work zone travel time

Figure 3. 11 Comparison of empirical, uncalibrated, and best-calibrated output distributions

Figure 3.11(b) shows the shape of CDF of empirical and uncalibrated WZTTD are considerably different (i.e., dark lines vs. red lines). This is similar to the findings from the SHD analysis. After the calibration, the shape of the calibrated CDF (black lines) and empirical CDF (green lines) match closely. The calibrated WZTTD of the northbound direction has an IQR of

124.6-155.5 s. This is similar to the empirical WZTTD's IQR of 125.0-157.0 s. In contrast, the uncalibrated IQR is 179.1-188.2 s. Similar results are found for the southbound direction where the IQR of the calibrated, empirical and uncalibrated WZTTD are 137.7-166.9 s, 136.0-168.0 s, and 188.4-198.6 s, respectively. The KS tests confirm there is no statistically significant difference between the empirical and calibrated WZTTD at the 95% confidence level.

In summary, it is found the uncalibrated VISSIM model gives results not statistically similar to the empirical data. In fact, it is found the uncalibrated simulation results are statistically different. Therefore, using the Distribution approach, the calibrated VISSIM model is able to capture the traffic behavior for the test site.

Comparisons between Distribution and Mean Approach

Intuitively, the mean approach may require less effort in data collection and calibration. However, based on the author's experience, it is unlikely that calibrating a model to mean values will result in valid distributions of the traffic metric (Kim et al. 2005; Tufuor et al. 2020). To demonstrate this concept, the process shown in Figure 3.10 is repeated using the means of the distribution (e.g., the Mean approach) rather than the distributions themselves.

Table 3.3 shows the results when the calibration is based on i) matching the mean (e.g., Mean approach) and ii) matching the distribution (e.g., Distribution approach) for the case study for saturation headway and work zone travel time, respectively.

Table 3. 3 Comparative Model Outcomes of Mean and Distribution Approach for Saturation Headway.

Statistics for Saturation Headway		Empirical	Uncalibrated	Mean Approach			Distribution Approach		
				1	2	3	1	2	3
Northboun	Mean	4.1	2.1	4.1	4.0	3.9	3.9	4.0	4.0
	SD	1.6	0.9	1.0	1.2	1.2	1.6	1.5	1.5
	IQR	2.2	1.1	1.4	1.5	1.4	2.2	1.9	1.9
	KS test (p-value)		**<0.001**	**<0.001**	**<0.001**	**<0.001**	**0.2**	**0.4**	**0.3**
Southbound	Mean	4.0	2.0	4.1	4.0	4.1	3.9	3.8	3.9
	SD	1.7	1.0	1.0	1.2	1.2	1.6	1.6	1.6
	IQR	2.3	1.0	1.4	1.5	1.6	2.1	2.2	2.1
	KS test (p-value)		**<0.001**	**<0.001**	**<0.001**	**<0.001**	**0.3**	**0.3**	**0.4**

Note: All measures are in second except the p-values of the KS test.

Table 3.3 lists the corresponding numerical statistical results of the best three calibration solutions (e.g., Calibrated 1, Calibrated 2, and Calibrated 3) for both the Mean and the Distribution approach for saturation flow headway and work zone travel time, respectively. These results include the mean, standard deviation (SD), and interquartile range (IQR). In addition, the results of the KS tests are shown when empirical data is compared to the uncalibrated simulation, and the calibrated simulation is performed by both approaches. Note the results for the best calibration for the Distribution approach (e.g., 7th column in both Tables) is portrayed visually CDF in Figure 3.11.

As can be seen in Table 3.3, for the northbound direction, the average results of the saturated headway from Mean and Distribution approach are 4.1 and 3.96 s, respectively. This may be compared to the empirical mean of the saturated headway of 4.0 s. In summary, both approaches predict the mean saturated headway with 3.4% accuracy. However, the difference between the empirical standard deviation and the standard deviation from the Mean and

Distribution approach is 29.3% and 4.3%, respectively. Similarly, the difference between the empirical IQR and the IQR of the Mean and Distribution approach is 31.8% and 9%, respectively.

On the other hand, Table 3.4 shows, for the northbound direction, the average results of travel time from the Mean and Distribution approach are 141.3 and 138.5 s, respectively. Therefore, both approaches can predict the field mean observation with 1.2% accuracy. However, the difference between the empirical standard deviation and the standard deviation from the Mean and Distribution approach is 6.2% and 1.6%, respectively. Similarly, the difference between the empirical IQR and the IQR of the Mean and Distribution approach is 17.7% and 5.9%, respectively.

Table 3. 4 Comparative Model Outcomes of Mean and Distribution Approach for Work Zone Travel Time.

Statistics for Work Zone Travel Time		Empirical	Uncalibrated	Mean Approach			Distribution Approach		
				1	2	3	1	2	3
Northboun	Mean	140.1	181.1	141.8	141.3	140.3	138.6	137.8	139.1
	SD	20.5	11.0	19.3	19.3	19.1	20.9	20.8	20.8
	IQR	32.0	9.1	25.8	26.8	26.4	30.9	29.6	29.8
	KS test (p-value)		**<0.001**	**<0.001**	**<0.001**	**<0.001**	**0.1**	**0.1**	**0.1**
Southbound	Mean	150.8	191.4	152.3	155.2	154.3	150.3	149.8	150.3
	SD	20.9	10.9	21.9	21.8	22.5	21.9	21.9	21.9
	IQR	32.0	10.2	29.6	28.2	31.2	29.2	29.1	29.2
	KS test (p-value)		**<0.001**	**<0.001**	**<0.001**	**<0.001**	**0.1**	**0.1**	**0.1**

Note: All measures are in second except the p-values of the KS test.

The discussion above revealed the Distribution approach can predict the variability of field observation better than the Mean approach. However, KS test can confirm whether the results from these two approaches are different. Table 3.3 and Table 3.4 list the results of p-values of the KS test, when the Distribution and Mean approach are compared to field observed

performance measures. It may be seen under the Distribution approach, for all performance measures from both directions of traffic, p-values of the KS test are higher than 0.05. Therefore, the test cannot reject the null hypothesis that the two distributions (empirical vs. simulated) are similar at 5% significance level. In other words, simulated outcomes using the Distribution approach have statistically the same distribution of performance measures as observed in the field.

In contrast, Table 3.3 and Table 3.4 report all the KS tests conducted under the Mean approach have p-values less than 0.05. In other words, the test result rejects the null hypothesis that the empirical and simulated distribution found by the Mean approach is similar at 5% significance level. In conclusion, these tests statistically determine that, unlike the Mean approach, the Distribution approach can replicate the field observed variations of the performance measures.

In summary, both SHD and WZTTD results indicate, compared to the uncalibrated (or HCM-6 approach of modifying CC0 parameter only) and Mean approach, the calibration of the microsimulation model using the Distribution approach is promising when imitating the stochastic features of the field observations and replicating the performance of the two-lane work zone at the test site. Therefore, it is decided to utilize the Distribution approach for the rest of the section.

3.2.6 Two-lane Highway Model Validation and Transferability

To test the effectiveness of the proposed distribution method, this section further discusses the validation and spatial transferability of calibrated model parameters. The validation is performed by predicting performance using the same work zone, but utilizing a dataset not

applied in the calibration process. Spatial transferability refers to the performance prediction of the work zone calibrated model parameters when applied to a geographically different work zone location. In both cases, the best-calibrated model parameters are used to predict SHD and WZTTD.

Figure 3.12(a) shows the comparison of work zone performance when the calibrated model parameters are applied for the work zone on Highway 30. Data from the morning peak hour on October 14, 2020, is used. It may be seen the calibrated model is able to predict the variability of saturated headway and work zone travel time performance for both directions when compared to the empirical observations. All of them passed the KS test criteria at the 5% significance level to indicate field observations and simulation predictions are statistically the same.

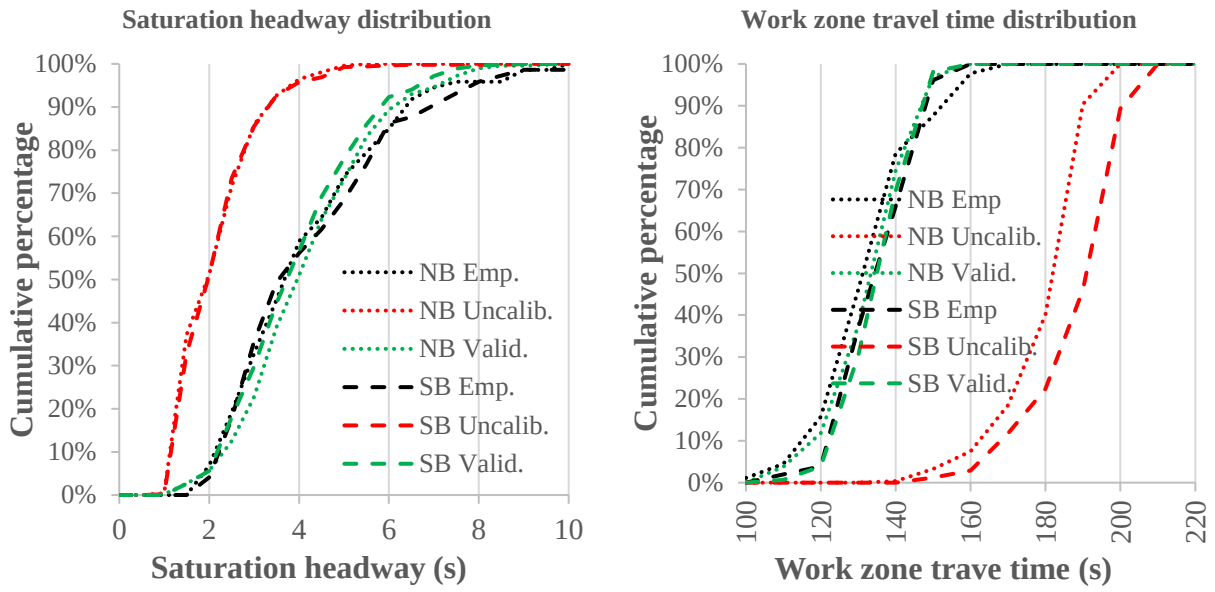

(a) Model validation

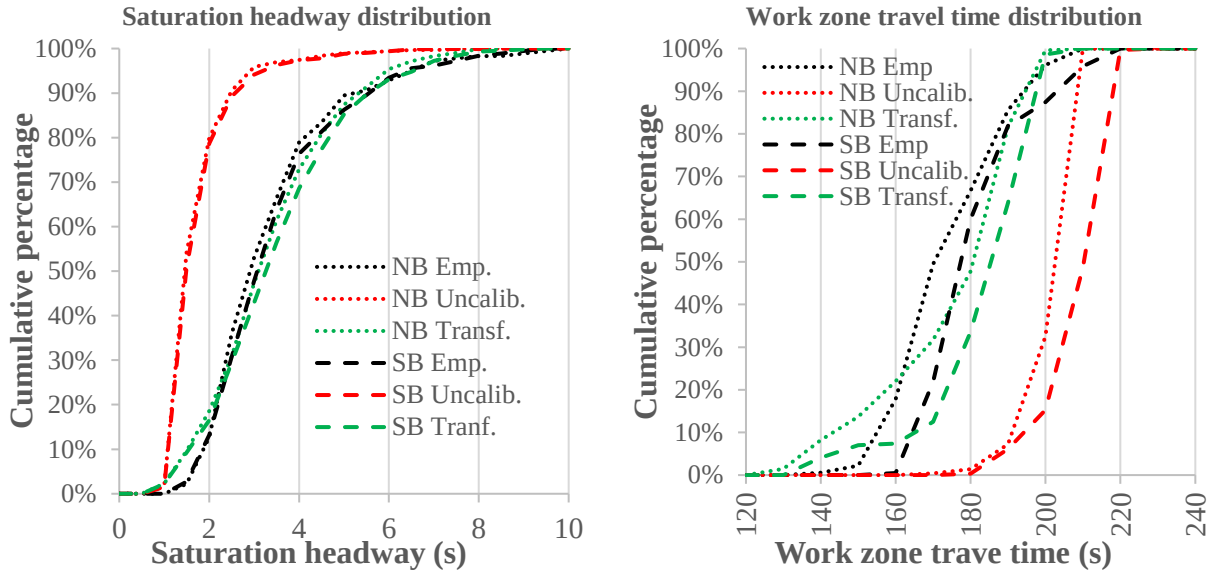

(b) Spatial transferability

Figure 3. 12 Validation and transferability of calibrated model parameters

For spatial transferability, the performance of the 1.5-mile work zone on Highway 77 is predicted using the calibrated model parameters. The Highway 77 work zone is approximately

140 miles northeast of the Highway 30 test site. The performance of Highway 77 is predicted using data from the evening peak hour (4 pm to 6 pm) from October 30, 2020.

Figure 3.12(b) shows the predicted performance of Highway 77 when compared to the empirical observations. It may be seen the predicted SHD of both directions matches the empirical observation as they pass the KS test criteria at the 5% significance level.

In Figure 3.12(b) the shape of CDF of predicted work zone travel time is close to the empirical observation. However, the KS test reveals the predicted distribution is statistically different than the field observations at the 5% significance level. For the southbound direction, the statistics suggest the prediction of the calibrated model for median, mean, standard deviation, and interquartile range are 186.5, 182.2, 14.9, and 14.8 s, respectively against the empirical observation of 178.0, 180.5, 13.3, and 14.0 s, respectively. Therefore, the model captures the median and mean value closely (within 4.7% accuracy); however, the predicted standard deviation is approximately 13% higher than field observation.

This case study shows that as the calibrated model is transferred spatially, it is able to capture the SHD. Therefore, it may be hypothesized the saturated headway does not vary across drivers. However, the WZTTD is a function of the work zone characteristics e.g., the intensity of work zone activities, operation of the pilot car, and different work zone lengths. It may explain the underlying results of the transferred calibrated model parameter for work zone travel time. Regardless, it was found using a calibrated model developed elsewhere produces better results than using an uncalibrated model as demonstrated by the shape of CDF of work zone travel time in Figure 3.12(b).

3.2.7 Two-lane Highway Model Development Concluding Remarks

A microsimulation model needs proper calibration to produce reliable outcomes. This section has established a guideline to calibrate a two-lane work zone microsimulation model. The proposed model enhances the credibility of microsimulation studies by capturing the field observed variations of performance measures. To the best of the authors' knowledge, existing literature does not provide a methodology of microsimulation model calibration based on field observed distribution of performance measures for the two-lane work zone.

In addition to describing the proposed calibration model, an example is provided on how the proposed methods are applied in an automated process using empirical data from a Highway 30 work zone in Nebraska. The automated calibration model includes a genetic algorithm that continuously updates microsimulation parameter sets and statistically compares the simulation and field observed distributions of the saturation headways and the work zone travel time to search for the optimal solution.

This section also found that when the microsimulation model was calibrated using measures of central tendency, such as the mean, the resulting model was unable to replicate field observed variations of performance measures. However, when the model was calibrated using the full distribution of field observations, the model was able to replicate field observed conditions.

The model developed using the proposed calibration technique has been validated using empirical data from the Highway 30 test site. This section also tested the transferability of the calibrated parameter. It was found that, when calibrated model parameters were spatially transferred, they were able to statistically predict saturation headways. Even though the model

produced similar mean values as the observed mean travel time, the corresponding travel time distributions were statistically different.

In summary, eliminating the current literature gap, this section has proposed and demonstrated a microsimulation calibration and validation technique able to replicate the field traffic conditions for lane closures at two-lane work zones. The authors recommend further studies to investigate the impact of the pilot car movement, intensity of work zone activities, and work zone length on vehicle speed profiles within the two-lane work zone.

4 SENSITIVITY ANALYSIS OF WORK ZONE CALIBRATED MICROSIMULATION MODEL FOR NEBRASKA

The calibrated models (i.e., the Multilane/Freeway Work Zone Model and the Two-lane Highway Model) in the previous chapter are used to provide estimates of capacity reduction, delay increases, and fuel usage increases related to various work zone/lane closure conditions. Specifically, the following work zone/lane closure cases are examined:

- Freeway or Multilane Highway
    1. Six-Lane Divided Highway: 3 lanes per direction, 1 lane closed (3-to-2)
    2. Six-Lane Divided Highway: 3 lanes per direction, 2 lanes closed (3-to-1)
    3. Four-Lane Divided Highway: 2 lanes per direction, 1 lane closed (2-to-1)
- Two-Lane (Undivided) Highway: 1 lane closed (Flag controlled operations)

The sensitivity analysis of each of these cases is conducted with respect to different lengths of the work zone, vehicle volume, percent of trucks, and speed limit combination of scenarios. Specifically, the impact of these factors on work zone performance (e.g., capacity, delay, and average queue length) are estimated for each scenario. Table 4.1 shows the breakdown of the number of scenarios analyzed as a function of the facility type. It may be seen a total of 1460 scenarios are analyzed across all facilities. Each of the scenarios is repeated five times using different random seeds in the calibrated VISSIM traffic microsimulation model and each output (e.g., delay, queue length, etc.) is averaged using the five different runs so the results are robust and not dependent on a single run (Tufuor et al. 2020). In other words, there are 7,300 different results for both the six-lane cases, the four-lane case, and the two-lane case, respectively.

Table 4. 1 The Total Number of Scenarios

Facility Case Type	Work Zone Length, mi	Traffic Volume, vphpl	Percent of Trucks, %	Posted Speed, mph	Scenarios = 1460
Six-Lane Divided Highway: 3 lanes per direction, 1 lane closed (3-to-2)	(4 no) 1 – 8	(5 no) 500 – 1500	(4 no) 10 – 40 %	(2 no) 55 – 75	160
Six-Lane Divided Highway: 3 lanes per direction, 2 lanes closed (3-to-1)	(4 no) 1 – 8	(5 no) 500 – 1500	(4 no) 10 – 40 %	(2 no) 55 – 75	160
Four-Lane Divided Highway: 2 lanes per direction, 1 lane closed (2-to-1)	(4 no) 1 – 8	(5 no) 500 – 1500 @ 250 interval	(4 no) 10 – 40 %	(3 no) 45 – 75	240
Two-lane Undivided Highway: 1 lane closed	(5 no) 0.25 – 4	(9 no) 100 – 500	(5 no) 0 – 40 %	(4 no) 50 – 65	900

4.1 Sensitivity Analysis of the Four-lane Work Zone Case

An active work zone on the westbound traffic movement on the I-80 at Waco, Nebraska is used as the test site. The empirical data collection process, the work zone model calibration, and validation results were discussed in Section 3.1. Figure 4.1 shows 1) the test site, 2) the data collection setup, and 3) the model calibration results. It may be seen the model simulation results are similar to the observed travel data. This calibrated model is used to undertake the sensitivity analysis and a sample of the results is discussed in subsequent sections. Details of all of the scenario results will be presented in the Appendix of this report.

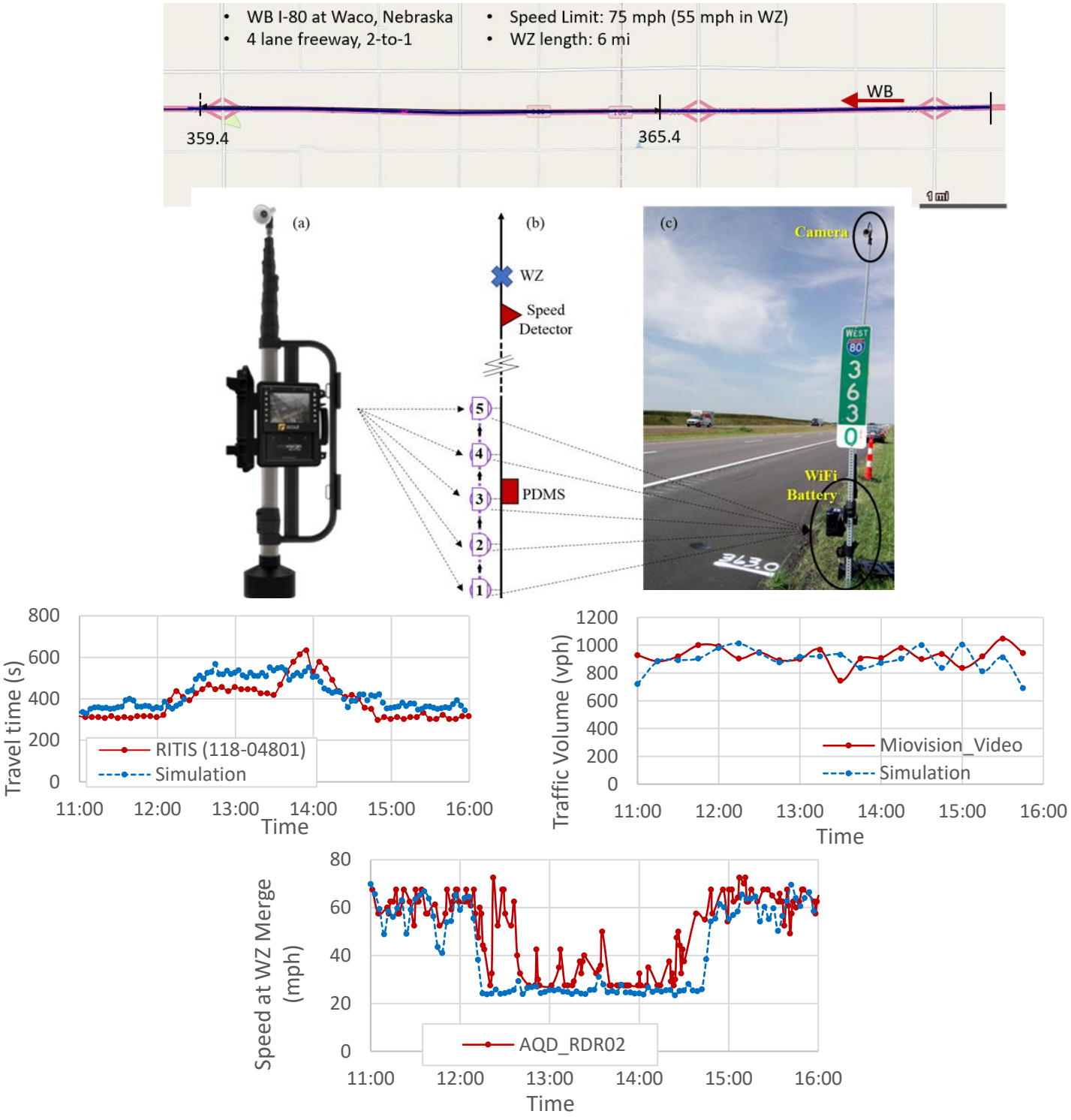

Figure 4. 1 Test site and calibration results for four-lane work zone

4.1.1 Four-lane Work Zone Model Capacity Estimates

The latest and 6th edition of the Highway Capacity Manual (HCM6) listed five factors that influence the work zone capacity of a freeway/multilane highway as discussed in Section 2.2 of this report. Based on these variables, the HCM6 estimates the work zone capacity (C) by adjusting the average queue discharge flow rate (QDR) using Equations 3.1 and 3.2 formulated in the NCHRP Report 03-107.

Figure 4.2 shows the sensitivity of the QDR as a function of speed, traffic volume, and percent of trucks from the simulation results.

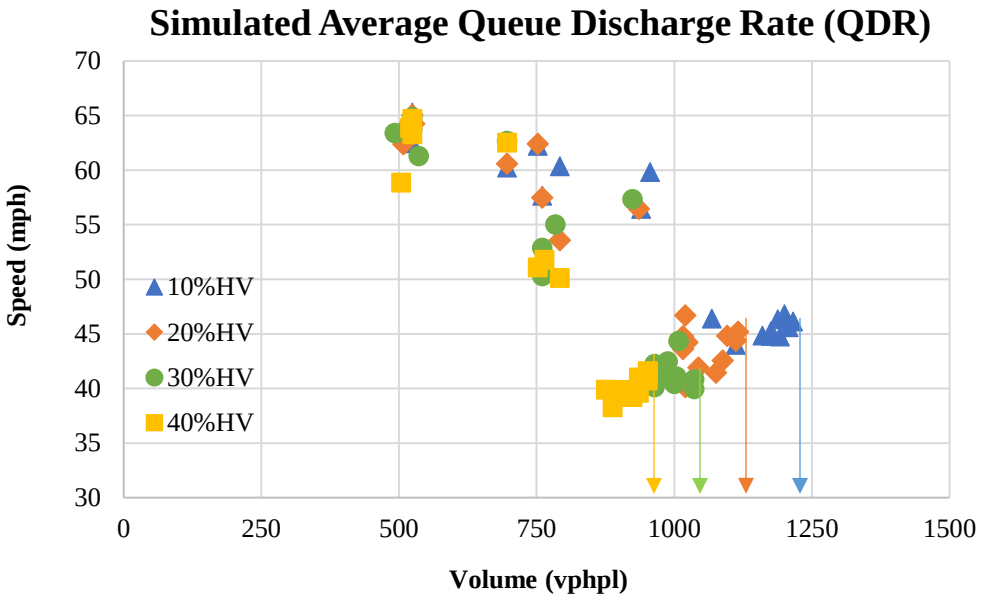

Figure 4. 2 Average queue discharge flow rate

The simulated QDR values are adjusted to estimate the work zone capacity as per the HCM methodology discussed in Section 2.2 of this report. Table 4.2 shows the estimated work zone capacity for the test site as a function of the percent of heavy vehicles.

Table 4. 2 Estimated Work Zone Capacity as a Function of Truck Percentage

HV%	QDR (vphpl) From Fig. 4.9	QDR (pcphpl) Using HCM PCE conversion	Capacity (pcphpl) From Equation 2.3
10	1216	1398	1503
20	1116	1451	1560
30	1039	1462	1572
40	952	1523	1638

It may be seen from Table 4.2 that the work zone capacity ranges from approximately 1500-1650 pcphpl. It is not surprising that the higher the percentage of heavy trucks present, the higher the capacity required to meet an acceptable operational queue discharge flow rate. The results are comparable to HCM and what other states have adopted as shown in Table 4.3. Exhibit 10-14 of the HCM provide more details of the different work zone capacities across the US.

Table 4. 3 Other State DOT Operational Work Zone Capacities

State	Capacity	Unit
Florida	1800	vph
Wisconsin	1500	pcphpl
Nevada	1500-1600	pcphpl
Massachusetts	1500	vph
Hawaii	1600	pcphpl
Iowa	1450	vphpl
New York	1800	pcphpl
New Jersey	1300-1400	vphpl
HCM (2010)	1400 (long-term WZ)	pcphpl
HCM (2010)	1600 (short-term WZ)	pcphpl
HCM (2016)	1455 – 2035	pcphpl

4.1.2 Four-lane Work Zone Model Performance Estimates

Four performance measures are used: 1) Average queue length, which measures the current queue length upstream by the queue counter in each time step, and thus the arithmetic mean is calculated per time interval; 2) Average vehicle delay, which refers to the average delay time of all vehicles; 3) Average travel time, which measures the arithmetic mean of the individual vehicle travel time as they traverse the work zone; and 4) Average queue delay, which measures the arithmetic mean of the individual vehicle delay when in a queue.

Figure 4.3 shows the trends in the four-work zone performance as a function of traffic volume and the percentage of heavy vehicles for one of the four-lane scenarios (i.e., posted speed of 75 mph to 55 mph for a 1-mile work zone length). The unshaded and shaded blocks show the undersaturation and oversaturation conditions, respectively. Similar analyses are conducted for the other scenarios.

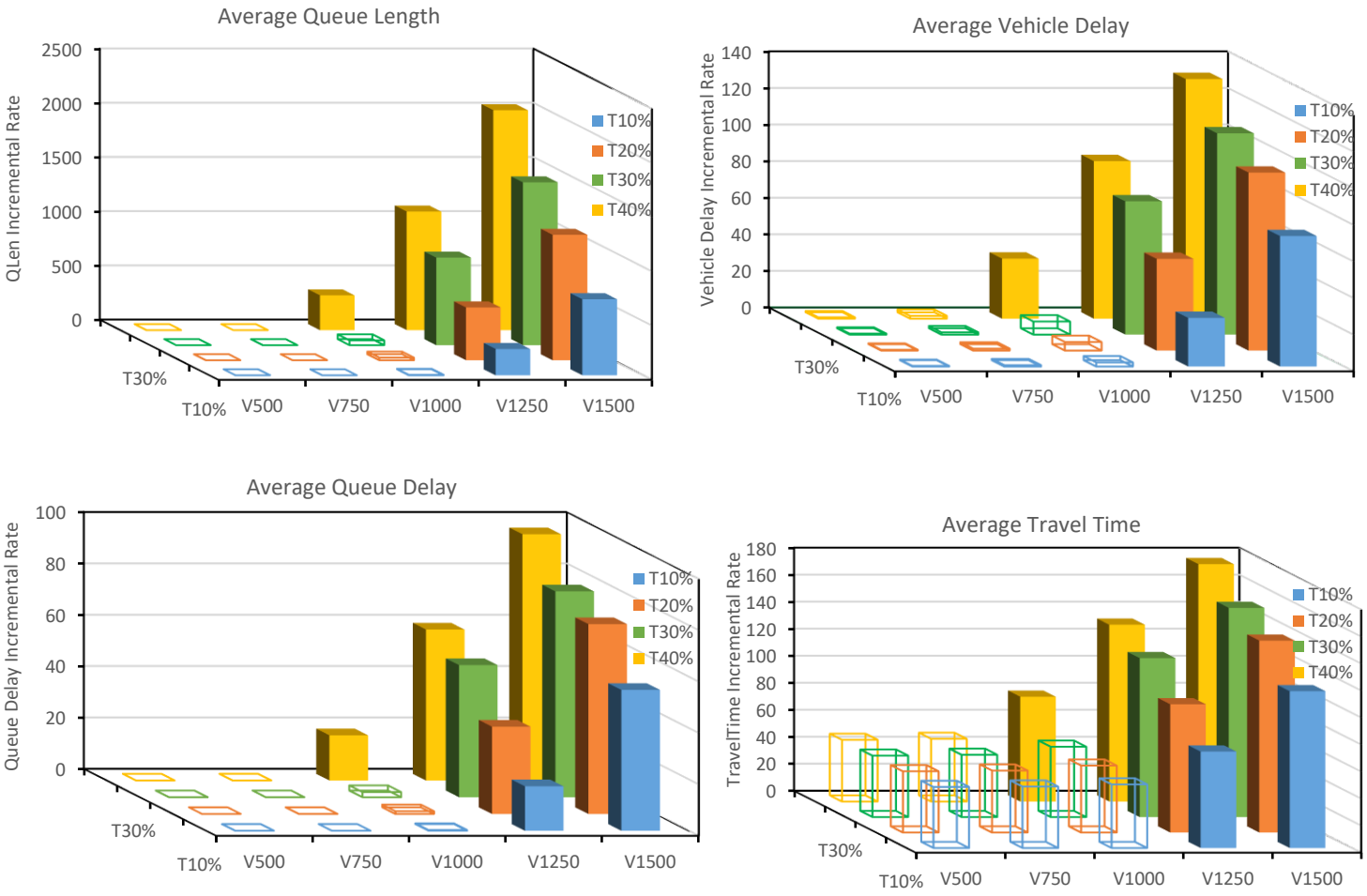

Figure 4. 3 Simulation results of undersaturated and oversaturated conditions for a four-lane work zone scenario

It may be seen from Figure 4.3 that there is an exponential deteriorative effect on the work zone performance when operating in oversaturated conditions. Results show a four-lane case scenario (2 lanes with 1 lane closed) where posted speed is reduced from 75 mph to 55 mph for a 1-mile work zone results in oversaturation when operated for one-hour for the following conditions:

1. Volume of 1000 vphpl with 40% of heavy vehicles.

2. Volumes greater than 1250 vphpl with 10% of heavy vehicles.

It is easy to hypothesize operating the work zone under Nebraska conditions below 90% of work zone capacity will result in minimal impact on travelers.

4.2 Sensitivity Analysis of the Six-lane Work Zone Case

An active work zone on I-80 westbound traffic movement at Ashland, Nebraska is used as the test site. The work zone model calibration and validation processes were discussed in Section 3.1. Figure 4.4 shows the test site and the model calibration results. It may be seen that the model simulation results are similar to the observed travel data. This calibrated model is used to undertake the sensitivity analysis and a sample of the results is discussed in subsequent sections. Details of all of the scenario results are presented in the Appendix of this report.

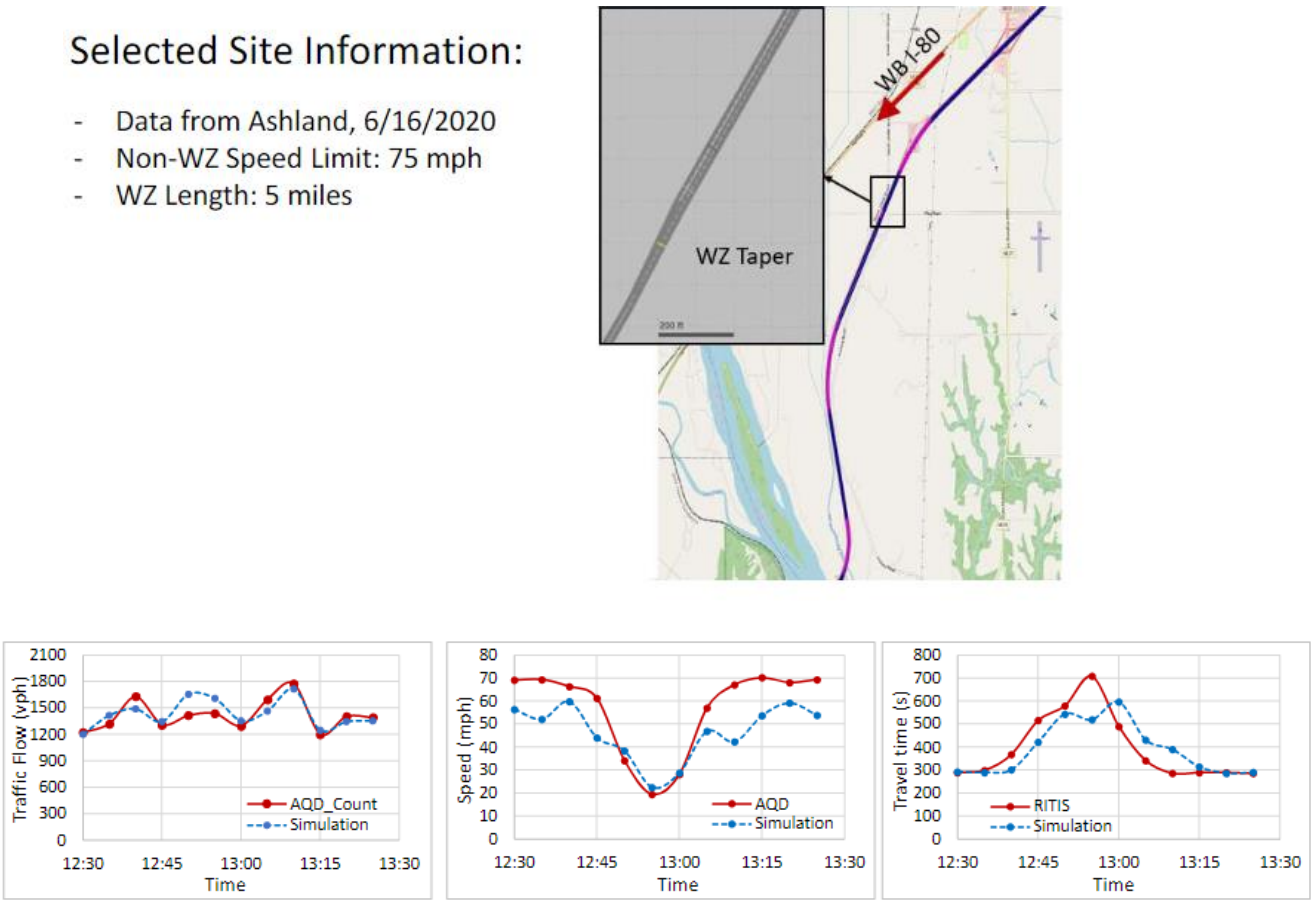

Figure 4. 4 Test site and model calibration results for six-lane divided work zone

4.2.1 Six-lane Work Zone Model Capacity Estimates

Applying the HCM6 procedure (from Eq. 2.2 in this report), the recommended capacity estimates for the six-lane work zone cases are shown in Table 4.4.

Table 4. 4 HCM6 Predicted Work Zone Capacities

Lane Config.	HCM 6 Estimated Capacity
3-to-2	1841 – 1918 pcphpl
3-to-1	1469 – 1545 pcphpl

Figures 4.5a and 4.5b show the relationship between the simulated capacity and heavy truck percentage for a two-lane work zone on a three-lane interstate highway (e.g. one lane is closed to traffic) and for a one-lane work zone on a three-lane interstate highway (e.g two lanes are closed to traffic), respectively. The graphs on the left show the capacity in terms of vphpl and the graphs on the right show the capacity, using the same data, in terms of pcphpl. Note the PCE used to make the conversion is obtained from the Highway Capacity Manual. The estimated HCM capacities in pcphpl for these cases are shown as dotted horizontal lines in the graphs on the left.

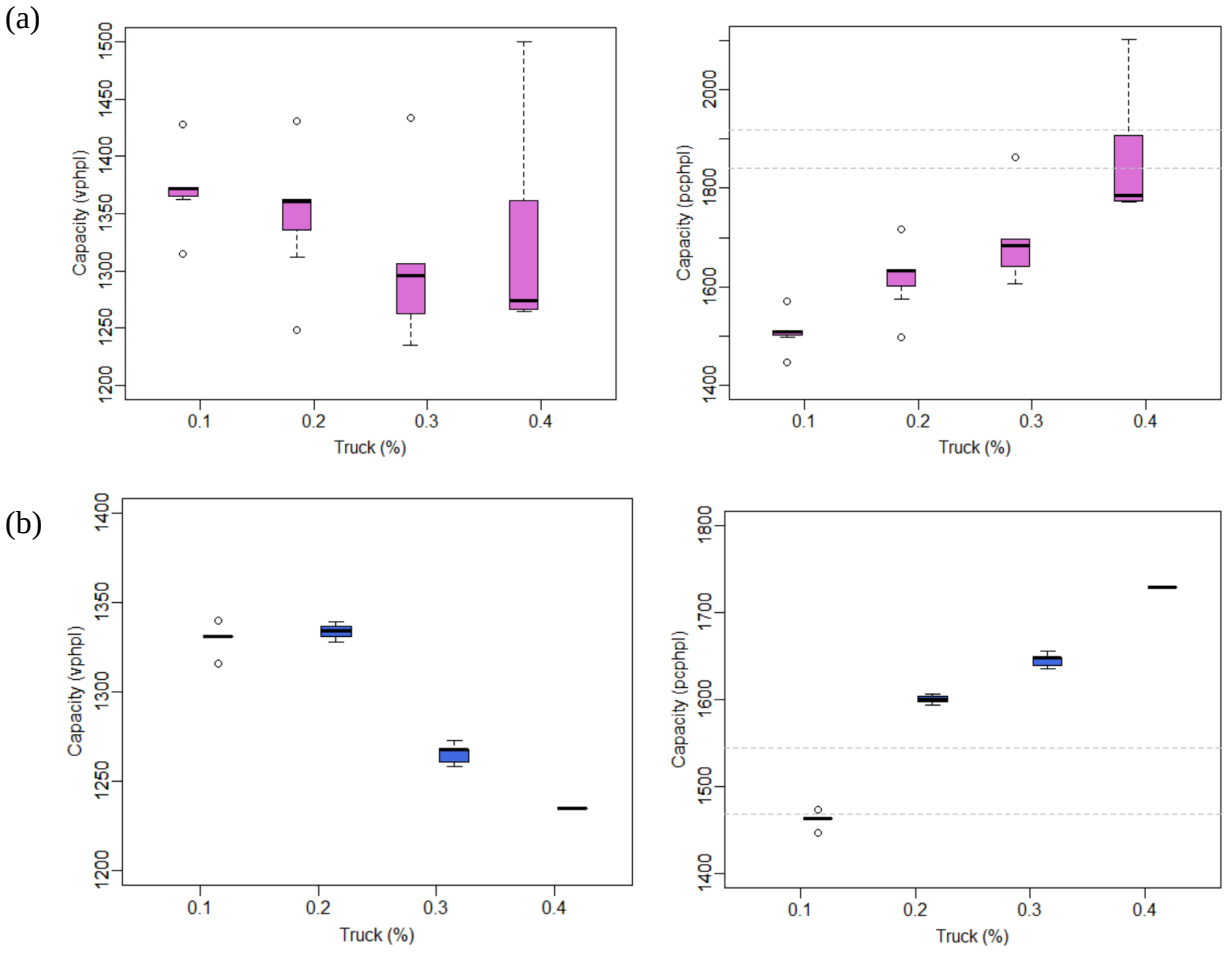

Figure 4. 5 Simulated capacities as a function of truck percentages (a) 3-lanes to 2-lanes work zone case, (b) 3-lanes to 1-lane work zone case

It may be seen from Figure 4.5 that as the truck percentage increases so too does the capacity as measured in pcphpl. In addition, the variability in capacity also increases with truck percentage when one out of the three lanes is closed to traffic. Similar variability in the capacity trend is found when two lanes are closed to traffic except for a 40% truck percentage where the variability in capacity decreased. The range of the simulated capacities for the two-lane configurations (3-to-2 and 3-to-1) seems reasonable when compared to other state values shown in Table 2.5 of this report.

4.2.2 Six-lane Work Zone Model Performance Estimates

Two performance measures are used: 1) Average queue length, where VISSIM outputs the current queue length upstream of the work zone at each step. The average queue length is the arithmetic mean used to calculate the average queue length over the one-hour steady-state simulation time; and 2) Average vehicle delay, where VISSIM outputs the average delay for all vehicles at user-defined intervals. In this research, the average delay is calculated over the one-hour steady-state simulation time. VISSIM calculates delay by subtracting the theoretical travel time from the actual travel time. The theoretical travel time is the travel time achieved if there are no other vehicles and/or no signal controls or other reasons to stop and assumes the vehicle travels at the speed limit for a given link. The actual travel time is the time it takes a vehicle to travel from its origin to its destination. Note that VISSIM automatically accounts for partial trips.

Figure 4.6 shows the incremental rate of increase in travel time as a function of traffic volume, truck percentage, work zone length, and work zone speed limit at 3-to-1 work zones (in hot pink color) and 3-to-2 work zones (in blue color), respectively.

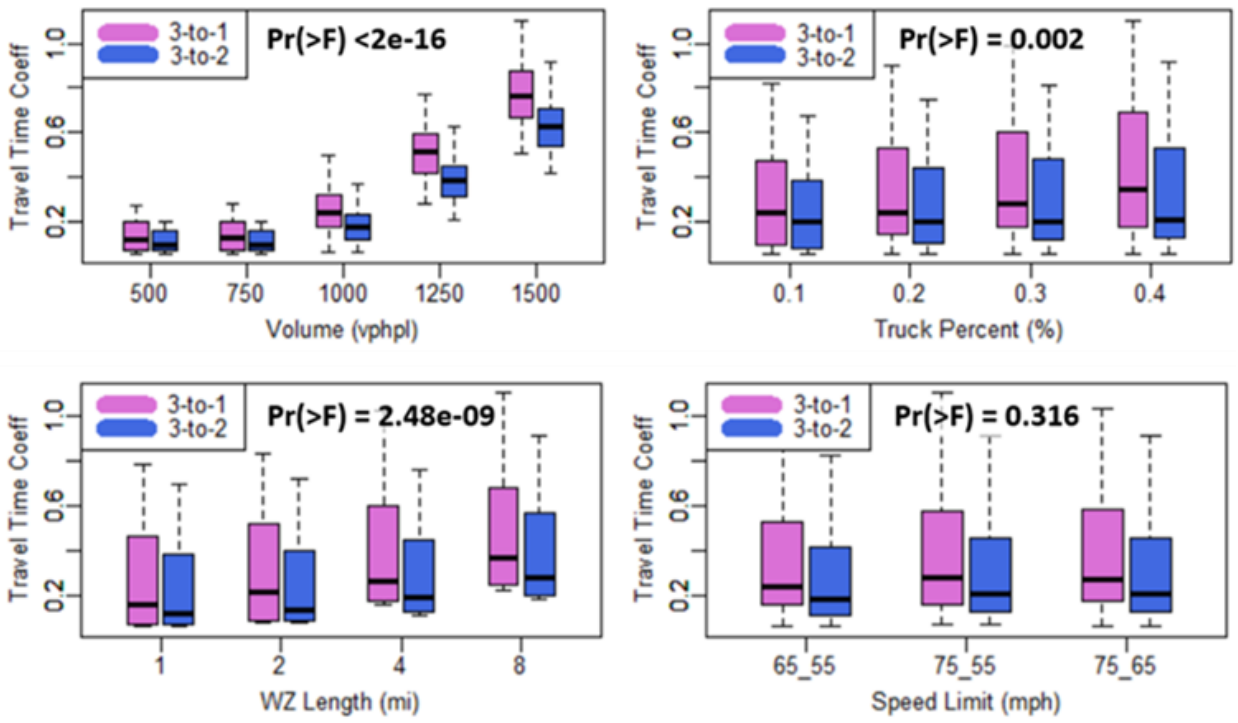

Figure 4. 6 Travel time metric changes as a function of volume, truck percent, WZ length, and the speed limit at the 6-lane work zone.

Figure 4.7 shows the incremental rate of increase in vehicle delay as a function of traffic volume, truck percentage, work zone length, and work zone speed limit at 3-to-2 work zones (in hot pink color) and 3-to-1 work zones (in blue color), respectively.

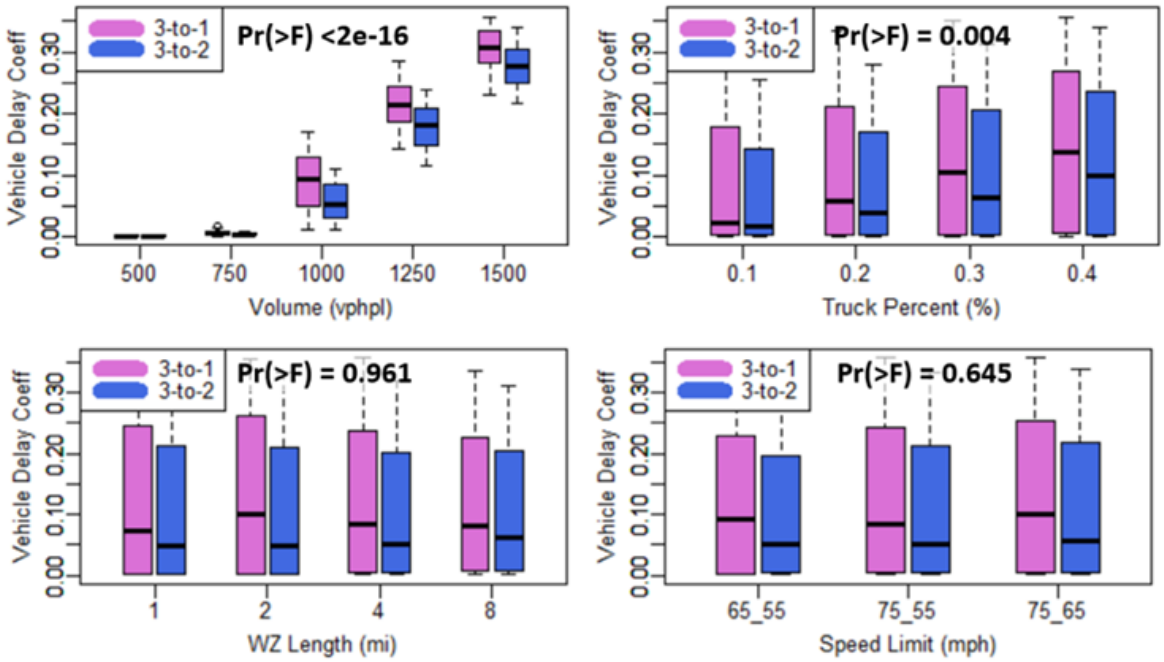

Figure 4. 7 Vehicle delay metric changes as a function of volume, truck percent, WZ length and speed limit at 6-lane work zone.

Figure 4.8 shows the incremental rate of increase in queue length as a function of traffic volume, truck percentage, work zone length, and work zone speed limit at 3-to-2 work zones (in hot pink color) and 3-to-1 work zones (in blue color), respectively.

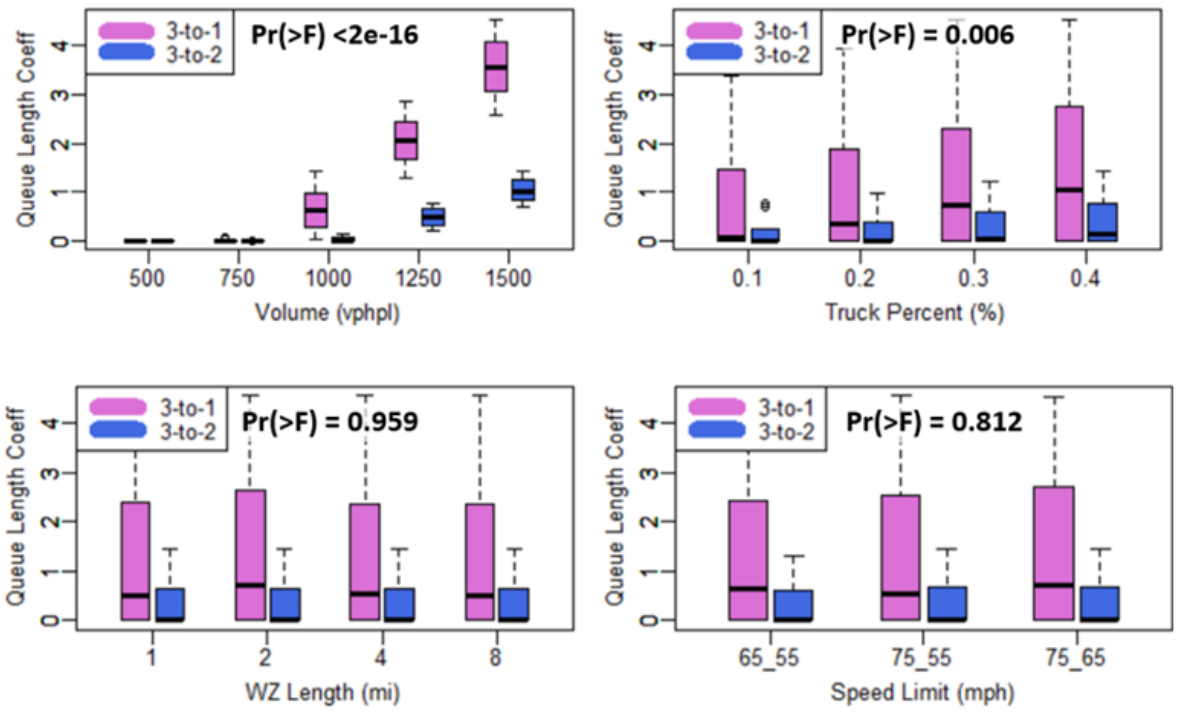

Figure 4. 8 Queue length metric changes as a function of volume, truck percent, WZ length and speed limit at 6-lane work zone.

Three observations can be concluded from Figure 4.6 to Figure 4.8 regarding the travel time, vehicle delay, and queue length, which share similar trends.

- As results show in the previous example scenario, the operational performance metrics (e.g., travel time, vehicle delay, and queue length) increase considerably as traffic volume increases. The Welch t-test is used to statistically test the difference between the mean values of the performance metrics of the 3-to-1 and 3-to-2 work zone configurations. The p-values for the variable significance are all smaller than 0.05, indicating a statistically significant difference between the two groups (i.e., 3-to-1 and 3-to-2).
- The increase in truck percentage also shows significance in contributing to the increase in travel time, vehicle delay, and queue length. The contribution of the truck percentage

is less than the factor of traffic volume.

- Work zone length and speed limit do not seem to be significant factors because they do not increase significantly as traffic volume, truck percentage, work zone length, and/or work zone speed limit increase. They have p-values larger than 0.05, the significance level.
- Travel time, vehicle delay, and queue length at 3-to-1 work zones perform worse compared to operations at 3-to-2 work zones. These show a longer travel time, a longer vehicle delay, and a longer queue length under the impact of different factors.

4.3 Sensitivity Analysis of the Two-lane Work Zone Case

An operational work zone for traffic movement on Highway 30 at Clarks, Nebraska is used as the test site. The empirical data collection process, the work zone model calibration, and validation results were discussed in Section 3.2. Figure 4.9 shows 1) the test site, 2) the data collection setup, and 3) the model calibration results. It may be seen the model simulation results are similar to the observed travel data. This calibrated model is used to undertake the sensitivity analysis and a sample of the results is discussed in subsequent sections. Details of all of the scenario results are presented in the Appendix of this report.

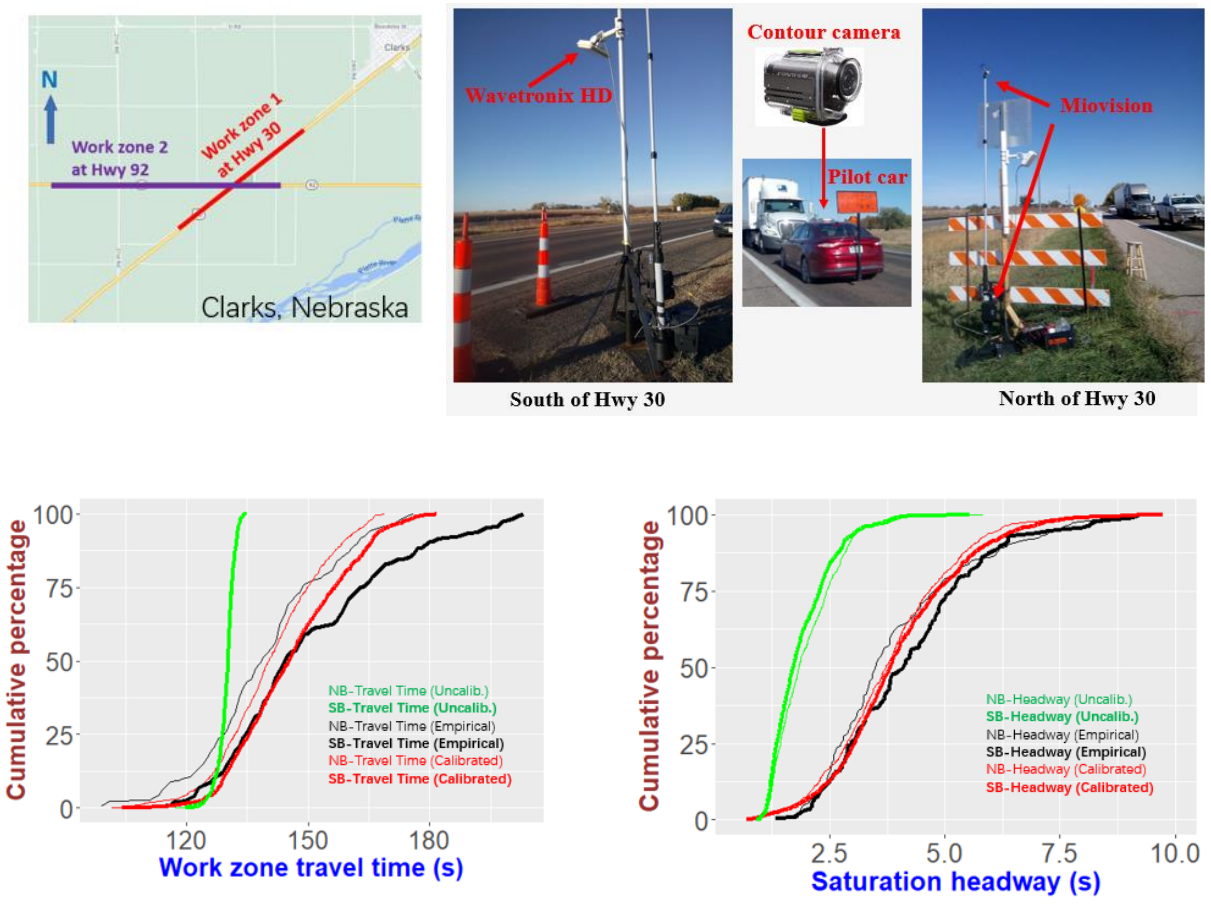

Figure 4. 9 Test site description and calibration results of the two-lane case.

4.3.1 Two-lane Work Zone Model Capacity Estimates

Sensitivity analyses of estimated capacity for various truck percentages (i.e., 0%, 20%, and 40%), work zone length (i.e., 0.25 to 4 miles), and speed limit (i.e., 50 and 65 mph) are conducted. Results are shown in **Error! Reference source not found.**.

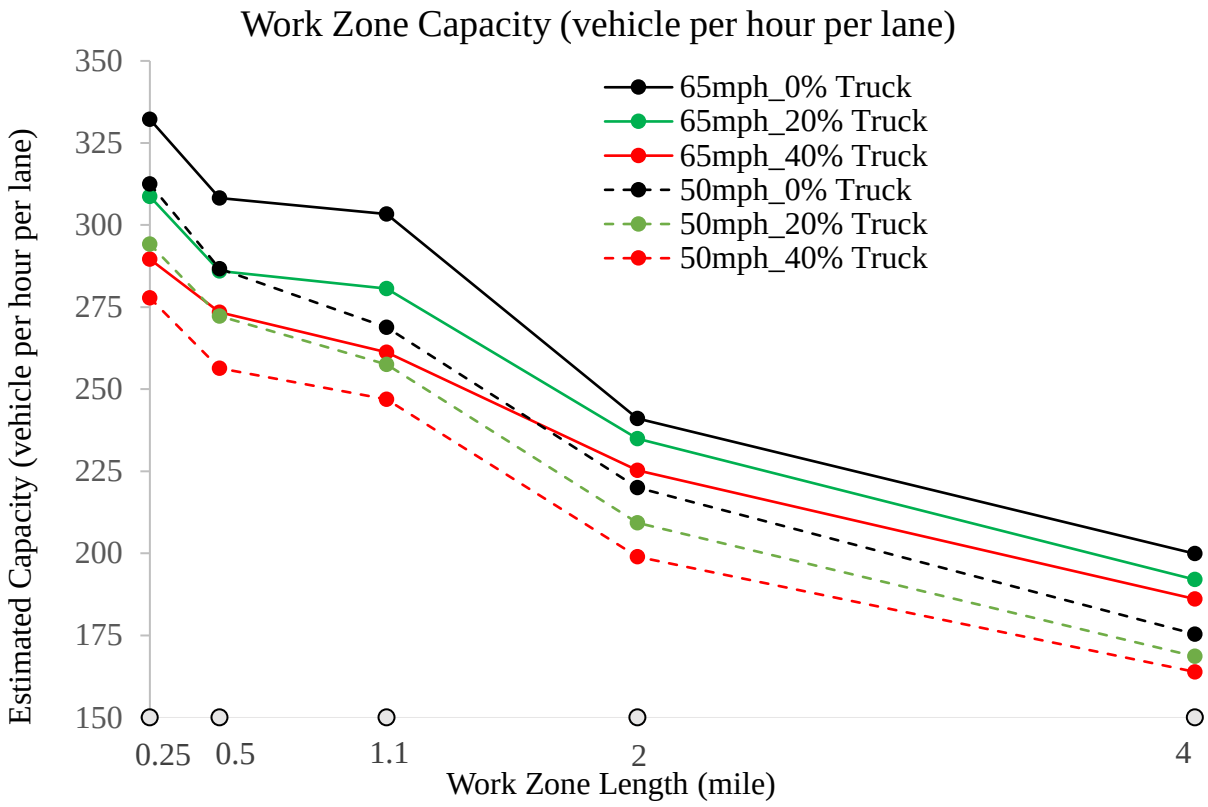

Figure 4. 10 Estimated work zone capacity analysis

As can be found in Figure 4.10, the capacity reduction is up to 12% when truck percentage varies from 0% to 40%. When work zone length varies from 0.25 miles to 4 miles, capacity is reduced up to 45%. Note the speed limits at 50 mph (i.e., dashed lines) and 65 mph (i.e., solid lines) do not show substantial differences at different levels of truck percentage and work zone lengths. It can therefore be argued that work zone length has the greatest impact on work zone capacity.

4.3.2 Two-lane Work Zone Model Queue Length Estimates

When the posted speed limit of a two-lane highway is 65 mph, the results of the maximum queue length from work zones are shown in Figure 4.11 for various truck percentages (0%, 20%, 40%), work zone lengths (0.25 to 4 miles), and traffic demand (150 vphpl and 300 vphpl).

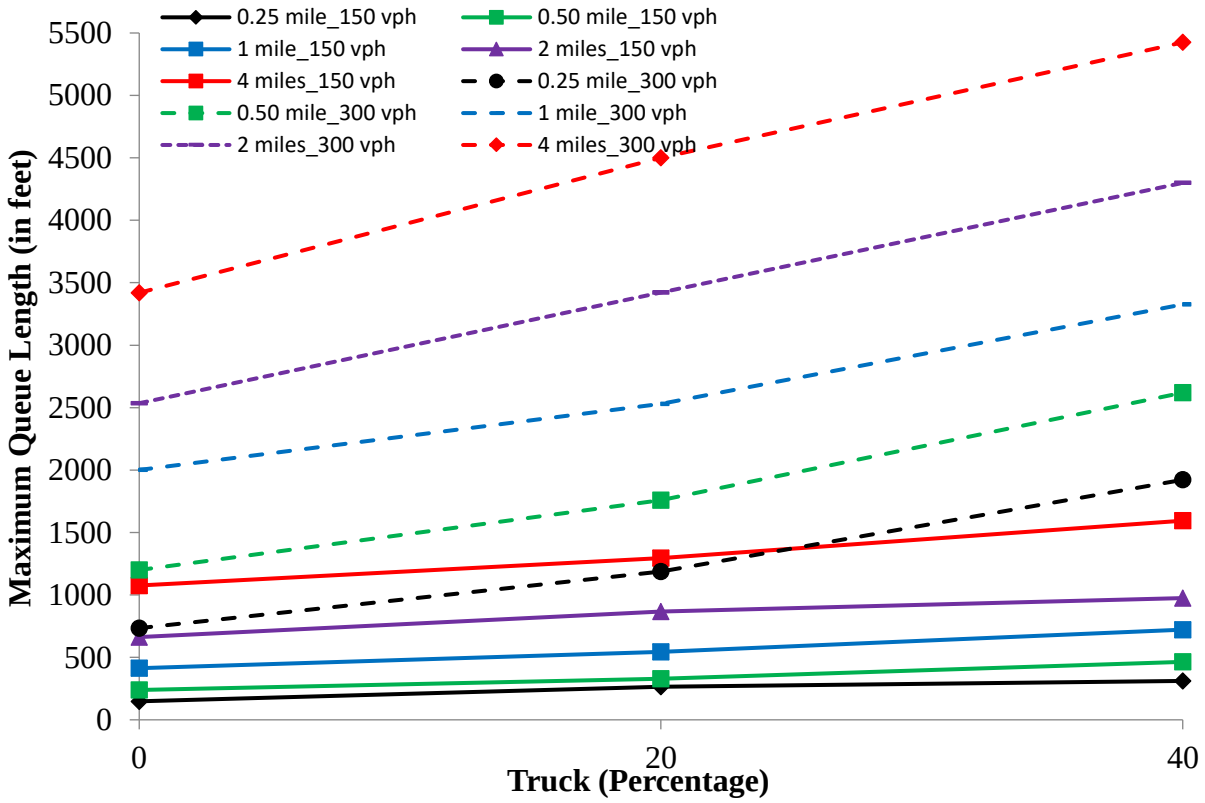

Figure 4. 11 Sensitivity analysis for active work zone duration of 1 hour

As can be seen in Figure 4.11, the maximum queue length increases with increases in traffic volume, truck percentage, and work zone length. Not surprisingly, queue length is impacted the most when there is an increase in traffic volume. This impact is amplified when the work zone length increases at a given traffic volume.

In the case of 0.25 miles of work zone, the maximum queue length is approximately 311 and 1920 feet for 150 and 300 vph with 40% truck, respectively. If work zone length is increased to four miles, the maximum queue length increases to approximately 1600 feet and 5500 feet. Note that any higher traffic volume than this can cause substantial growth in queues, and it will keep increasing as the length of work zone operation increases.

4.3.3 Two-lane Work Zone Model Delay Estimates

The result of delay change is shown in Figure 4.12 for various traffic demand (150 and 300 vphpl), truck percentage (0%, 20%, and 40%), work zone length (0.25 to 4 miles).

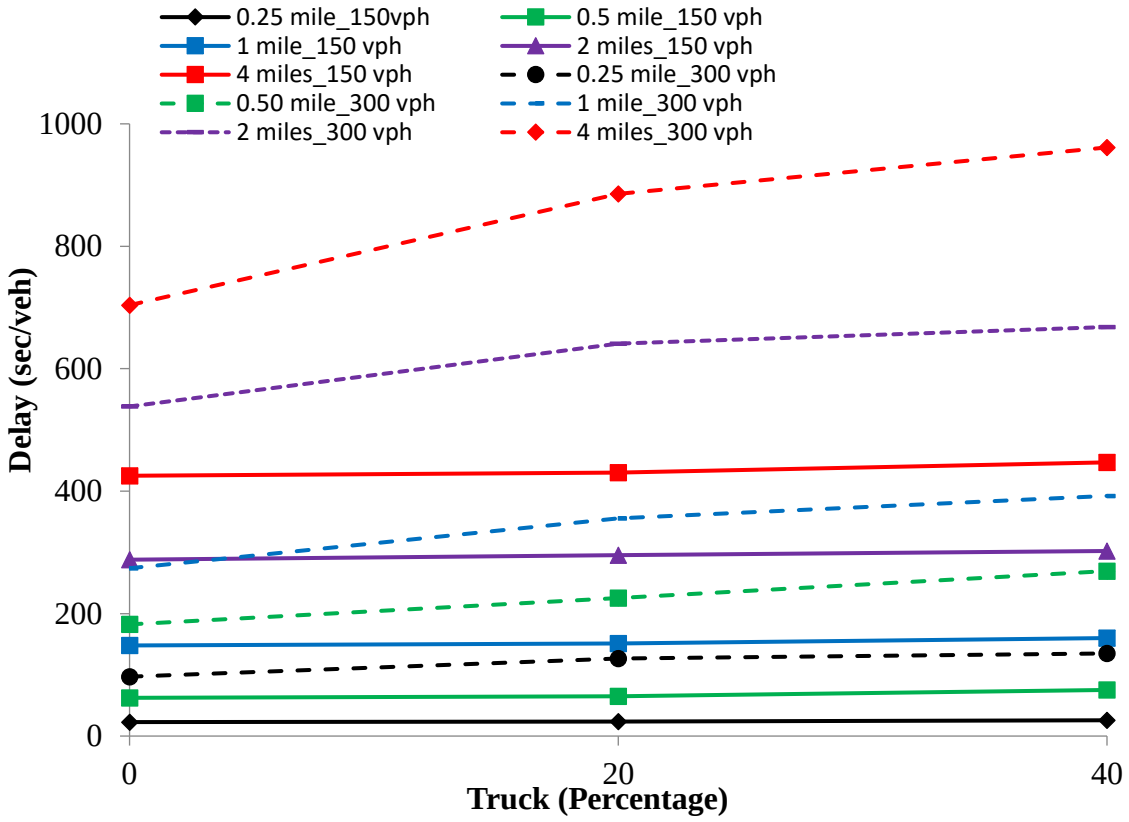

Figure 4. 2 Delay varies over truck percentage, demand, and work zone length

As can be seen in Figure 4.12, the sensitivity analysis for an active work zone duration of 1-hour results in the average vehicle delay increasing by 450 seconds when the work zone length increases from 0.25 to 4 miles for 150 vphpl with 40% truck. With demand of 300 vphpl, the delay substantially doubles to 961 seconds. It demonstrates that if traffic demand approaches capacity, work zones can experience substantial delays.

4.4 Sensitivity Analysis of Vehicle Emission Performance

A MOtor Vehicle Emission Simulator (MOVES) is used to model the sensitivity of the vehicle emission performance using the outcome of the calibrated work zone models as a key input. MOVES is the state-of-the-science emission modeling software and the most accurate tool for estimating transport sector emissions (US EPA https://www.epa.gov/moves/latest-version-motor-vehicle-emission-simulator-moves). It incorporates the latest data on emission rates and fuel supply information in the US. The MOVES output emissions (in grams) and total energy usage (in joules) are functions of vehicle type and fuel type e.g., CO_2, CO_2_Eq, CO, NO_2, NO, N_2O, NO_x, Total Energy, HC, VOC, PM_{10}, PM_{25}.

The MOVES Simulator has 10 different on-road algorithms i.e., Running Exhaust, Start Exhaust, Hoteling Emissions, Crankcase, Brake Wear, Tire Wear, Evaporative Permeation, Evaporative Fuel Vapor Venting, Evaporative Fuel Leaks, and Refueling Displacement Vapor and Spillage Loss.

In this project, the Running Exhaust (RE) algorithm is used – because it is the typical mobile source emission algorithm to estimate exhaust emissions from running vehicles at operating temperature. The major project-level emission components for the RE algorithm are

Link information, Vehicle population information, and Vehicle characteristics and activity data. Figure 4.15 shows the flow chart of the RE algorithm.

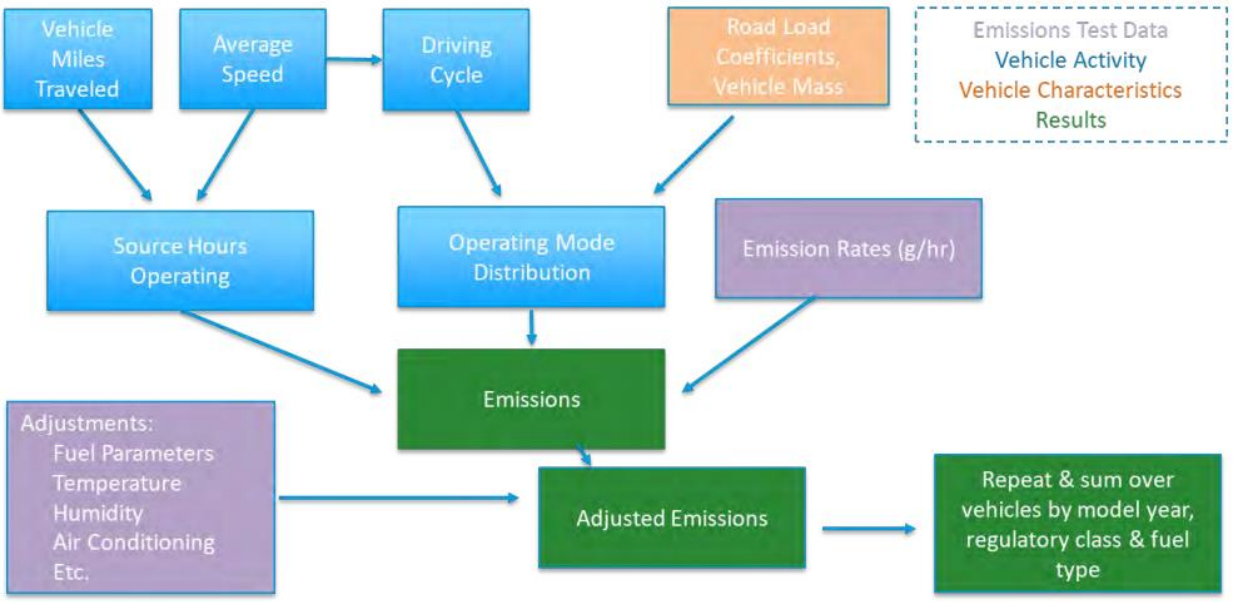

Figure 4. 3 Running exhaust algorithm flow chart
(Source: EPA 2021 https://nepis.epa.gov/Exe/ZyPDF.cgi?Dockey=P1011KV2.pdf)

4.4.1 MOVES Work Zone Model & Results – Nebraska Conditions

Each outcome of the 1460 scenarios discussed in the previous chapter was used as input in the MOVES model. It is important to note that only the outcome of one run is used in the emission model. Every scenario is modeled with or without lane closure and the differences in emission outcome are used as the net emission. In summary, there are a total of 2560 scenarios analyzed. E.g.,

- 6-lane case: 640 scenarios - [Length (4), Volume (5), Truck % (4), Speed (2), Type (2), Lane closure (2)]

- 4-lane case: 480 scenarios - [Length (4), Volume (5), Truck % (4), Speed (3), Lane closure (2)]

- 2-lane case:1440 scenarios - [Length (5), Volume (9), Truck % (4), Speed (4), Lane closure (2)]

For each scenario, there are seven different combinations modeled consisting ted of three vehicle types (PC, SU Long-haul Truck, and Combination Long-haul truck) and four fuel types (Gasoline, Diesel Fuel, Compressed Natural Gas, and Ethanol). Each of these seven combinations results in 12 different vehicle emission outcomes, i.e., running emissions in grams of CO_2, CO_{2_equiv}, CO, NO_2, N_2O, NO, NO_x, Total HC, VOC, $PM_{10,}$ and $PM_{2.5,}$ and energy consumptions in joules. Consequently, there are 215,040 outcomes comprising *2560 scenarios x 7 combinations x 12 outcomes.* These are presented in the Appendix of this report.

Table 4.5 shows a sample of 84 outcomes for scenario #41. This scenario consists of 1000 vphpl, 10% truck, work zone length of 2 mi, work zone approach lanes reduced from three to one, and a 75-mph posted speed in non-WZ reduced to 55 mph at the work zone. It is important to note that five miles of the non-work zone segment from the taper of the work zone are included in the emission analysis e.g., a total segment length of seven miles is analyzed if the work zone length is two miles.

Table 4. 5 Sample Scenario Emission Results

Scenario	Volume	Truck %	WZL	WZT	Speed	Source	Fuel	CO2	CO2_Eq	CO	NO2	NO	N2O	NOx	TotalEnergy	TotalHC	VOC	PM10	PM25
41	1000	10	2	3_1	75_55	21	1	1825049	1827188	19075	171	1528	7	1713	25394989056	366	293	21	19
41	1000	10	2	3_1	75_55	21	2	13133	13137	101	1	4	0	6	178291424	1	1	0	0
41	1000	10	2	3_1	75_55	21	5	1107	1108	8	0	0	0	0	15561118	0	0	0	0
41	1000	10	2	3_1	75_55	53	1	14630	14708	216	2	28	0	30	203570400	6	6	0	0
41	1000	10	2	3_1	75_55	53	2	48791	48834	137	20	163	0	184	662368576	31	35	13	12
41	1000	10	2	3_1	75_55	53	3	513	519	11	0	0	0	0	8684490	6	0	0	0
41	1000	10	2	3_1	75_55	62	2	351982	352206	903	218	1388	1	1620	4778400768	130	143	71	66

Legend		
Emission Data	**Value**	**Exmplanation**
sourceTypeID	21	Passenger Car
sourceTypeID	53	Single Unit Long-haul Truck
sourceTypeID	62	Combination Long-haul Truck
fuelTypeID	1	Gasoline
fuelTypeID	2	Diesel Fuel
fuelTypeID	3	Compressed Natural Gas (CNG)
fuelTypeID	5	Ethanol (E-85)
Mass Units		g
Energy Units		J

The model is validated by comparing the outcome with data from the US Bureau of Transportation Statistics. It finds the results are within the acceptable range of values of the national estimates. Table 4.6 shows a sample validation of the outcome for Scenario # 57 (with and without lane closure as in Figure 4.14).

No lane closure

Scenario	Volume	Truck %	WZL	WZT	Speed	Source	Fuel	CO2	CO2_Eq	CO	NO2	NO	N2O	NOx	TotalEnergy	TotalHC	VOC	PM10	PM25
57	1000	10	2	3_1	75_65	21	1	1841798	1843803	19651	176	1566	7	1756	25627918336	363	290	20	18
57	1000	10	2	3_1	75_65	21	2	13250	13253	104	1	4	0	6	179874304	1	1	0	0
57	1000	10	2	3_1	75_65	21	5	1117	1118	9	0	0	0	0	15707300	0	0	0	0
57	1000	10	2	3_1	75_65	53	1	13850	13923	204	2	27	0	29	192719280	6	5	0	0
57	1000	10	2	3_1	75_65	53	2	46258	46298	129	19	155	0	175	627990912	30	33	13	12
57	1000	10	2	3_1	75_65	53	3	485	491	11	0	0	0	0	8217015	5	0	0	0
57	1000	10	2	3_1	75_65	62	2	333884	334093	853	207	1319	1	1538	4532704256	122	135	67	62

Lane closure

Scenario	Volume	Truck %	WZL	WZT	Speed	Source	Fuel	CO2	CO2_Eq	CO	NO2	NO	N2O	NOx	TotalEnergy	TotalHC	VOC	PM10	PM25
57	1000	10	2	3_1	75_65	21	1	2080571	2082785	33773	207	1846	7	2069	28950478848	476	381	36	32
57	1000	10	2	3_1	75_65	21	2	14944	14948	180	1	5	0	7	202880400	2	2	0	0
57	1000	10	2	3_1	75_65	21	5	1263	1264	15	0	0	0	0	17752420	0	0	0	0
57	1000	10	2	3_1	75_65	53	1	15798	15878	249	2	29	0	31	219817792	7	6	0	0
57	1000	10	2	3_1	75_65	53	2	58737	58781	142	26	217	0	244	797390912	31	35	15	14
57	1000	10	2	3_1	75_65	53	3	590	597	12	0	0	0	1	9990852	6	0	0	0
57	1000	10	2	3_1	75_65	62	2	448817	449047	965	299	1911	1	2227	6092990976	131	144	89	81

Figure 4. 44 Output of a sample emissions scenario analysis

Table 4. 6 National Emission Estimates Vs Simulation Estimations

Vehicle	Pollutant	*National estimation (g/mi)	MOVES (g/mi)	
			No closure	Closure
PC (gasoline)	CO	**4.15**	19651/(900*7) **3.12**	33773/(900*7) **5.36**
Heavy Truck (diesel)	CO	**2.00**	853/(80*7) **1.52**	965/(80*7) **1.72**

* US Bureau of Statistics

It may be seen from Table 4.6 the estimated emissions are realistic and similar to the national estimates. Similar results are obtained when other scenarios are randomly sampled and checked with the national estimates. It should be noted that EPA default model values e.g., fuel-related data such as fuel usage fractions, vehicle weight & resistance (e.g., rolling, rotating, & aerodynamic) based on the national estimates are applied.

As previously stated, the detailed model results are presented in the Appendix of this report. Figures 4.15 to 4.17 illustrate a sample of the results showing the impact of volume, work zone length, and speed on the estimated vehicle emissions.

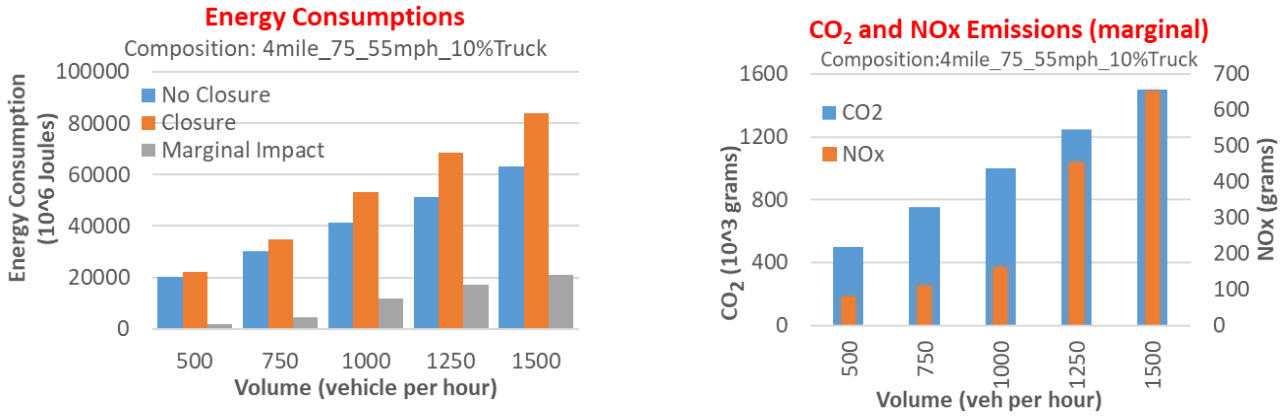

Figure 4. 5 The impact of traffic volume changes on vehicle emissions

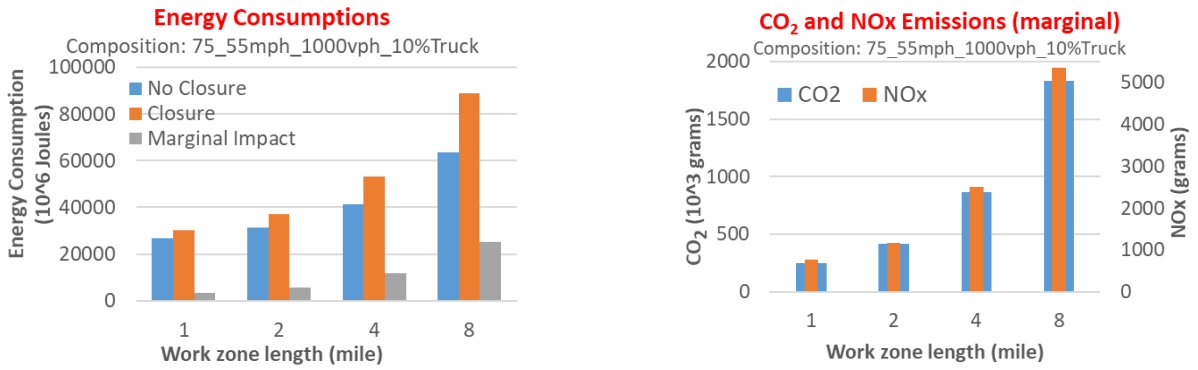

Figure 4. 66 The impact of work zone length on vehicle emissions

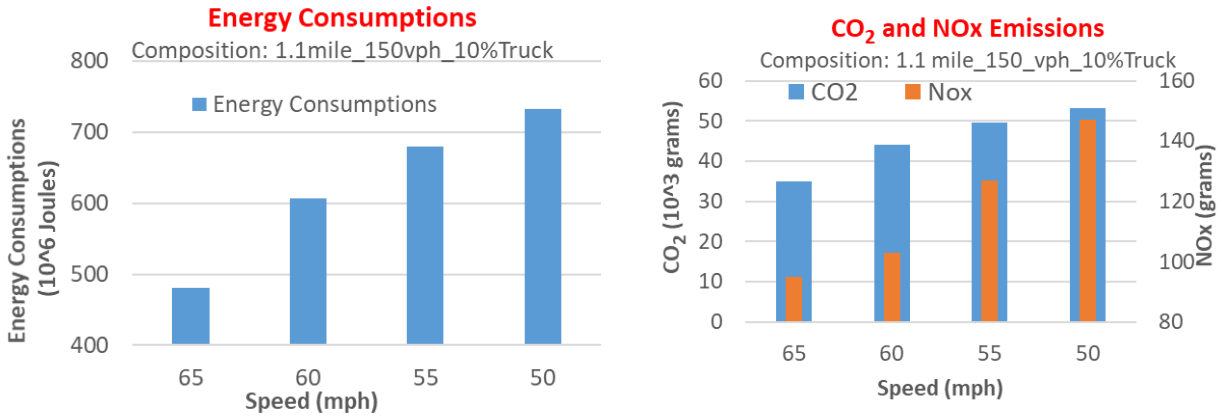

Figure 4. 7 The impact of posted speed on vehicle emissions

The results from Figures 4.15 to 4.17 are not surprising. For example, in all cases, it is evident that vehicle emissions are higher for lane closure conditions than for no-closure conditions. In addition, the higher the traffic volume, the longer the work zone length, and the slower the speeds, resulting in higher vehicle emissions. Interestingly, the marginal differences between lane closure and non-lane closure conditions increase linearly as traffic volume increases. Similar trends are observed as work zone length increases, and as speed reduces. Comparable results are found for all other scenarios.

5 THE COSTS OF LANE CLOSURE MODEL

5.1 Introduction

The lane closure cost simulation model examines the cost of changes in road user time, emissions, and fuel cost under hundreds of alternative lane closure scenarios. The model utilizes changes in travel time, emissions of various greenhouse gases (i.e., CO2, CO, NOx, VOC) and fuel use (gasoline, diesel, CNG, E-85 Ethanol) under 1,460 lane closure scenarios developed by engineers who are part of the research team. Those scenarios span the type of road, traffic volume, reduction in speed, share of vehicles which are trucks, and the length of the lane closure. The economics team estimates values related to travel time, greenhouse gas emission, and fuel use in order to simulate the daily cost of lane closures.

Cost estimate methodologies for travel time, emissions, and fuel use are described in more detail in the sections below, but detailed information about the scenarios is provided here.

There are three specific road types examined: two-lane roads, four-lane roads and six-lane roads. Lane closure on two-lane roads lead to shared use of a single lane (1B) by traffic coming in both directions. Lane closure on a four-lane road leads to sharing of a single lane by travelers heading in one direction (2-1). Lane closure on a six-lane road leads to the sharing of two-lanes in one scenario (3-2), or a single lane in the other scenario (3-1) by travelers heading in one direction. Analysts using the model for daily cost simulations would enter whether the lane closure takes place on a two-lane (1B), four-lane (2-1) or six-lane (3-2 or 3-1) highway.

Analysts running a simulation would also enter the length of the work zone for the lane closure. The length of the work zone could be as little as 0.25 miles to as much as four miles on a

two-lane road. Work zone lengths would vary between one mile and eight miles on four-lane and six-lane roads.

Scenarios also differ by the amount of hourly traffic on each remaining open lane (lanes). There is significant variation in hourly traffic volumes based on the type of road (two-lane, four-lane or six-lane) and under congested or uncongested conditions. Traffic volume on open lanes could vary from 100 to 1500. The potential that traffic volume can vary by time of day means analysts need to enter a traffic volume for each of the 24 one-hour periods during a day.

Analysis using the model to run daily cost simulations would also enter the expected change in speed in the work zone. On a two-lane road, the work zone could cause a decline from 65, 60, or 55 miles per hour to a "slow" speed. On a four-lane road, drivers would slow from 65 to 45, 65 to 55, or 75 to 55, depending on the scenario. On a six-lane road, drivers would slow from 75 to 65 or 75 to 55.

Cost scenarios would also vary by the truck and passenger vehicle mix. The share of trucks could be 10%, 20%, 30%, or 40% on a four-lane or six-lane road. The costs of delay and idling in terms of travel time, emissions, and fuel use can obviously vary substantially between trucks and passenger vehicles.

The fact values for traffic volume, change in speed, share of trucks, and work zone lengths are discrete implies it may not be possible to find a lane closure scenario that precisely matches all possible work zone designs that occur in Nebraska over a year. However, the 1,280 scenarios that are available mean it should be feasible to simulate a very similar scenario.

From a traffic perspective, each of the lane closure scenarios yields a different result in terms of the change (typically an increase) in travel time (trucks and passenger cars), emissions (by type of greenhouse gas) and fuel use (by type of fuel). The economic analysis develops estimates of time, emissions, and fuel use costs to simulate the increase in hourly road user costs associated with a lane closure. Methods for discussing time costs, emissions costs, and fuel costs are discussed in the sections which follow.

5.2 Travel Time Costs

Separate travel time costs per hour were estimated for trucks and passenger vehicles. Costs reflected both vehicle occupancy rates and the value of an hour of time. The value of the hour of time varied based on hourly wages and/or benefits for truckers (trucks) and the public at large (passenger vehicles). For passenger vehicles, the value of an hour of time also varied depending on whether passengers were at work or at leisure.

The review of the approaches to valuing travel time and specific estimates of the value of time per vehicle hour presented in Section 2.3 are based on the *Revised Departmental Guidance on Valuation of Travel Time in Economic Analysis* from the Office of the Secretary of the U.S. Department of Transportation. The guidance was issued in September 2016, but the methodology provided can be used in later years. The value of time for business travel is hourly wages plus hourly benefits. The value of time for personal travel is calculated in a different way since not all members of a household are engaged in the labor force, and the value of leisure time may be less than hourly compensation. As a result, the value of personal travel is based on the "hourly" value of personal income, calculated by dividing median household income by 2,080 hours worked per year. Departmental guidance further indicates that the value of personal travel for each individual is valued at 50% of hourly income for local travel and 70% of hourly income for intercity travel.

Tables 5.1 and 5.2 below shows the method of calculating the value of travel time per vehicle mile for automobiles and trucks. Estimates in Table 5.1 and 5.2 use national values for relevant variables such as household income, wages, and benefits. While not shown in Tables 5.1 and 5.2, the value of time was also calculated using Nebraska income and wages using a similar methodology. Analysts have the option of using Nebraska values rather than national values.

In Table 5.1, the hourly value of personal travel time per person is calculated based on estimated 2021 median household income in United States[1] divided by 2080 hours. Personal travel time includes shopping, social, or recreation purposes and commuting to and from work. The time value per hour of vehicle travel by trip purpose is obtained by multiplying the value of time per person by vehicle by average vehicle occupancy, which is available from the 2017 *National Transportation Survey*. The aggregate time value for an hour of personal automobile travel is the weighted average of the value of time for shopping, other family/personal trips, social/recreational trips, and commuting to and from work. The weights are the share of U.S. miles driven for each purpose, again taken from the 2017 *National Travel Survey*. The aggregate time value for an hour of personal automobile travel is $28.08 for local travel and $29.18 for intercity travel.

[1] The American Community Survey reports at 2019 value of median household income in Nebraska of $65,712. The value was estimated to be $69,769 in 2021 based on data from the National Association of Realtors that median family income grew by 10.3 percent in nominal terms from 2019 to 2021.

Table 5. 1 Method for Calculating the Time Cost of an Hour of Vehicle Travel using U.S. Income and Wages

	House-hold Income	Annual Hours	Hourly Rate	Share of Time Value	Time Value Per Person Hour	Persons Per Vehicle	Time Value Per Vehicle Hour	Share of Travel	Time Cost Value Per Vehicle Hour
Local Personal Travel									
Shopping	$72,509	2080	$34.86	50%	$17.43	1.82	$31.72	17.1%	
Other Family/Personal	$72,509	2080	$34.86	50%	$17.43	1.82	$31.72	19.5%	
Social/Recreational	$72,509	2080	$34.86	50%	$17.43	2.10	$36.60	28.3%	
To/From Work	$72,509	2080	$34.86	50%	$17.43	1.18	$19.79	35.1%	
Hourly Value of Auto Travel for Personal Local Use (Weighted Average)									$29.18
Intercity Personal Travel									
Shopping	$72,509	2080	$34.86	70%	$24.40	1.82	$44.41	17.1%	
Other Family/Personal	$72,509	2080	$34.86	70%	$24.40	1.82	$44.41	19.5%	
Social/Recreational	$72,509	2080	$34.86	70%	$24.40	2.10	$51.24	28.3%	
To/From Work	$72,509	2080	$34.86	70%	$24.40	1.18	$28.79	35.1%	
Hourly Value of Auto Travel for Personal Intercity Use (Weighted Average)									$40.85
Hourly Value of Auto Travel Work (Local and Intercity)			$30.34	100%	$30.34	1.00	$30.34	100%	$30.34
Truck Travel (Local and Intercity)			$33.45	100%	$33.45	1.00	$33.45	100%	$33.45

The value of an hour of automobile travel at work is based on the median hourly wage for all occupations plus estimated hourly benefits. Median hourly wage data for all occupations comes from the May 2020 *Occupation Employment and Wage Statistics* of the U.S. Bureau of Labor Statistics.[2] Year 2020 values are updated to 2021 estimates using the inflation rate. The ratio of benefits to wages for all occupations is available from the *National Compensation Survey* of the U.S. Bureau of Labor Statistics.[3] That survey indicates there are $0.44 of benefits for each $1.00 in wages for all private industry workers.

The value of an hour of truck travel is assumed to always take place at work and is based on the median hourly wage for truck drivers plus estimate hourly benefits. The sources are the same as for calculating the value of an hour of automobile travel at work. The median hourly wage for truck drivers is the weighted average of the value for heavy and tractor trailer truck drivers and light truck and delivery drivers. Weights are based on the number of workers in each category in the United States. *The National Compensation Survey* indicates there are $0.52 of benefits for each $1.00 in wages for all private transportation and material moving workers.

Table 5.1 shows how the time value of an hour of automobile travel is calculated for local personal travel, intercity personal travel, and for work. The appropriate aggregate value for an hour of automobile travel will require a weighted average of the three values, based on local conditions.

Table 5.2 shows how the aggregate is calculated. The default values are that 20 percent of all automobile vehicle miles are for work travel and 80 percent of automobile vehicle miles are for personal travel. For personal travel, the default is that 50 percent of personal travel is local

[2] Available at https://www.bls.gov/oes/
[3] https://www.bls.gov/ncs/

and 50 percent is intercity. These default values can be adjusted based on the specific lane closure project. Table 5.2 shows an estimate of the time value of an hour of automobile travel under these default assumptions. The estimated time value is $34.08 per hour.

Table 5. 2 Aggregate Value for an Hour of Automobile Travel using U.S. Income and Wages

Type of Trip	Time Value of an Automobile Vehicle Hour	Weight (Default Share)	Time Value of an Automobile Vehicle Hour
Work	$30.34	20%	
Local Personal	$29.18	40%	
Intercity Personal	$40.85	40%	
Weighted Average			$34.08

Summing up, Table 5.1 showed the time value of an hour of truck travel is $33.45, and Table 5.2 showed that the time value of an hour of automobile travel is $34.08 under default assumptions. These two values can be applied to engineering estimates of the time delay resulting from a particular lane closure project. An example is provided in Table 5.3 below for a single hour of the day for a particular lane closure project.

The characteristics of the example lane closure project are:

- single lane closure is on a six-lane divided highway (three to two lanes)
- work zone length is eight miles
- speed reduces from 75 to 55 miles
- 10 percent of vehicles are trucks
- 750 vehicles per hour travel on each of the two open lanes

Table 5. 3 Hourly Value of Increased Travel Time for an Example Lane Closure Project

Increase in Vehicle Hours Traveled During Hour	Percent Trucks	Value of an Hour of Truck Travel	Value of an Hour of Auto Travel	Value of Increased Truck Travel During Hour	Value of Increased Automobile Travel During Hour	Total Value of Increased Vehicle Travel During Hour
3.894	10%	$33.45	$34.08	$13.03	$119.44	$132.48

Under the scenario described in conditions one through five above, the travel time costs of a lane closure would be $132.48 during the hour. Most of these costs would be due to delays for automobiles as autos account for 90% of the vehicles.

5.3 Emissions Costs

Engineering estimates identified the change in emissions of multiple types of greenhouse gases as a result of lane closure projects. Most types of emissions rise as vehicles spend more time idling or traveling in halting traffic with more fluctuation of speed. Engineering estimates assessed the change in each type of emissions in grams under alternative lane closure scenarios. The types of greenhouse gases modeled in engineering estimates are reported in Table 5.4 below.

Table 5.4 also provides estimates of the dollar value per gram of increased emissions for each type of greenhouse gas. A review of economic research found the health and environmental cost of these emissions on a metric ton or short-ton basis. Table 5.4 shows the value, year, and source of those estimates and shows how each estimate is updated to produce costs for gram of emissions in 2021 dollars.

Table 5. 4 Method for Estimate the Cost Per Gram of Greenhouse Gas Emissions

Green-house Gas	Cost Per Ton	Grams/Ton	Cost/Gram	Year of Estimate	Conversion Factor to 2021 Dollars	Cost Per Gram in 2021 Dollars	Source
CO_2	$51/Metric Ton	1,000,000	$0.000051	2020	1.047	$0.000053	Interagency Working Group on the Cost of Green House Gases, Table ES.1
CO	$145/Short Ton	907,185	$0.000160	2010	1.243	$0.000199	The Economic and Societal Impact of Motor Vehicle Crashes, Table 3-22
N_20	$18,000/Metric Ton	1,000,000	$0.018000	2020	1.047	$0.018846	Interagency Working Group on the Cost of Green House Gases, Table ES.3
NO_X	$12,000/Short Ton	907,185	$0.013228	2010	1.243	$0.016438	The Economic and Societal Impact of Motor Vehicle Crashes, Table 3-22
VOC	$2,800/Short Ton	907,185	$0.003086	2010	1.243	$0.003835	The Economic and Societal Impact of Motor Vehicle Crashes, Table 3-22
PM10	$46,094/Short Ton	907,185	$0.050810	2010	1.243	$0.063140	The Economic and Societal Impact of Motor Vehicle Crashes, Table 3-22
PM2.5	$270,000/Short Ton	907,185	$0.297624	2010	1.243	$0.369846	The Economic and Societal Impact of Motor Vehicle Crashes, Table 3-22

Values are either gathered for 2020 from the Interagency Working Group on Social Cost of Greenhouse Gases[4] or for 2010 from The Economic and Societal Impact of Motor Vehicle Crashes 2010 (Revised)[5]. Estimates from both years are updated to 2021 values in Table 5.4 using the inflation rate in relevant years. The value per gram is lowest for CO_2 and highest for PM2.5.

Table 5.4 shows the value of a gram for each type of emissions. These values can be applied to engineering estimates of the quantity of emissions in grams for a single hour of the day for all lane closure scenarios. An example of a calculation is provided in Table 5.5 below. Once again, the characteristics of the example lane closure project are:

1) single lane closure (three to two lanes)
2) work zone length of eight miles
3) speed reduction from 75 to 55 miles
4) 10 percent of vehicles are trucks
5) 750 vehicles per hour on each of the two open lanes

[4] Interagency Worker Group on Social Cost of Green house Gases, United States Government, *Technical Support Document: Social Cost of Carbon, Methane and Nitrous Oxide, Interim Estimates* under Executive Order 13990, Tables ES.1 and ES.3 (February 2021)

[5] Blincoe, L. J., Miller, T. R., Zaloshnja, E., & Lawrence, B. A., *The Economic and Societal Impact of Motor Vehicle Crashes 2010 (Revised),* Table 3-22 (updated to 2020 using CPI), DOT HS 812 013 (May 2015)

Table 5. 5 Hourly Value of Increased Emissions for an Example Lane Closure Project

Greenhouse Gas	Change in Hourly Emissions Due to Lane Closure (grams)	Value of Emissions Per Gram	Hourly Value of Emissions
CO_2	389,940	$0.000053	$20.82
CO	18,098	$0.000199	$3.59
N_20	1	$0.018846	$0.02
NO_X	1,000	$0.016438	$16.44
VOC	147	$0.003835	$0.56
PM10	65	$0.063140	$4.10
PM2.5	60	$0.369846	$22.19
Total			**$67.73**

Under the scenario described in conditions one through five above, the value of emissions costs of a lane closure would be $67.73 during the hour. Most of these costs would be due to CO_2 and PM2.5 emissions.

5.4 Fuel Costs

Engineering estimates related to vehicle operating costs focus on the change in costs for multiple types of fuel as a result of lane closure projects. Fuel costs rise for vehicles that use gasoline, diesel, compressed natural gas (CNG), and E-85 ethanol as vehicles spend more time idling or traveling in halting traffic with more fluctuation of speed. Engineering estimates assessed the change in each type of fuel use in joules under alternative lane closure scenarios. In order to estimate increased fuel costs, the price per gallon is converted into the price per joule of energy based on the joules contained in each gallon of gasoline, diesel, CNG (gallon

equivalents), and E-85 ethanol.[6] The costs per joule for each type of fuel is calculated in Table 5.6. Data on the 2021 cost of a gallon of each fuel is gathered from sources such as *Monthly Energy Review* of the U.S. Department of Energy[7], the Alternative Fuels Data Center[8], or the web site E85 prices.[9]

Table 5. 6 Method for Estimate the Cost Per Joule of Fuel Use

Type of Fuel	2021 Cost Per Gallon	Joules/Gallon	2021 Cost Per Joule	Source
Gasoline	$3.05	122474950	$2.49 x 10^{-8}	U.S. Energy Information Administration, Monthly Energy Review, January 2022, Table 9.4, Average Price 2021 Unleaded Regular Gasoline
Diesel	$3.29	135554840	$2.42 x 10^{-8}	U.S. Energy Information Administration, Monthly Energy Review, January 2022, Table 9.4, Average Price 2021 On Highway Diesel Fuel
CNG	$2.23	3757739	$5.93 x 10^{-7}	Alternative Fuels Data Center, available at https://afdc.energy.gov/fuels/prices.html
E85	$2.33	93112190	$2.51 x 10^{-8}	E85 Prices, available at https://e85prices.com/

Costs per joule in Table 5.6 are applied to engineering estimates of the increase in joules of energy use in a single hour of the day in all lane closure scenarios. An example of a

[6] Joules/gallon, available at https://nhcleancities.org/2017/04/can-compare-energy-content-alternative-fuels-gasoline-diesel/
[7] U.S. Energy Information Administration, Monthly Energy Review, January 2022, Table 9.4, Average Price 2021 Unleaded Regular Gasoline and Average Price 2021 On Highway Diesel Fuel
[8] Alternative Fuels Data Center, available at https://afdc.energy.gov/fuels/prices.html
[9] E85 Prices, available at https://e85prices.com/

calculation is provided below in Table 5.7. Once again, the characteristics of the example lane closure project are:

1) single lane closure (three to two lanes)
2) work zone length of eight miles
3) speed reduction from 75 to 55 miles
4) 10 percent of vehicles are trucks
5) 750 vehicles per hour on each of the two open lanes

Table 5. 7 Hourly Value of Increased Fuel Costs for an Example Lane Closure Project

Type of Fuel	Change in Hourly Joules of Energy	Value of Energy Per Joule	Hourly Value of Fuel Use
Gasoline	3,920,551,168	$\$2.49 \times 10^{-8}$	$97.67
Diesel	1,464,876,608	$\$2.42 \times 10^{-8}$	$35.52
CNG	1,477,720	$\$5.93 \times 10^{-7}$	$0.88
E85	2,393,368	$\$2.51 \times 10^{-8}$	$0.06
Total			**$134.12**

Under the scenario described in conditions one through five above, the value of fuel use of a lane closure would be $134.12 during the hour. Most of these costs would be due to the increased use of gasoline and diesel fuel.

5.5 Lane Closure Costs

Total lane closure costs for a particular hour of a day would be the sum of the travel time costs, emissions costs, and fuel costs. In the case of the example used above, the total hourly cost for a time of day with a traffic volume on the open lane of 750, would be the sum of $132.48, $67.73, & $134.12. That sum is $334.33. The same lane closure project could have different

hourly costs at different times of the day, when traffic volume in the open lane is either higher or lower than 750. The cost for each hour is summed across all 24 hours to yield the total daily cost of a lane closure.

6 CONCLUDING REMARKS

Lane closures are used to facilitate activities related to construction and maintenance/operations. However, there are economic costs associated with lane closures and these may accrue to both the traveling public as well as to traffic agencies. While it is sometimes necessary to prohibit lane closures during the day to alleviate traffic congestion, there are consequences of this decision related to project delivery timelines, construction costs, and safety within the work zone. The goal of this project is to assist NDOT in effectively managing the operations of work zones to maximize the effectiveness of lane closures under Nebraska conditions. Accurate evaluation of critical performance measures (e.g., delay, capacity, costs) are key to efficient work zone management and road users' satisfaction.

The latest and 6th edition of the Highway Capacity Manual (HCM6) provides methodologies to estimate lane closure capacity reductions and delays related to various work zone conditions. The HCM6 methodology is based on a microsimulation model, and it is critical to calibrate this model to represent Nebraska conditions.

Calibration of freeways/multilane highway work zones

This study recommends calibrating the freeway intelligent work zone equipped with an advanced queue detection system in three steps. These three steps are 1) configure the desired speed distributions, by scenario, from empirical data, 2) identify the car-following headways from observation and/or from the literature, and 3) calibrate the HV acceleration characteristics. Specifically, ($\hat{\mu}$, $\hat{\sigma}$), (*CC0*, *CC1*, *CC2*), and (k_1, k_2, c, φ) are the three groups of calibrated parameters closely related to driver behavior under the AQD system. Empirical data collected from a test site was used for demonstrating the calibration process in the case study. A user may choose to calibrate the same, more, or fewer parameters than used in this section. The goal was

to demonstrate the methodology and not argue which set of microsimulation models should be observed in the field and which should be calibrated. It should be noted using a simulation would not remove the need for the local DOT to study the safety and efficiency of the work zone being implemented.

It is worth mentioning, due to issues with the AQD system, the case study did not differentiate the warning status of the traffic between slow traffic (i.e., speed between 25 and 45 mph) and the stopped traffic (i.e., speed below 25 mph). It was argued that although the detection of the speed data may affect the understanding of the lower queued speed at the work zone site, it did not necessarily affect the simulation of the AQD system in terms of when to start and end the warning message on PDMS.

Traffic simulation of the intelligent work zone is beneficial in that it provides a cost-efficient method to assess the work zone impact before the system is installed. As a follow-up study, the calibrated simulation model could be used in various studies of the AQD system such as:

- PDMS locations for the optimal distance upstream of the work zone;
- Speed thresholds for different traffic status and types of warning messages;
- Rolling interval for averaging vehicle speeds at each detector location;
- Detector spacing between speed detectors deployed upstream of the lane closure; and
- The impact of platooning of connected and automated heavy vehicles on interstate freeway work zone operations.

Calibration of two-lane highway work zones

To the best of the authors' knowledge, existing literature does not provide a methodology of microsimulation model calibration based on field observed distribution of performance measures for the two-lane work zone. In addition to describing the proposed calibration model, an example is provided on how the proposed methods are applied in an automated process using empirical data from a Highway 30 work zone in Nebraska.

This report also tested the transferability of the calibrated parameter. It was found that, when calibrated model parameters were spatially transferred, they were able to statistically predict saturation headways. Even though the model produced similar mean values as the observed mean travel time, the corresponding travel time distributions were statistically different.

In summary, eliminating the current literature gap, this report has proposed and demonstrated a microsimulation calibration and validation technique that is able to replicate the field traffic conditions for lane closures at the two-lane work zone. The authors recommend further studies to investigate the impact of the pilot car movement, intensity of work zone activities, and work zone length on vehicle speed profiles within the two-lane work zone.

Sensitivity analysis of the performance of the calibrated work zone models

The sensitivity analysis was conducted with respect to different lengths of the work zone, vehicle volume, percent trucks, and speed limit combinations that makes up 1460 scenarios. Specifically, the impact of these factors on work zone performance (e.g., capacity, delay, and average queue length) were estimated for each scenario. Each scenario was repeated five times using different random seeds in the calibrated VISSIM traffic microsimulation model and each

output (e.g., delay, queue length, etc.) was averaged using the five different runs so the results are robust and not dependent on a single run. It was found that:

1. *Multilane scenarios (Six-lane and four-lane cases)*
    - As expected, the operational performance metrics (e.g., travel time, vehicle delay, and queue length) increase considerably as traffic volume increases.
    - The increase in truck percentage also shows significance in contributing to the increase in travel time, vehicle delay, and queue length. The contribution of the truck percentage is less than the factor of traffic volume.
    - Work zone length and speed limit do not seem to be significant factors because they do not increase significantly with the increase in traffic volume, truck percentage, work zone length, and/or work zone speed limit.
    - The simulated capacities were within the range of values used in other states. A clear distinction between unsaturated and oversaturated conditions were made. It is recommended that NDOT work zone managers insist on operating below 90% capacity to avoid any oversaturated conditions that have exponential effects on travelers in terms of excessive delays, longer queue lengths and travel time.

2. *Two-lane case (2 lane undivided highway with one lane closed)*
    - The simulated capacity estimates are reasonable compared to the HCM6 estimates. The capacity ranges from 164 vphpl to 332 vphpl for different work zone lengths and truck percentages.
    - The work zone capacity is reduced by 45% when the work zone length is increased from 0.25 mi to 4 mi. Meanwhile, there is only a 12% work zone capacity reduction when truck percentage changes from 0% to 40%.

- Not surprisingly, the work zone performance is negatively affected with increasing travel volume, percentage of trucks, work zone length, and reduced speeds.
- Changes in work zone length and traffic volume can be argued to have the greatest impact on work zone capacity.

Lane Closure Costs

A lane closure cost simulation model that examines the cost of changes in road user time, emissions, and fuel costs under hundreds of alternative lane closure scenarios was developed in this project. The model utilizes changes in travel time, emissions of various greenhouse gases (i.e., CO2, CO, NOx, VOC), and fuel use (gasoline, diesel, CNG, E-85 Ethanol) under lane closure scenarios.

From a traffic perspective, each of the lane closure scenarios yields a different result in terms of the change (typically an increase) in travel time (trucks and passenger cars), emissions (by type of greenhouse gas), and fuel use (by type of fuel). Economic analysis develops estimates of time, emissions, and fuel use costs in order to simulate the increase in hourly road user costs associated with a lane closure.

A working spreadsheet has been developed to assist NDOT engineers to estimate the cost of lane closures for various closure scenarios. The fact that values for traffic volume, change in speed, share of trucks, and work zone length are discrete implies that it may not be possible to find a lane closure scenario that precisely matches all possible work zone designs that occur in Nebraska over a year. However, the hundreds of scenarios that are available imply that it should be feasible to simulate a similar scenario.

REFERENCES

Agdas, D., D. J. Warne, J. Osio-Norgaard, and F. J. Masters. Utility of Genetic Algorithms for Solving Large-scale Construction Time-cost Trade-off Problems. Journal of Computer in Civil Engineering. 2018. 32 (1): 04017072.

Algers S, Bergström P, Dahlberg M, et al. Mixed logit estimation of the value of travel time[R]. Working paper, 1998.

Al-Kaisy, A. and E. Kerestes. 2006. "Evaluation of the Effectiveness of Single-Lane Two-Way Traffic Control at Maintenance and Reconstruction Zones," Canadian Journal of Civil Engineering, Canadian Science Publishing, 33(9), pp. 1217–1226.

Ambarwati, Lasmini, Amelia K. Indraistuti, and Pretiwindya Kusumawardhani. "Estimating the Value of Time and Its Application." Open Science Journal 2.2 (2017).

Angelova, M., and T. Pencheva. Tuning Genetic Algorithm Parameters to Improve Convergence Time. International Journal of Chemical Engineering. 2011: 1–7. https://doi.org/10.1155/2011/646917.

Appiah Justice, Bhaven Naik, Scott Sorensen. Calibration of Microsimulation Models for Multimodal Freight Networks. Final Report No. MATC-UNL: 429. University of Nebraska Lincoln, 2012.

Appiah, B. Naik, R. Wojtal, and L. R. Rilett. Safety Effectiveness of Actuated Advance Warning Systems. Transportation Research Record, 2011, 2250: 19–24.

Appiah, J., B. Naik, L. Rilett, Y. Chen, and S.-J. Kim. Development of a State of the Art Traffic Microsimulation Model for Nebraska. Lincoln, NE: Nebraska DOT. 2011.

Appiah, J., L. Rilett., B. Naik, and S. Sorensen. Calibration of Microsimulation Models for Advance Warning Systems. Journal of Modern Traffic and Transportation Engineering

Research, 2012, 2(1): 41-47.

Athira I C, Muneera C P, Krishnamurthy K, et al. Estimation of value of travel time for work trips[J]. Transportation Research Procedia, 2016, 17: 116-123.

Becker, G.S., 1965. A theory of the allocation of time. Economic Journal 75 (299), 493–517

Bham, G.H., and M. C. Leu. A Driving Simulator Study to Analyze the Effects of Portable Changeable Message Signs on Mean Speeds of Drivers. Journal of Transportation Safety & Security, 2018, 10(1-2): 45-71.

Blayac T, Causse A. Value of travel time: a theoretical legitimization of some nonlinear representative utility in discrete choice models[J]. Transportation Research Part B: Methodological, 2001, 35(4): 391- 400.

Bledsoe, J., Raghunathan, D., & Ullman, J. (2014). Kansas Demonstration Project: Improvements to the Homestead Lane/I-35 Interchange in Johnson County.

Brownstone D, Ghosh A, Golob T F, et al. Drivers' willingness-to-pay to reduce travel time: evidence from the San Diego I-15 congestion pricing project[J]. Transportation Research Part A: Policy and Practice, 2003, 37(4): 373-387.

Buck, H. S., N. Mallig., and P. Vortisch. Calibrating VISSIM to analyze Delay at Signalized Intersections. Transportation Research Record 2615, no. 1 (2017): 73-81.

Button, K. (1995). What can meta-analysis tell us about the implications of transport? Regional Studies, 29(6), 507–517.

CA4PRS Software, FHWA, 2019. https://www.fhwa.dot.gov/construction/ca4prsbroc.cfm, last accessed on September 21, 2020.

Calfee J, Winston C. The value of automobile travel time: implications for congestion policy[J]. Journal of Public Economics, 1998, 69(1): 83-102.

Carlson, P. J., L. L. Higgins, M. P. Pratt, M. D. Finley, L. Theiss, W. F. Williams, V. Iragavarapu, M. Ko, and A. A. Nelson. 2015. Traffic Control Device Evaluation Program: Technical Report, Texas Department of Transportation.

Carrion C, Levinson D. Value of travel time reliability: A review of current evidence[J]. Transportation research part A: policy and practice, 2012, 46(4): 720-741.

Cassidy, M. J. and L. D. Han. 1993. "Proposed Model for Predicting Motorist Delays at Two-Lane Highway Work Zones," Journal of Transportation Engineering 119(1), pp. 27–42.

Ceder, A. An Application of an Optimal Traffic Control During Lane Closure Periods of a Two-Lane Road. Journal of Advanced Transportation, 2000. 34 (2): 173–190.

Chen. C. H., and P. Schonfeld. Work Zone Optimization for Two-Lane Highway Maintenance Projects. Transportation Research Record: Journal of the Transportation Research Board, Vol. 1877, No. 1, 2007, pp. 95–105.

Chien, Steven I-Jy, Dimitrios G. Goulias, Shmuel Yahalom, and Shoaib M. Chowdhury. "Simulation-based estimates of delays at freeway work zones." Journal of Advanced Transportation 36, no. 2 (2002): 131-156.

Chien, S., Y. Tang, and P. Schonfeld. Optimizing work zones for two-lane highway maintenance projects. Journal of Transportation Engineering, 2002. 128 (2): 145-155.

Chitturi, M. V. Methodology for Development of Delay-based Passenger Car Equivalents of Heavy Vehicles in Work Zones. PhD diss., University of Illinois at Urbana-Champaign, 2007.

Chitturi, Madhav, and Rahim Benekohal. "Comparison of QUEWZ, FRESIM and QuickZone with field data for work zones." In 83rd Annual Meeting of the Transportation Research Board, Washington, DC. 2004.

Chitturi, Madhav, and Rahim Benekohal. "Work zone queue length and delay methodology." Transportation Letters 2, no. 4 (2010): 273-283.

Daly A, Hess S. VTT or VTTS: a note on terminology for value of travel time work[J]. Transportation, 2020, 47(3): 1359-1364.

Daly, A., Tsang, F., Rohr, C.: The value of small time savings for non-business travel. In: Transport Economics and Policy, vol. 48, 2 May (2014)

Daniels, G., S. Venglar, and D. Picha. 2000. Guidelines for the Use of Portable Traffic Signals in Rural Two-Lane Maintenance Operations, Texas Department of Transportation.

de Almeida Correia G H, Looff E, van Cranenburgh S, et al. On the impact of vehicle automation on the value of travel time while performing work and leisure activities in a car: Theoretical insights and results from a stated preference survey[J]. Transportation Research Part A: Policy and Practice, 2019, 119: 359- 382.

De Borger B, Fosgerau M. The trade-off between money and travel time: A test of the theory of reference-dependent preferences[J]. Journal of urban economics, 2008, 64(1): 101-115.

De Donnea, F.X., 1972. Consumer behaviour, transport mode choice and value of time: some micro- economic models. Regional and Urban Economics 1 (4), 355–382.

Deacon, R.T., Sonstelie, J., 1985. Rationing by waiting and the value of time: results from a natural experiment. Journal of Political Economy 93, 627–647.

DeSerpa, A., 1971. A theory of the economics of time. Economic Journal 81, 828–846.

Devarasetty P C, Burris M, Shaw W D. The value of travel time and reliability-evidence from a stated preference survey and actual usage[J]. Transportation research part A: policy and practice, 2012, 46(8): 1227-1240.

Discrete choices and the trade-off between money and time: Another test of the theory of reference- dependent preferences. Paper presented at the European Transport Conference, Strasbourg, France, 2006

Domenichini, L., F. L. Torre., V. Branzi., and A. Nocentini. Speed Behaviour in Work Zone Crossovers. A driving Simulator Study. Accident Analysis & Prevention, 2017, 98: 10-24.

Dong, J., A. J. Houchin, N. Shafieirad, C. Lu., N.R. Hawkins, and S. Knickerbocker. VISSIM Calibration for Urban Freeways. Iowa State University, 2015.

Edara, P., Estimation of Traffic Impacts at Work Zones: State of the Practice, Report No. VTRC 06- R25, Virginia Department of Transportation, Richmond, VA, 2006.

Edara, Praveen, Carlos Sun, and Andrew Robertson. Effectiveness of Work Zone Intelligent Transportation Systems. Final Report, Midwest Smart Work Zone Deployment Initiative, 2013.

Ellis, R., Herbsman, Z., and Ellias, A. M. (1997). Development for improved motorist user cost determinations for FDOT construction projects, Florida Dept. of Transportation, Univ. of Florida, Gainesville, Fla.

Ettema D, Verschuren L. Multitasking and value of travel time savings[J]. Transportation Research Record, 2007, 2010(1): 19-25.

Farid, Y. Z., A. N. David., V. C. Madhav., Y. Song., W. F. Bremer., and A. R. Bill. Practices in One-lane Traffic Control on a Two-lane Rural Highway. No. Project 20-05, Topic 48-11. 2018.

Fatality Analysis Reporting System (FARS) 2019 Annual Report File. National Highway Traffic Safety Administration (NHTSA).

Federal Highway Administration. Manual on uniform traffic control devices for streets and highways, 2009 Edition. Federal Highway Administration, U.S. Department of Transportation, Washington, D.C.: 2009.

Federal Highway Administration. Office of Safety Research and Development. Surrogate safety measures from traffic simulation models. Updated on Mar. 8, 2016. https:\www.fhwa.dot.gov\publications\research\safety\03050\04.cfm. Accessed May 25, 2021.

Fezzi C, Bateman I J, Ferrini S. Using revealed preferences to estimate the value of travel time to recreation sites[J]. Journal of Environmental Economics and Management, 2014, 67(1): 58-70.

FHWA, WZ RUC. Mallela, Jagannath, and Suri Sadavisam. Work zone road user costs: Concepts and applications. No. FHWA-HOP-12-005. United States. Federal Highway Administration, 2011.

FHWA. 2009. Manual on Uniform Traffic Control Devices (MUTCD) for Streets and Highways, Federal Highway Administration.

FHWA. Guideline for Applying Traffic Modeling Simulation Software. https://ops.fhwa.dot.gov/trafficanalysistools/tat_vol3/sect5.htm. Accessed July 26, 2021.

Finley, M. D., P. Songchitruksa, and S. R. Sunkari. 2014. Evaluation of Innovative Devices to Control Traffic Entering from Low-Volume Access Points within a Lane Closure," Texas Department of Transportation.

Finley, M.D.; Songchitruksa, P.; Jenkins, J. Evaluation of Alternative Methods of Temporary Traffic Control on Rural One-Lane, Two-way Highways; Texas A&M Transportation Institute: College Station, TX, USA, 2015.

Florida DOT. 2017. Standard Specifications for Road and Bridge Construction, Florida Department of Transportation.

Fosgerau M, Engelson L. The value of travel time variance[J]. Transportation Research Part B: Methodological, 2011, 45(1): 1-8.

Fosgerau M. Investigating the distribution of the value of travel time savings[J]. Transportation Research Part B: Methodological, 2006, 40(8): 688-707.

Fosgerau M. Using nonparametrics to specify a model to measure the value of travel time[J]. Transportation Research Part A: Policy and Practice, 2007, 41(9): 842-856.

Fosgerau, M. 2005 Unit income elasticity of the value of travel time savings.

Hallmark. S., A. Sharma., B. Lawton., G. Basulto-Elias., A. Bilek., N. Oneyear., and T. Litteral. Assessing Driver Behavior at Back of Queues: Implications for Queue Warning System in Work Zones. Iowa State University, 2020.

Hanemann, W. M. (1991) Willingness to pay and willingness to accept: how much can they differ? American Economic Review, 81, pp. 635–647.

Hardy, M., and K. Wunderlich, Traffic Analysis Tools Volume VIII: Work Zone Analysis - A Guide for Decision-Makers, Report No. FHWA-HOP-08-029, Office of Operations, Federal Highway Administration, Washington, DC, 2008.

Hensher, D.A., 2001. Measurement of valuation of travel time savings. Journal of Transport Economics and Policy 35 (1), 71–98.

Horowitz, J. K. and McConnell, K. E. (2002) A review of WTP/WTA studies, Journal of Environmental Economics and Management, 44, pp. 426–447.

Hourdos, J., Z, Liu., P. Dirks., H. X. Liu., S. Huang., W. Sun., and L, Xiao. Development of a Queue Warning System Utilizing ATM Infrastructure System Development and Field-testing (No. MN/RC 2017-20). Minnesota Deparmtent of Transportation, 2017.

Hua, X., Y. Wang., W. Yu., W. Zhu., and W. Wang. Control Strategy Optimization for Two-Lane Highway Lane-Closure Work Zones. Sustainability 11, no. 17 (2019): 4567.

Huang, Q. and J. Shi. Optimizing Work Zones for Two-Lane Urban Road Maintenance Projects. Tsinghua Science and Technology, 2008. 13 (5): 644–650.

Huebschman, C. R., C. Garcia., D. M. Bullock., and D. M. Abraham. Construction Work Zone Safety (Report No. FHWA/IN/JTRP-2002/34). West Lafayette, IN: Purdue University, Joint Transportation Research Program, 2003.

Hultkrantz, L. and Mortazavi, R. (2001) Anomalies in the value of travel-time changes, Journal of Transport Economics and Policy, 35, pp. 285–300.

Huq M. Explaining Variations in the Value of Time Saving, The All China Economics (ACE) International Conference[C]//The Second Conference, City University of Hong Kong. 2007.

Hurtado-Beltran, A., & Rilett, L. R. (2021). Alternative Regression Model Structure for the HCM-6 Equal-Capacity Passenger Car Equivalency Methodology. Transportation Research Record, 2675(7): 581-596

Iowa DOT. 2015. Flaggers Handbook, Iowa Department of Transportation.

Ishimaru, John, and Mark Hallenbeck. QUEWZ Work Zone Software: Literature Search and Methodology Review. No. WA-RD 888.1. Washington (State). Department of Transportation, 2019.

Jara-Diaz, S., 2007. Allocation and valuation of travel-time savings. In: Handbook of Transport Modelling. second ed. Emerald Group Publishing Limited, pp. 303–319.

Jehn, N. L., and Rod E. T. Calibration of Vissim Models for Rural Freeway Lane Closures: Novel Approach to the Modification of Key Parameters. Transportation Research Record, 2019, 2673 (5): 574-583.

Jiang M, Morikawa T. Theoretical analysis on the variation of value of travel time savings[J]. Transportation Research Part A: Policy and Practice, 2004, 38(8): 551-571.

Johnson, M., 1966. Travel time and the price of leisure. Western Economic Journal 4, 135–145.

Kan, X., L. Xiao, H. Liu. et al. Cross-Comparison and Calibration of Two Microscopic Traffic Simulation Models for Complex Freeway Corridors with Dedicated Lanes. Journal of Advanced Transportation, 2019, Article ID 8618476.

Kansas DOT. 2015. Standard Specification: Section 805, Work Zone Traffic Control and Safety, Kansas Department of Transportation.

Khazraeian, S., M. Hadi., and Y. Xiao. Safety Impacts of Queue Warning in a Connected Vehicle Environment. Transportation Research Record, 2017, 2621(1): 31-37.

Kim, Seung-Jun., W. Kim., and L. R. Rilett. Calibration of Microsimulation Models using Nonparametric Statistical Techniques. Transportation Research Record 1935, no. 1 (2005): 111-119.

Kochenderfer, M. J., and T. A. Wheeler. Algorithms for optimization. Cambridge, MA: MIT Press, 2019.

Kou wenhoven M, de Jong G. Value of travel time as a function of comfort[J]. Journal of choice modelling, 2018, 28: 97-107.

Kramer, O. Genetic algorithm. Genetic algorithm essentials. New York: Springer, 2017.

Kremers, H., Nijkamp, P., & Rietveld, P. (2000). A meta-analysis of price elasticities of transport demand in a general equilibrium framework. Tinbergen Institute Discussion Paper. Tinbergen Institute, Amsterdam/Rotterdam.

Li, Yanning, Juan Carlos Martinez-Mori, and Daniel Work. Improving the Effectiveness of Smart Work Zone Technologies. ICT-16-023, Springfield: Illinois Department of Transportation (SPR), 2016.

Lu, X.Y., J.Y. Lee., D.J. Chen., and et al. Freeway Micro-simulation Calibration: Case Study using Aimsun and VISSIM with Detailed Field Data. In 93rd Annual Meeting of the Transportation Research Board, Washington, D.C., 2014.

Mackie P J, Jara-Dıaz S, Fowkes A S. The value of travel time savings in evaluation[J]. Transportation Research Part E: Logistics and Transportation Review, 2001, 37(2-3): 91-106.

Martín-Fernández, Jesús; del Cura-González, Ma Isabel; Gómez-Gascón, Tomás; Oliva-Moreno, Juan; Domínguez-Bidagor, Julia; Beamud-Lagos, Milagros; Pérez-Rivas, Francisco Javier (2010-05-10). "Differences between willingness to pay and willingness to accept for visits by a family physician: A contingent valuation study". BMC Public Health. 10 (1): 236.

MassDOT . Smarter Work Zones Technology Applicatins Case Study: Technology Applications on the Callahan Tunnel Project. 2014. https://tti.tamu.edu/featured-project/facilitating-deployment-decisions-of-highly-portable-end-of-queue-warning-systems/.

Mathew, T. V., and P. Radhakrishnan. Calibration of Microsimulation Models for Nonlane-based Heterogeneous Traffic at Signalized Intersections. Journal of Urban Planning and Development 136, no. 1 (2010): 59-66.

McCoy, P. T., G. Pesti. Effectiveness of Condition-responsive Advisory Speed Messages in Rural Freeway Work Zones. Transportation Research Record, 2002, 1794: 11–18.

Merkert R, Beck M. Value of travel time savings and willingness to pay for regional aviation[J]. Transportation Research Part A: Policy and Practice, 2017, 96: 29-42.

Metz D. The myth of travel time saving[J]. Transport reviews, 2008, 28(3): 321-336.

Michigan DOT. 2010. Traffic Regulator’s Instruction Manual, Michigan Department of Transportation.

Minnesota DOT. 2014. Minnesota Flagging Handbook, Minnesota Department of Transportation.

Missouri DOT. 2017. Typical Applications (MUTCD 6H), Missouri Department of Transportation.

Montana DOT. 2014. Standard Specifications for Road and Bridge Construction, Montana Department of Transportation.

MVAConsultancy, ITS Leeds University, TSU Oxford University, 1994. Time savings: Research into the value of time. In: Layard, R., Glaister, S. (Eds.), Cost-Benefit Analysis, pp. 235–271. Cambridge University Press, 1994.

Nam D, Park D, Khamkongkhun A. Estimation of value of travel time reliability[J]. Journal of Advanced Transportation, 2005, 39(1): 39-61.

Nebraska Annual Average Daily Traffic Counts Map. https://gis.ne.gov/portal/home/item.html?id=9da1b7650dfe4f07af4911a5bdf95e6a. Accessed, June 26, 2021.

Nebraska DOT. 2017. Standard Specifications for Highway Construction, Nebraska Department of Roads. Nebraska Department of Transportation.

Nevada DOT. 2017. Standard Plans for Road and Bridge Construction, Nevada Department of Transportation.

Ohio MUTCD. Manual on Uniform Traffic Control Devices. Ohio Department of Transportation, Columbus, Ohio, January 13, 2012. Available at http://www.dot.state.oh.us/Divisions/Engineering/Roadway/DesignStandards/traffic/OhioMUT D/Pages/OMUTCD2012_current_default.aspx. Accessed March 31, 2014.

Ohio TEM. Traffic Engineering Manual. Office of Traffic Engineering, Ohio Department of Transportation, Columbus, Ohio, January 17, 2014 Revision.

Oregon DOT. 2016. Oregon Temporary Traffic Control Handbook for Operations of Three Days or Less, Oregon Department of Transportation.

Paracha, J., & Ostroff, R. (2018). Improving Work Zones Every Day, in Every Way. Public Roads, 82(2).

Pennsylvania DOT. 2014. Temporary Traffic Control Guidelines, Publication 213, Pennsylvania Department of Transportation.

Pesti, G., C. L. Chu., H. Charara., G. L. Ullman., and K. Balke. Simulation Based Evaluation of Dynamic Queue Warning System Performance. In Transportation Research Board 92nd Annual Meeting (No. 13-5086), Washington D.C., 2013.

Pesti, G., P. Wiles., R. L. K. Cheu., P. Songchitruksa., J. Shelton., and S. Cooner. Traffic Control Strategies for Congested Freeways and Work Zones (No. FHWA/TX-08/0-5326-2). Texas Transportation Institute, 2018.

PTV VISSIM 2020 Software. User Manual. https://www.ptvgroup.com/en/solutions/products/ptv-vissim/. Accessed, May 26, 2021.

Ramjerdi F, Lindqvist Dillén J. Gap between willingness-to-pay (wtp) and willingness-to-accept (WTA) measures of value of travel time: Evidence from Norway and Sweden[J]. Transport Reviews, 2007, 27(5): 637-651.

Ramjerdi, F., Rand, L., Sætermo, I.-A. and Sælensminde, K. (1997) The Norwegian Value-of-Time Study.TØI Report No. 379/1997 (Oslo: Institute of Transport Economics).

Roelofs, T. and C. Brookes. Synthesis of Intelligent Work Zone Practices. ENT-2014-1.

ENTERPRISE Pooled Fund Study TFP-5(231), Michigan DOT, 2014.

Schoen, J. M., J. A. Bonneson., C. Safi., B. Schroeder., A. Hajbabaie., C. H. Yeom., N. Rouphail., Y. Wang., W. Zhu, and Y. Zou. NCHRP Project 3-107: Work Zone Capacity Methods for the Highway Capacity Manual, 2015.

Schonfeld, P. and S. Chien. Optimal Work Zone Lengths For Two-Lane Highways. Journal of Transportation Engineering.1999. 125 (1): 21–29.

Shibuya, S., T. Nakatsuji, T. Fujiwara, and E. Matsuyama. Traffic Control at Flagger-Operated Work Zones on Two-Lane Roads. Transportation Research Record: Journal of the Transportation Research Board, 1996. 1529: 3–9.

Shires J D, De Jong G C. An international meta-analysis of values of travel time savings[J]. Evaluation and program planning, 2009, 32(4): 315-325.

Small, K.A., Noland, R., Chu, X., Lewis, D., 1999. Valuation of Travel-Time Savings and Predictability in Congested Conditions for Highway User-Cost Estimation. National Cooperative Highway Research Program Report 431, National Academy Press, Washington, DC.

Son, Y. T. Queueing Delay Models for Two-Lane Highway Work Zones. Transportation Research Part B: Methodological, 1999. 33 (7): 459471.

Spiegelman, C., E. S. Park, and L. R. Rilett. Transportation Statistics and Microsimulation. Boca Raton, FL: CRC Press. 2010.

Strawderman, L., Y. Huang., and T. Garrison. The Effect of Design and Placement of Work-zone Warning Signs on Driver Speed Compliance: A Simulator-based Study. IIE Transactions on Occupational Ergonomics and Human Factors, 2013, 1(1): 66-75.

Tawfeek, M. H., M. E. Esawey., K. El-Araby., and H. Abdel-Latif. Calibration and Validation of Micro-simulation Models Using Measurable Variables. In Proceedings of the Annual Conference. Canadian Society for Civil Engineering. 2018.

Texas A&M Transportation Institute. Facilitating Deployment Decisions of Highly Portable End-of-Queue Warning Systems. 2018. https://tti.tamu.edu/featured-project/facilitating-deployment-decisions-of-highly-portable-end-of-queue-warning-systems/.

Transportation Research Board. Highway Capacity Manual, 5th Edition, Washington, D.C., 2010.

Transportation Research Board. Highway Capacity Manual, 6th Edition, Washington, D.C., 2016.

Tseng, Y., Verhoef, E., 2008. Value of time by time of day: a stated-preference study. Transportation Research Part B 42, 607–618.

Tufuor, E. O., and L. R. Rilett. New Travel Time Reliability Methodology for Urban Arterial Corridors. Transportation Research Record (2021): 03611981211006104.

Tufuor, E. O., L. R. Rilett., and L. Zhao. Calibrating the Highway Capacity Manual Arterial Travel Time Reliability Model. Journal of Transportation Engineering, Part A: Systems 146, no. 12 (2020): 04020131.

Uchida K. Estimating the value of travel time and of travel time reliability in road networks[J]. Transportation Research Part B: Methodological, 2014, 66: 129-147.

Ullman, G., & Schroeder, J. (2014). Mitigating work zone safety and mobility challenges through Intelligent Transportation Systems: Case Studies (No. FHWA-HOP-14-007).

USDOT Federal Highway Administration. Benefits of Using Intelligent Transportation Systems in Work Zones. Summary Report, Washington DC: US Department of Transportation Federal Highway Administration, 2008.

USDOT Federal Highway Administration. ITS in Work Zones: Using an Automated Traffic Information System to Reduce Congestion and Improve Safety During Reconstruction of the I-55 Lake Springfield Bridge in Illinois. Case Study, Washington DC: USDOT Federal Highway Administration, 2004.

VDOT. 2020. Virginia, Department of Transportation. VISSIM user guide. http://www.virginiadot.org/business/resources/VDOT_Vissim_UserGuide_Version2.0_Final_2020-01-10.pdf._Accessed, June 26, 2021.

Virginia DOT. 2015. Virginia Work Area Protection Manual: Standards and Guidelines for Temporary Traffic Control, Virginia Department of Transportation.

Wackerly, D., W. Mendenhall., and R. L. Scheaffer. Mathematical Statistics with Applications. Cengage Learning, 2014.

Wardman et al. (2016) found 389 studies for Europe alone. A Scopus search in November 2017 finds 1805 papers mentioning “value of travel time”, or VTT,

Wardman M. The value of travel time: a review of British evidence[J]. Journal of transport economics and policy, 1998: 285-316.

Wardman, M. R. (2004). Public transport values of travel time savings. Transport Policy, 11, 363-377.

Washburn, S. S., T. Hilles, and K. Heaslip. Impact of Lane Closures on Roadway Capacity: Development of a Two-Lane Work Zone Lane Closure Analysis Procedure (Part A).

2008. Research Report TRC-FDOT-59056-a-2008 for Transportation Research Center, University of Florida.

Watson, J. D. C., T. W. Hiles and S. S. Washburn. Analysis Methodology for Two-Lane Highways with a Lane Closure. Transportation Research Board 94th Annual Meeting (No. 15- 1186), 2015.

Webster, F.V. Traffic Signal Settings; Road Research Technical Paper; Road Research Laboratory: London, UK, 1958.

Willig, R. D. (1976) Consumer's surplus without apology, American Economic Review, ,589–597.

Wunderlich, K. E., M. Vasudevan., and, P. Wang. TAT Volume III: Guidelines for Applying Traffic Microsimulation Modeling Software 2019 Update to the 2004 Version (No. FHWA-HOP-18-036). United States. Federal Highway Administration, 2019.

Yao, J., F. Shi, Z. Zhou, and J. Qin. Combinatorial Optimization of Exclusive Bus Lanes and Bus Frequencies in Multi-modal Transportation Network. Journal of Transportation Engineering, 2012. 138 (12): 1422–1429.

Yeom, C., N. M. Rouphail, W. Rasdorf, and B. J. Schroeder. Simulation Guidance for Calibration of Freeway Lane Closure Capacity. Transportation Research Record, 2016, 2553(1): 82-89.

Zaidi, Z., E. Radwan., and R. Harb. Evaluating Variable Speed Limits and Dynamic Lane Merging Systems in Work Zones: A Simulation Study. International Scholarly Research Notices, 2012.

Zamparini L, Reggiani A. Freight Transport and the Value of Travel Time Savings: A Meta-analysis of Empirical Studies[J]. Transport Reviews, 2007, 27(5): 621-636.

Zhao, J. and Kling, C. L. (2001) A new explanation for the WTP/WTA disparity, Economics Letters, 73,293–300.

Zhou, J., L. Rilett, and E. Jones (2019). Estimating Passenger Car Equivalent Using the HCM-6 PCE Methodology on Four-Lane Level Freeway Segments in Western US. Transportation Research Record, 2673 (11): 529-545.

Zhu, W. Two-Lane Highway Work Zone Capacity Model and Control Analysis. Masters Thesis, 2015.

Zhu, W. Two-Lane Highway Work Zone Capacity Model and Control Analysis. Masters Thesis, 2015.

Zwahlen, Helmut, and Andrew Russ. Evaluation of the Accuracy of a Real-Time Travel Time Prediction System in a Freeway Construction Work Zone. Paper No. 02-2371, Washington DC: Transportation Research Board, 2001.

APPENDICES

A. CALIBRATED MODEL PARAMETERS

B. SENSITIVITY ANALYSIS OF THE CALIBRATED MODELS

C. MOVES OUTCOME

D. ECONOMIC ANALYSIS SPREADSHEET

APPENDIX A: CALIBRATED MODEL PARAMETERS

Parameter	Reference	Default	Best Value (4 Lane)	Best Value (6 Lane)
cc0	Standstill distance	4.92 ft	**5**	**4.92**
			10	**4.92**
cc1	Headway time	0.9 s	**2.0**	**1.8**
			2.8	**3.0**
		0	**0.3/0.5**	**0.5/0.5**
cc2	Following variation	13.12 ft	**45**	**20**
Deceleration for cooperative braking (max)		–9.84 ft/s^2	**-15**	**-9.84**
Look ahead distance (max)		656.2 ft	**3000**	**1500**
Advanced merging		No	**Yes**	**Yes**
Cooperative merging		No	**Yes**	**Yes**
Routing decisions look ahead		No	**Yes**	**Yes**

Calibrated Values
Two-Lane Work Zone
CC0: 4.92
CC1: Mean (PC:4.75, Truck:6.17)
CC1:StdDev (PC:2.3, Truck: 2.73)
CC2: 5
CC3: -10
CC4 :-0.2
CC5: 0.33
CC6: 11.3

APPENDIX B: SENSITIVITY ANALYSIS OF THE CALIBRATED MODELS

Double Click to Open


TwoLaneWZ_1_B.xlsx


SixLaneWZ_3_2.xlsx


SixLaneWZ_3_1.xlsx


FourLaneWZ_2_1.xlsx

APPENDIX C: MOVES OUTCOME

Double Click to Open


TwoLaneWZ_Emission.xlsx


SixLaneWZ_3_2_Emission.xlsx


SixLaneWZ_3_1_Emission.xlsx


FourLaneWZ_2_1_Emission.xlsx

APPENDIX D: ECONOMIC ANALYSIS SPREADSHEET

Double Click to Open


Work_Benefit_Summary_021822.xlsx